Differential InSAR Techniques for Displacement Mapping

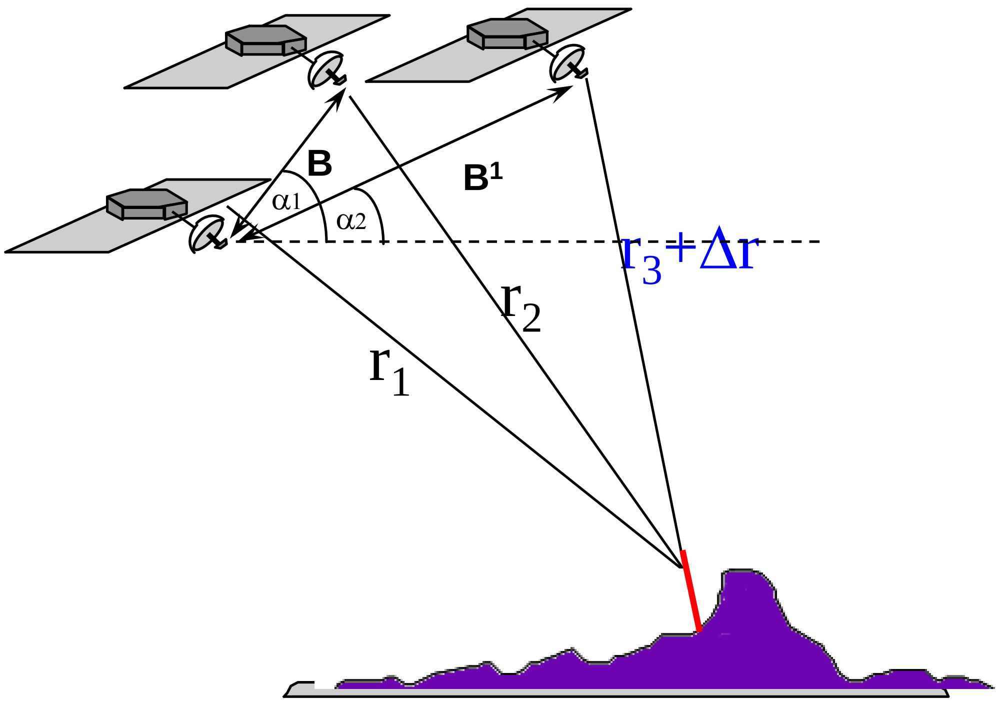

$$\Delta\phi = \phi^1 - (B_{\shortparallel}^1 / B_{\shortparallel})\phi = \frac{4\pi}{\lambda}\Delta r \qquad (1)$$

Δr = Surface Movement; Δφ= Differential Phase

Applications of Differential SAR Interferometry

- Earthquake Studies
- Volcano Monitoring
- Land Subsidence (oil or water)
- Landslides
- Glaciers and Ice Sheet Motion
- Land use/ Land Cover Analysis

3-Pass DInSAR

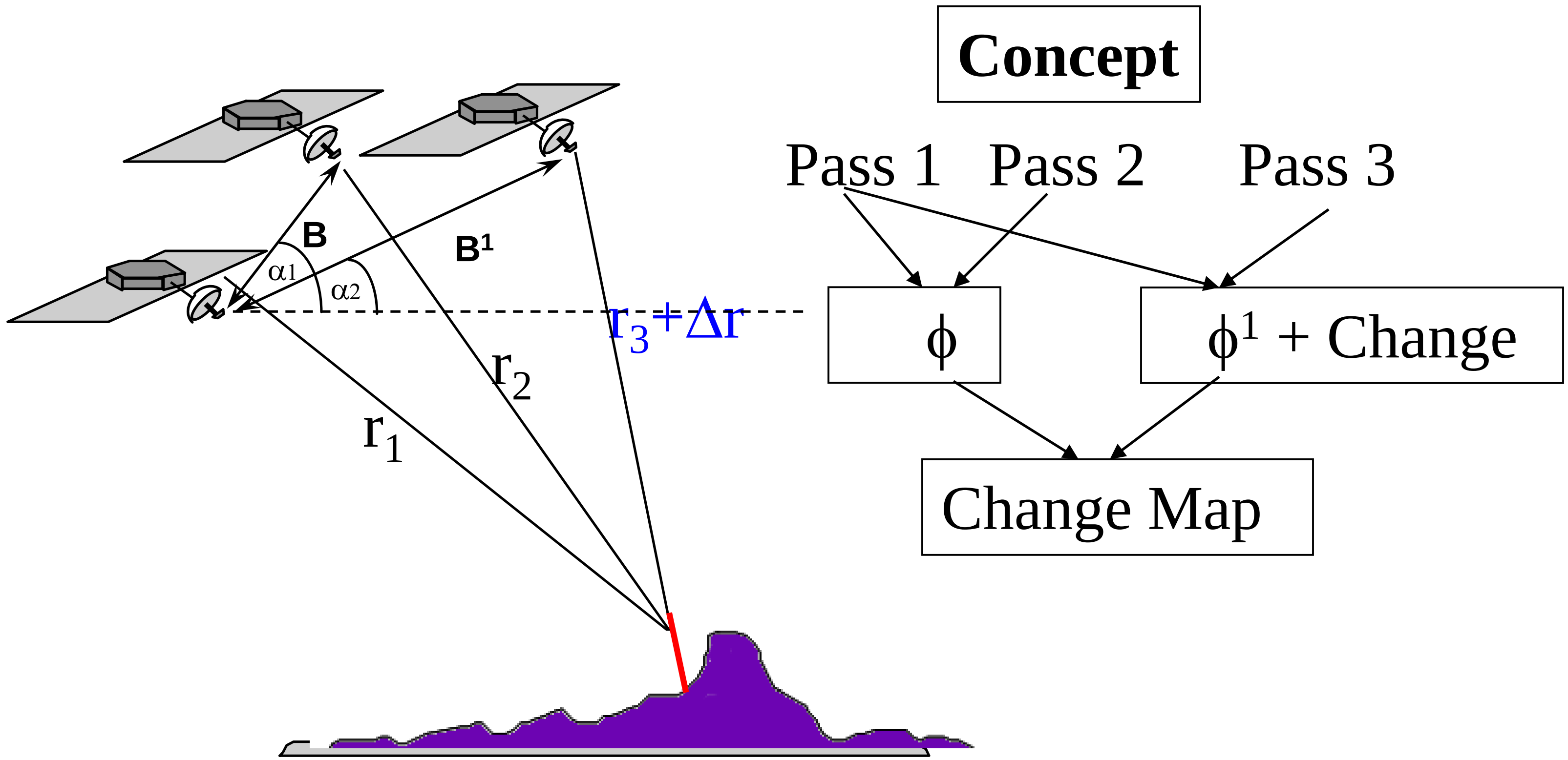

$$\Delta\phi = \phi^1 - (B_{II}^1 / B_{II})\phi = \frac{4\pi}{\lambda}\Delta r \qquad (1)$$

Δr = Surface Movement; $\Delta\phi$= Differential Phase

Derivation of Eq. (1)

Path difference is related to phase difference

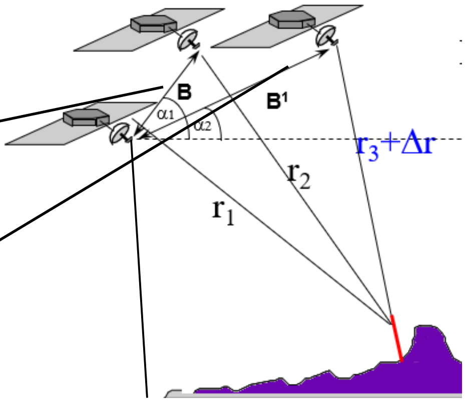

$$\varphi = -\frac{4\pi}{\lambda}(r_1 - r_2) \quad \text{(interferogram1)}$$

$$\varphi = -\frac{4\pi}{\lambda}B_{\parallel} \quad \text{since } r_1 - r_2 = B_{\parallel} \quad (2)$$

$$\varphi = -\frac{4\pi}{\lambda}(B_{\parallel} - B_{\parallel 0}) \quad \textit{Corrected for reference (flat surface) phase}$$

$$\varphi^1 = -\frac{4\pi}{\lambda}\{r_1 - (r_3 + \Delta r)\} \quad \text{(Interferogram 2) deformation}$$

$$\varphi^1 = -\frac{4\pi}{\lambda}(B_{\parallel}^1 - \Delta r)$$

$$\varphi^1 = \varphi\frac{B_{\parallel}^1}{B_{\parallel}} + \frac{4\pi}{\lambda}\Delta r \quad \textit{from eq}(2) \quad -4\pi/\lambda = \frac{\varphi}{B_{\parallel}}$$

$$\varphi^1 - \varphi\frac{B_{\parallel}^1}{B_{\parallel}} = \frac{4\pi}{\lambda}\Delta r$$

Displacement Map Generation (3-Pass)

May 17, 1993 earthquake

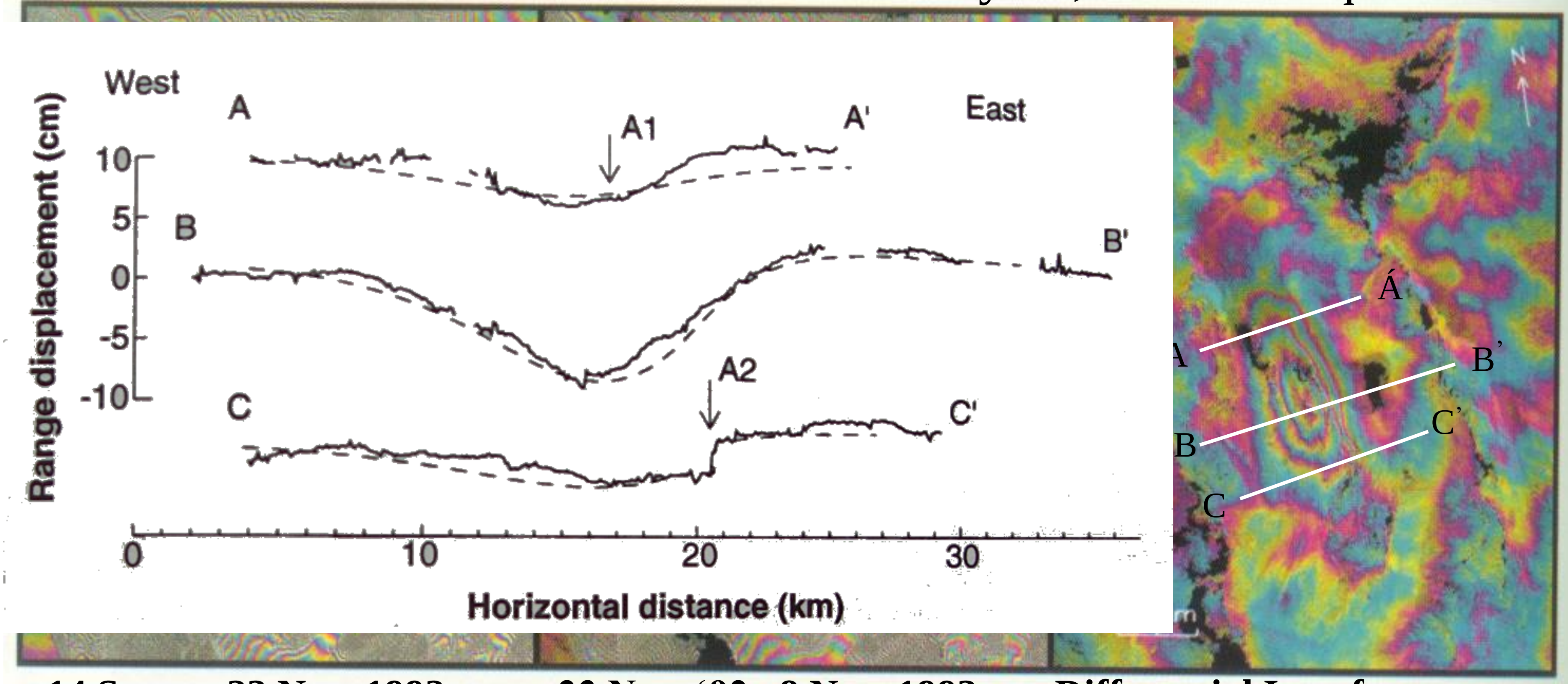

14 Sept. - 23 Nov, 1992 **23 Nov. '92– 8 Nov, 1993** **Differential Interferogram**

Interferometric mapping of a 9.5 cm elliptical depression in the **Eureka Valley** generated by a **May 17, 1993, magnitude 6.1 earthquake**. The interferometric phase is mapped onto a color wheel. Two way propagation results in a correspondence between a displacement of $\lambda/2$(=2.8 cm) and one revolution on the color wheel. The left interferogram is formed from data acquired before the earthquake, reflecting only topography; the center interferogram is formed from data acquired before and after the earthquake; and on the right the displacement map (determined by removing the topographic component from the center interferogram) is shown. The **9.5 cm** ellipsoidal depression is seen at the center of the right interferogram.

Iran, Bam Earthquake (M_w=6.6) on Dec. 26, 2003 (3-pass)

Topo
Inteferogram

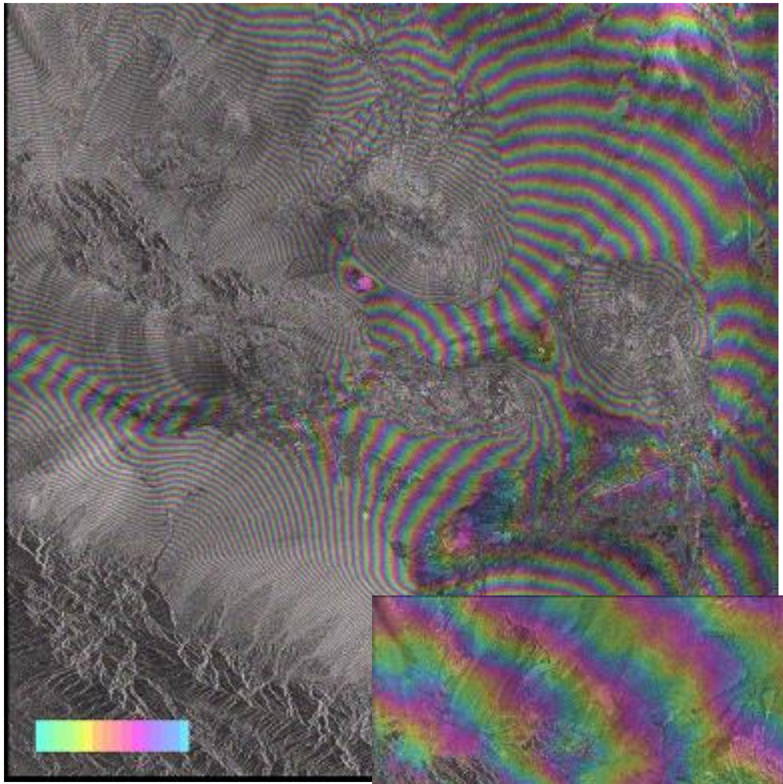

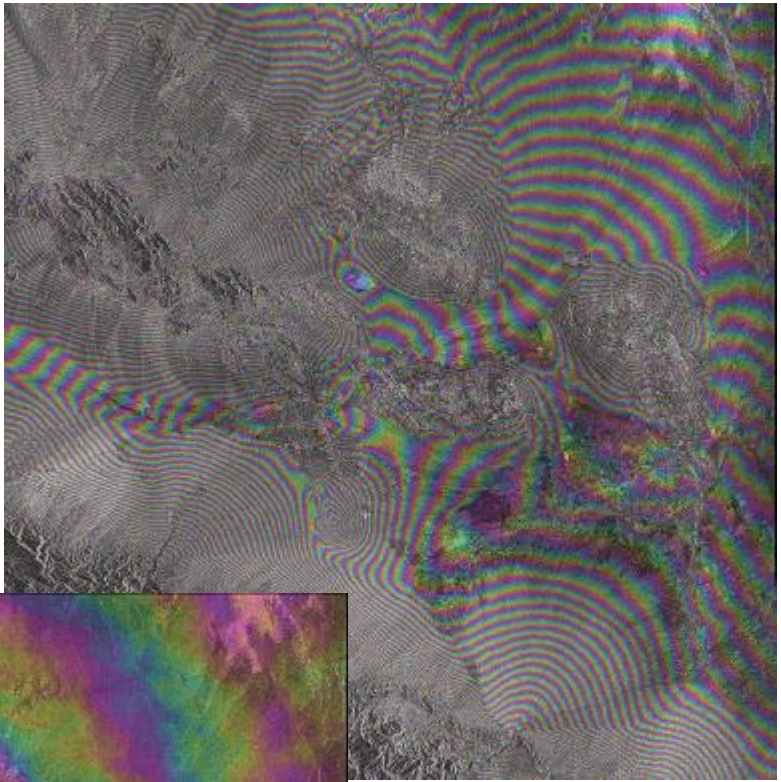

defo

Dec. 3, 2003
June 11, 2003,
Baseline 475m

Dec. 3, 2003
Jan. 7, 2004
Baseline 520m

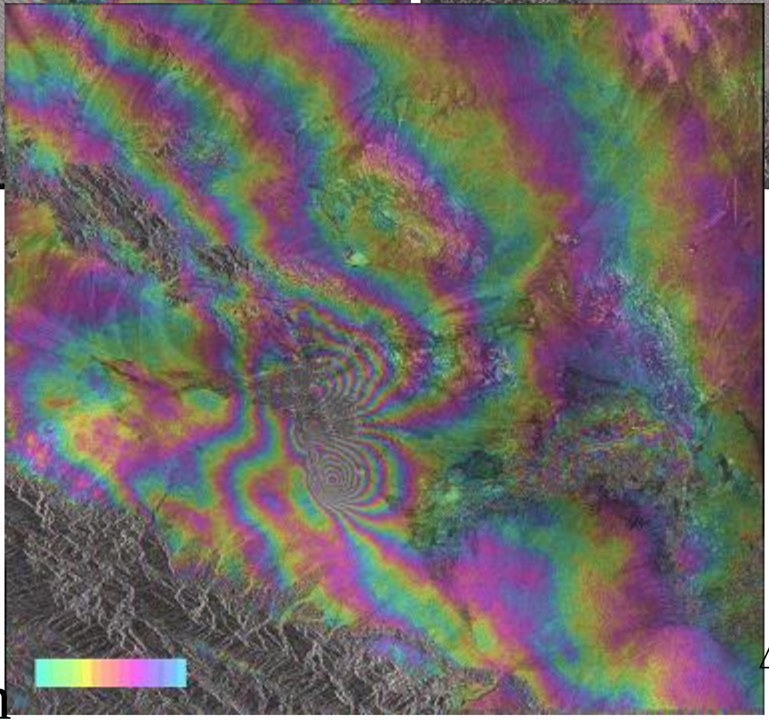

Differential
Interferogram

$$\Delta\phi = \phi^1 - (B_{\text{II}}^1 / B_{\text{II}})\phi = \frac{4\pi}{\lambda}\Delta r \qquad (1)$$

InSAR versus DInSAR (Sensitivity)

InSAR $$dh = \frac{\lambda}{4\pi} \frac{r_1 \sin\theta}{B_\perp} d\phi$$

For ERS-1, $B_\perp$ =200 m, r_1=850 km, θ=23^0

dh = 46 m   ***for dΦ = 2π***

DInSAR $$\Delta\phi = \phi' - (B'_{II} / B_{II})\phi$$

$$\Delta\phi = (4\pi/\lambda)\Delta r$$

For $\Delta\phi$ =2π *(one cycle), displacement Δr = λ/2 = 2.8 cm*

46 meters $\longrightarrow$ 2π ***in InSAR***

2.8 cm $\longrightarrow$ ***2π in DInSAR***

(46 m/2.8 cm) = 1642 times greater sensitivity in DInSAR as compared to InSAR for Baseline $B_\perp$ = 200 m

Other way of telling:

1m equal to phase change of 7.742^0 for InSAR

1m equal to phase change of 12857^0 for DInSAR

Two-Pass Method

Deformation measurements

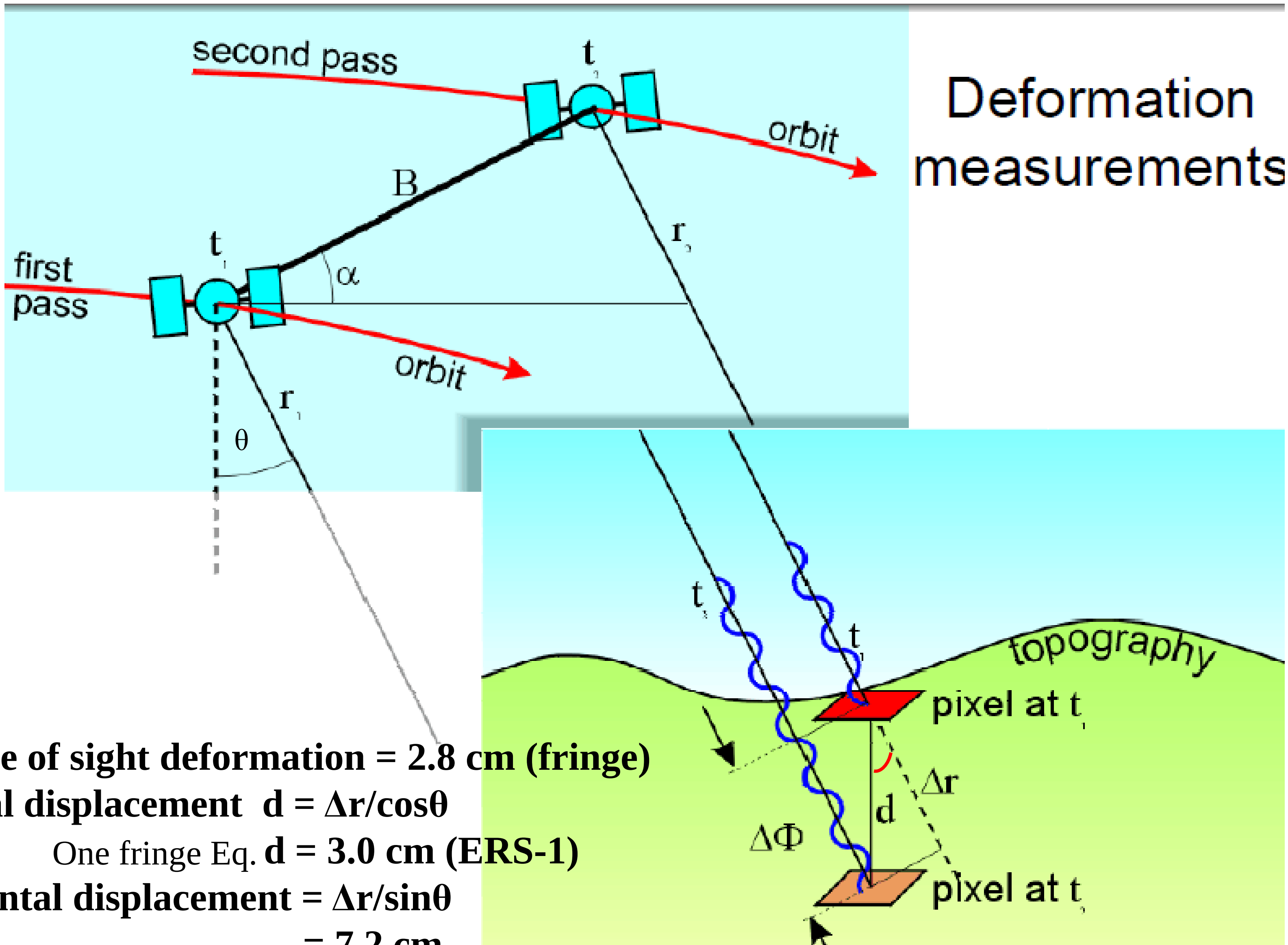

Δr= line of sight deformation = 2.8 cm (fringe)

Vertical displacement d = Δr/cosθ

One fringe Eq. **d = 3.0 cm (ERS-1)**

Horizontal displacement = Δr/sinθ

= 7.2 cm

Two-Pass Method for Deformation

Ideal case = Zero baseline

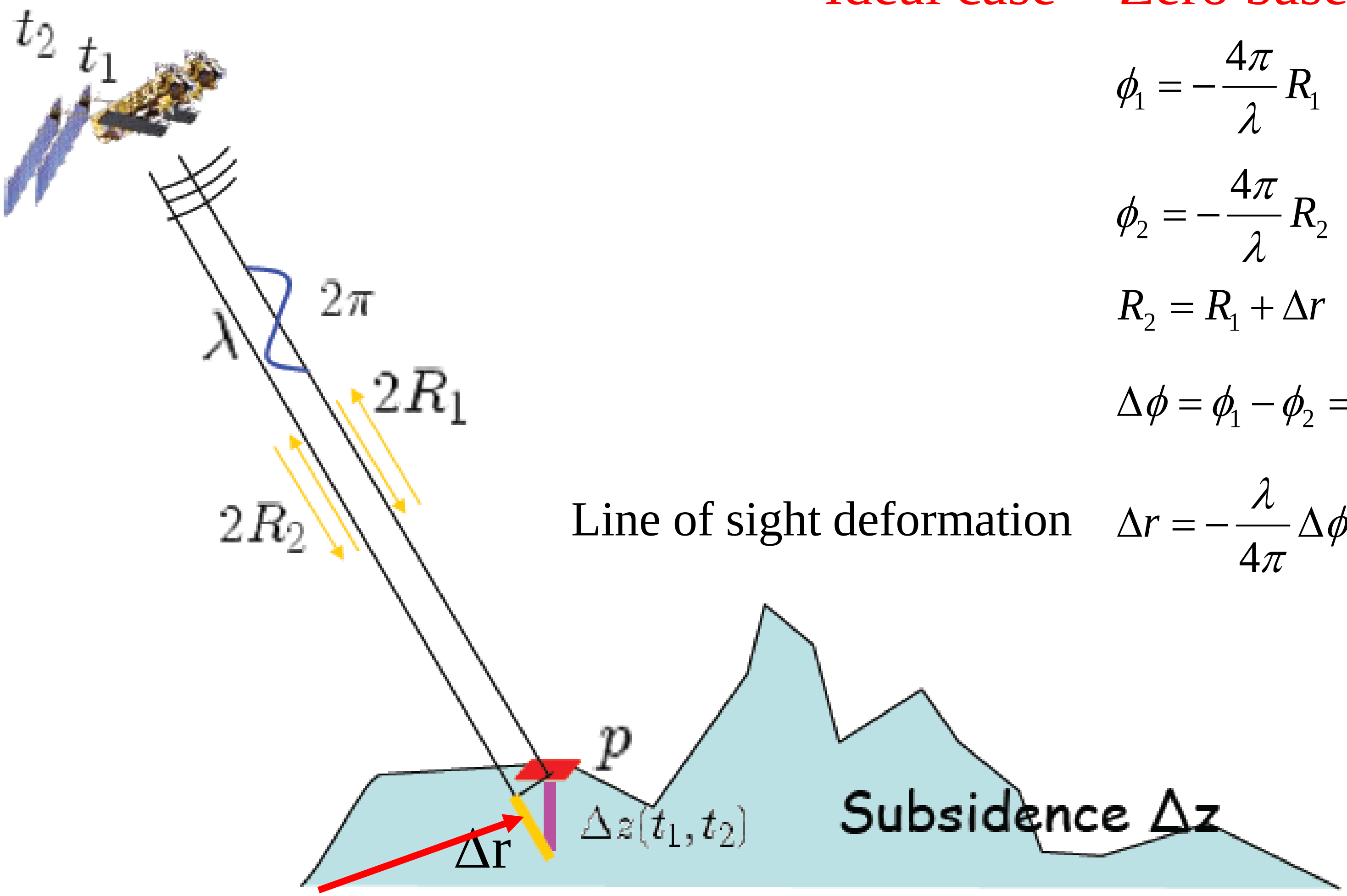

$$\phi_1 = -\frac{4\pi}{\lambda} R_1$$

$$\phi_2 = -\frac{4\pi}{\lambda} R_2$$

$$R_2 = R_1 + \Delta r$$

$$\Delta\phi = \phi_1 - \phi_2 = -\frac{4\pi}{\lambda} \Delta r$$

Line of sight deformation $$\Delta r = -\frac{\lambda}{4\pi} \Delta\phi$$

1 cycle LOS deformation is equal to **half** the physical wavelength

2-Pass Method for DInSAR

Pass 1 **Pass 2** **DEM**

Interferogram with differential effects

Simulated Interferogram

Change Map

Non-Ideal Case = Non zero baseline.

You need DEM to remove topography information

$$\text{Interferogram } \phi = \frac{4\pi B_{\perp}}{\lambda r \sin\theta} dh - \frac{4\pi}{\lambda} \Delta r$$

By removing the topographic phase (i.e. first term) through SRTM DEM, we get displacement map.

$$\Delta\phi_d = -\frac{4\pi}{\lambda}(\Delta r)$$

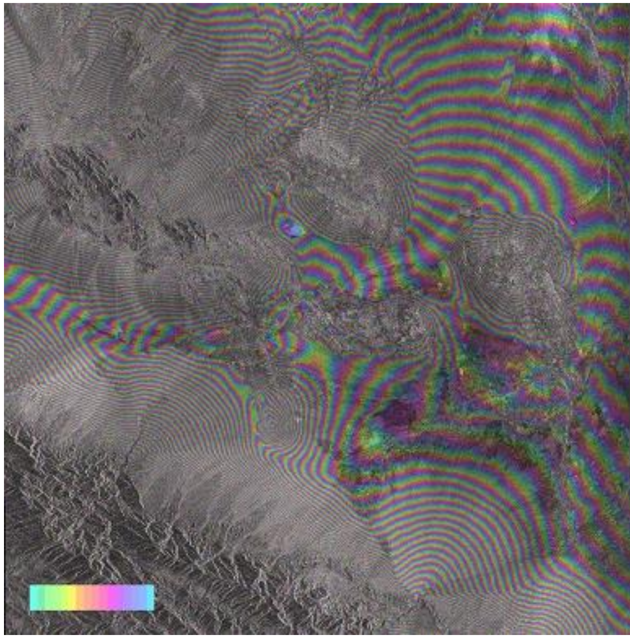

Deformation with topography interferogram

2-Pass Iran, Bam Earthquake(Dec 3, 03-Jan 7, 04)

SRTM DEM

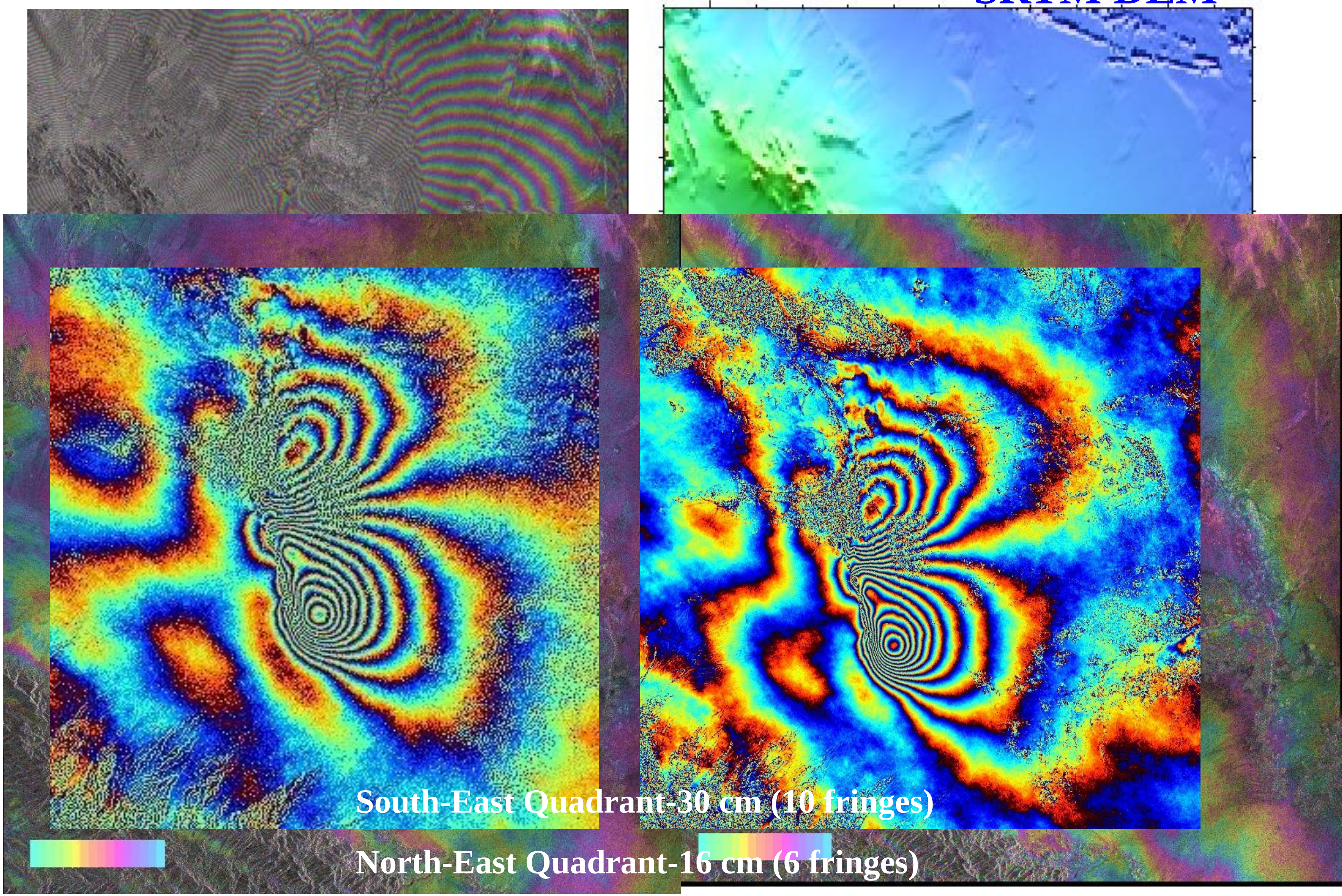

Influence of DEM error on DInSAR Results

Suppose SRTM DEM has an error of 30 m

Let us consider ERS-1 SAR parameters r_1=850km, θ=23^0 λ=5.6 cm,

B_{perp} =500 m

For InSAR dh = λ r sin θ / (4π B_|_)*($\Delta\phi$)

= (0.056*850000*sin(23)*(2 π)) / (4 π*500)

= 18.599m (one fringe equivalent value)

For DinSAR Δr = $\lambda\Delta\phi$ /4π = λ(2π)/4 π= λ/2 = 5.6/2 = 2.8 cm (one fringe equivalent value)

For 18.599 m --→ error is 30 m

2.8 cm ---> ?

DInSAR error = 0.028*30/18.599 = 4.5 cm (for B_{perp} = 500 m)

For baseline B_{perp} = 100 m.

InSAR dh = 93 m

DInSAR error = 0.028*30/93 = 0.0903 cm

For less baseline, we get less error

Influence of DEM error on DInSAR Results

Simple way of calculation of DInSAR error

InSAR dh = λ r sin θ / (4π B_|_)*(Δϕ)

Substitute dh value as error in DEM (30 m) and get Δ

From the above equation Δϕ = 4π B_|_dh/(λrsinθ)

Δϕ = 10.13 radians

Substitute Δϕ = 10.13 in the following DInSAR Equation

Δr = λΔϕ /4π = 4.5 cm

Four-pass Method (if no DEM is available)

Passes with no deformation **Pass4 with deformation**

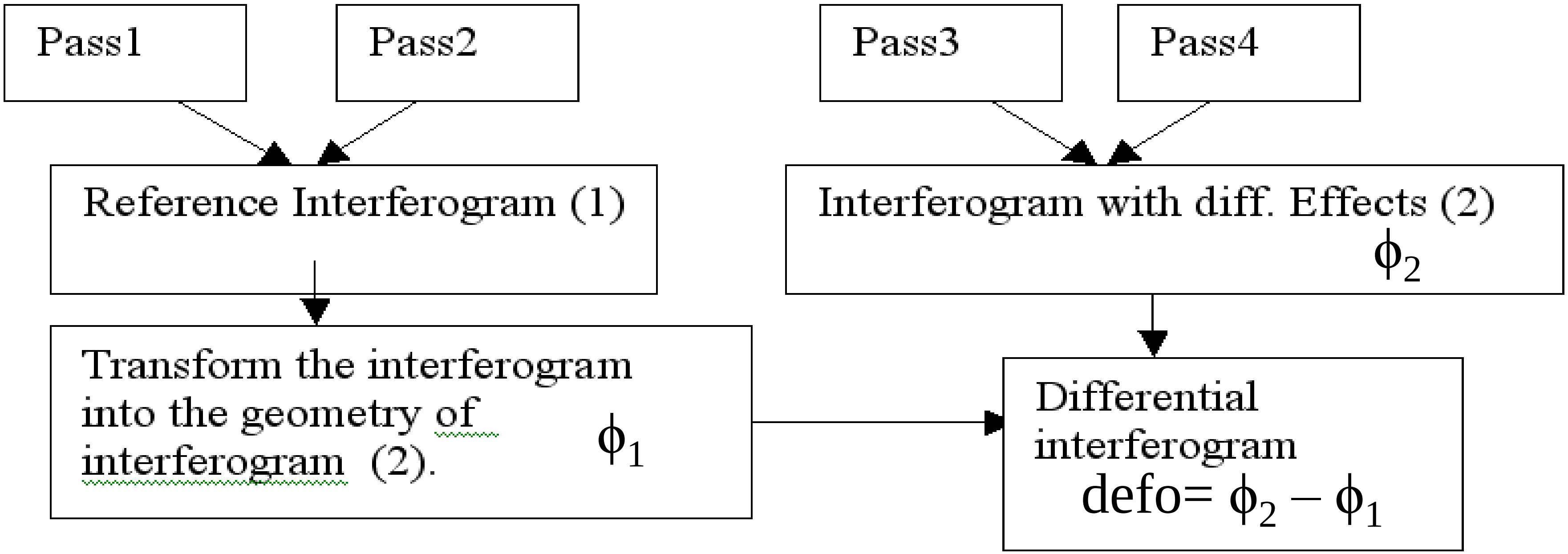

Iran, Bam Earthquake (M_w=6.6) on Dec. 26, 2003 (3-pass)

Topo
Inteferogram

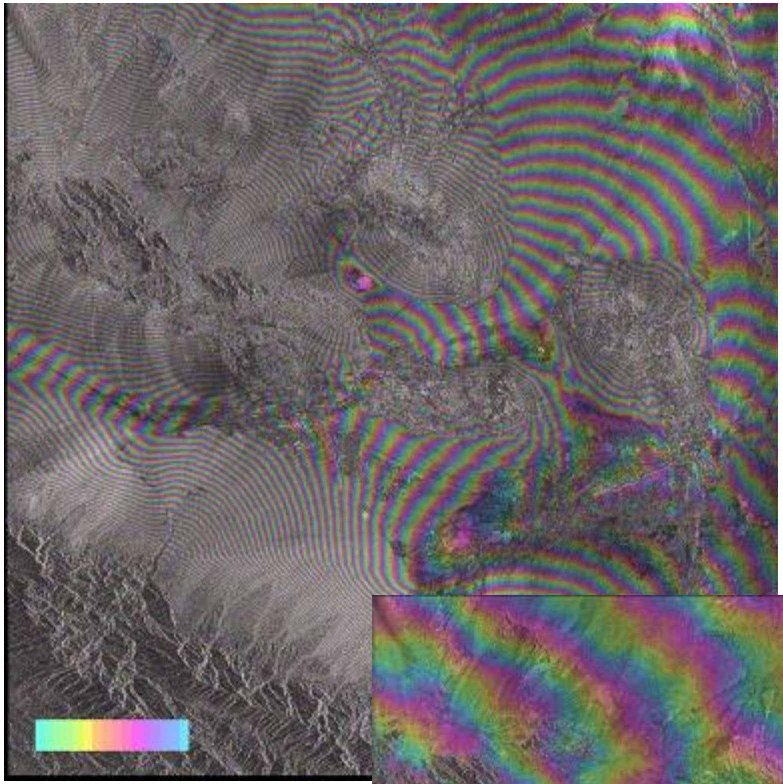

Dec. 3, 2003
June 11, 2003,
Baseline 475m

defo

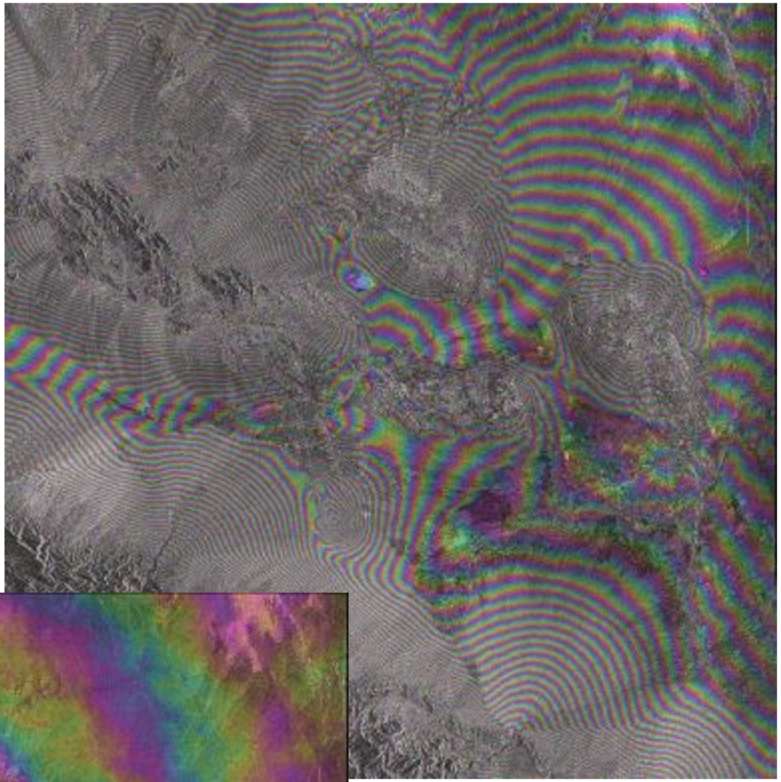

Dec. 3, 2003
Jan. 7, 2004
Baseline 520m

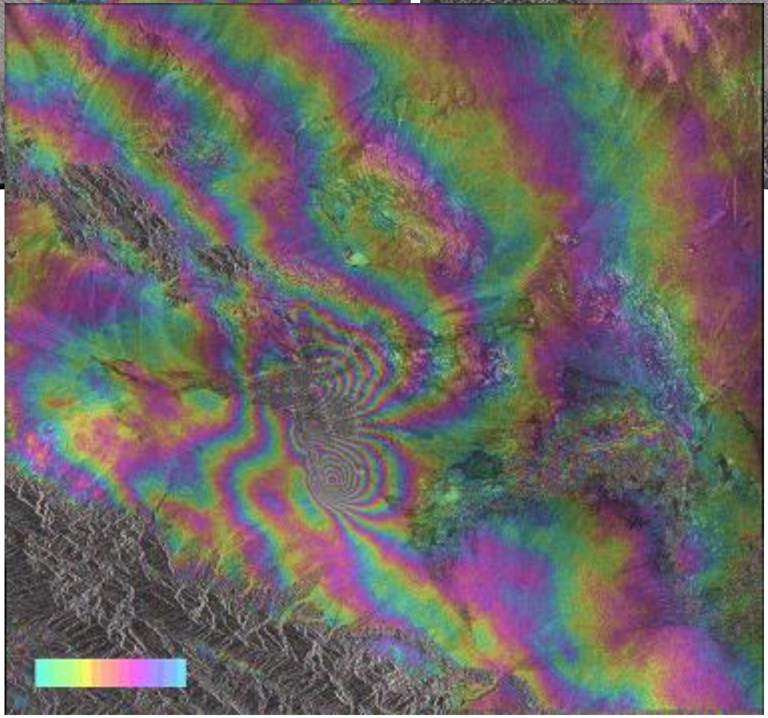

Differential
Interferogram

$$\Delta\phi = \phi^1 - (B_{II}^1 / B_{II})\phi = \frac{4\pi}{\lambda}\Delta r \qquad (1)$$

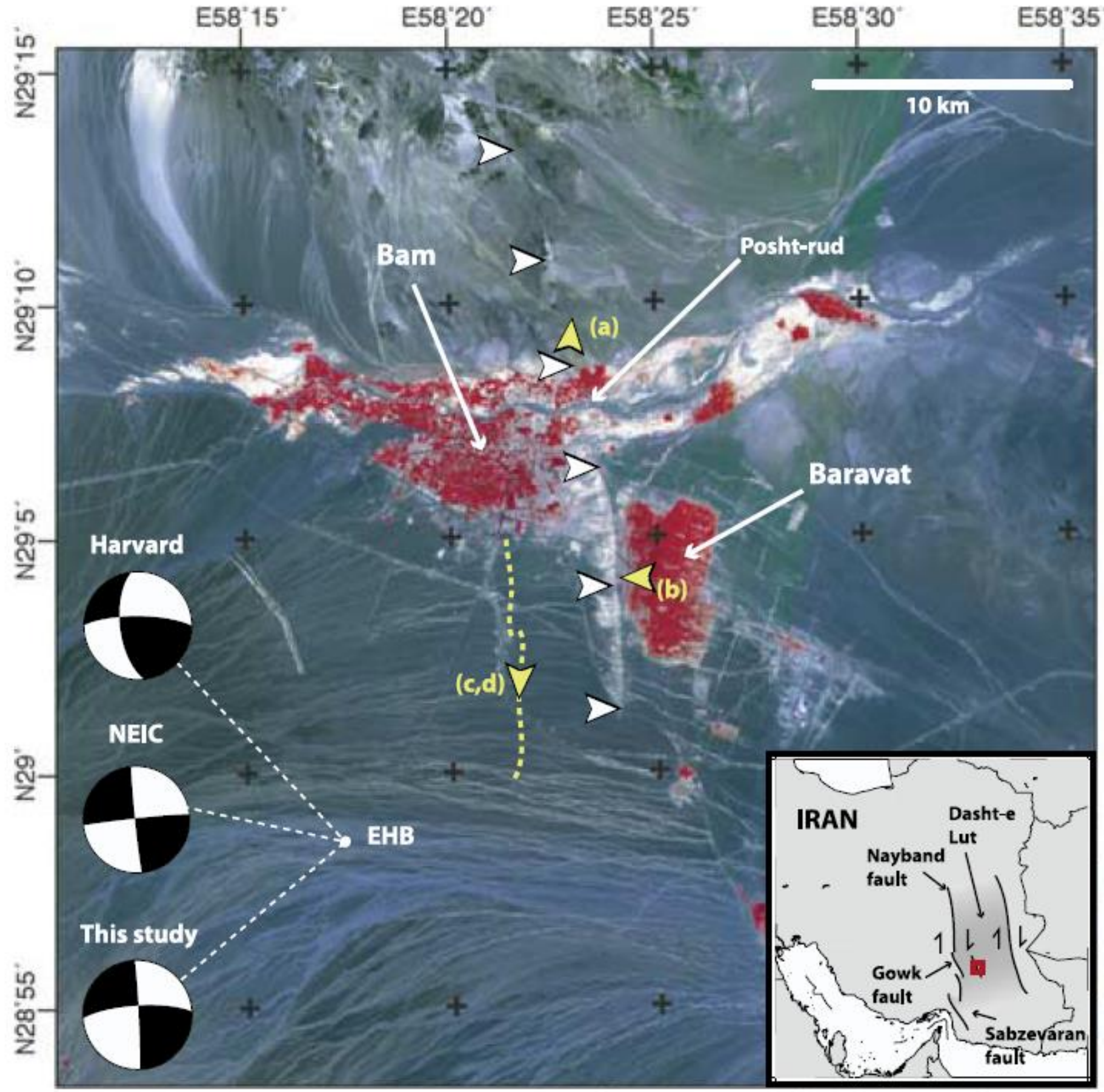

ASTER FCC Image. Red colour shows vegetation in Bam city. Arrows shows strike-slip fault. Dashed yellow shows newly found blind strike-slip fault

Yellow arrows:

(a) North of Bam (b) near Baravat, (c)&(d) South of bam

http://earthquake.usgs.gov/learn/glossary/?term=strike-slip

2-Pass Iran, Bam Earthquake(Dec 3, 03-Jan 7, 04)

SRTM DEM

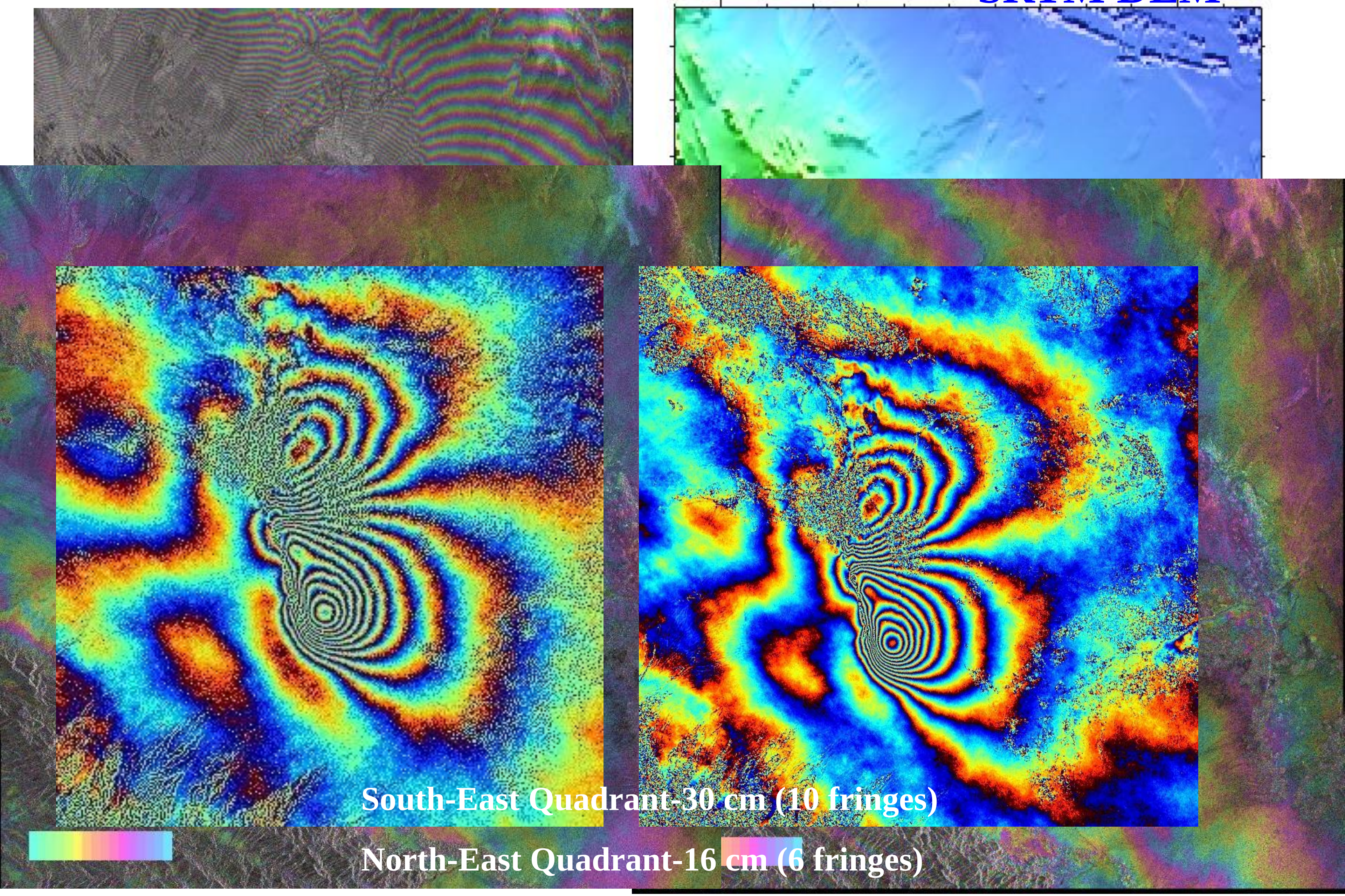

Master Dec. 3, 2003, Slave Jan. 7 , 2004

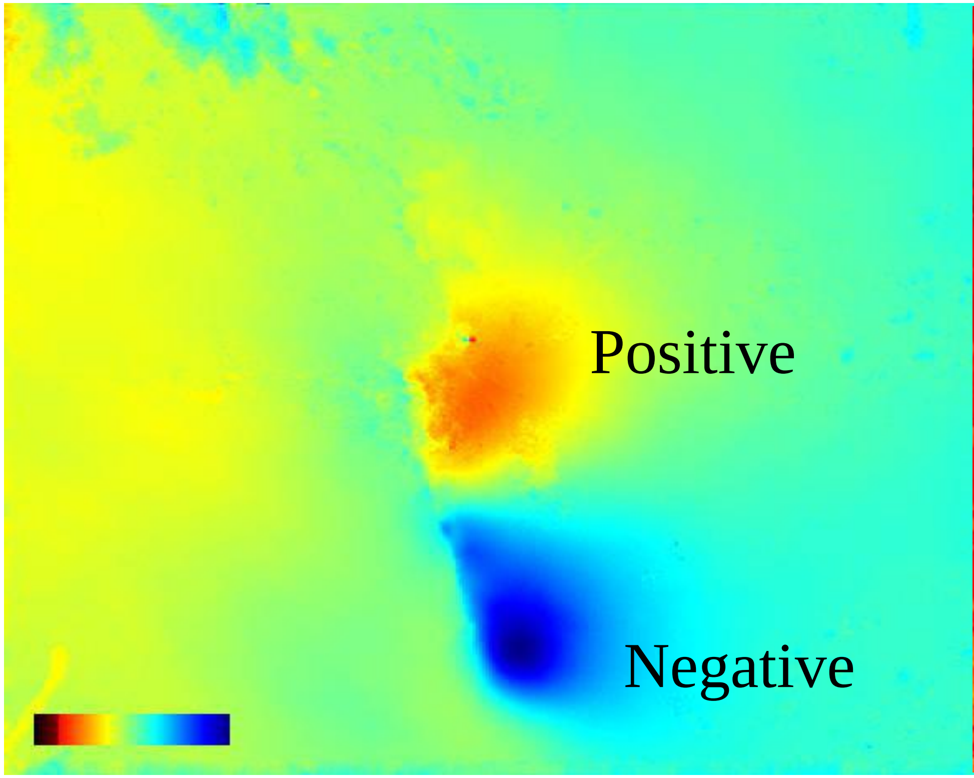

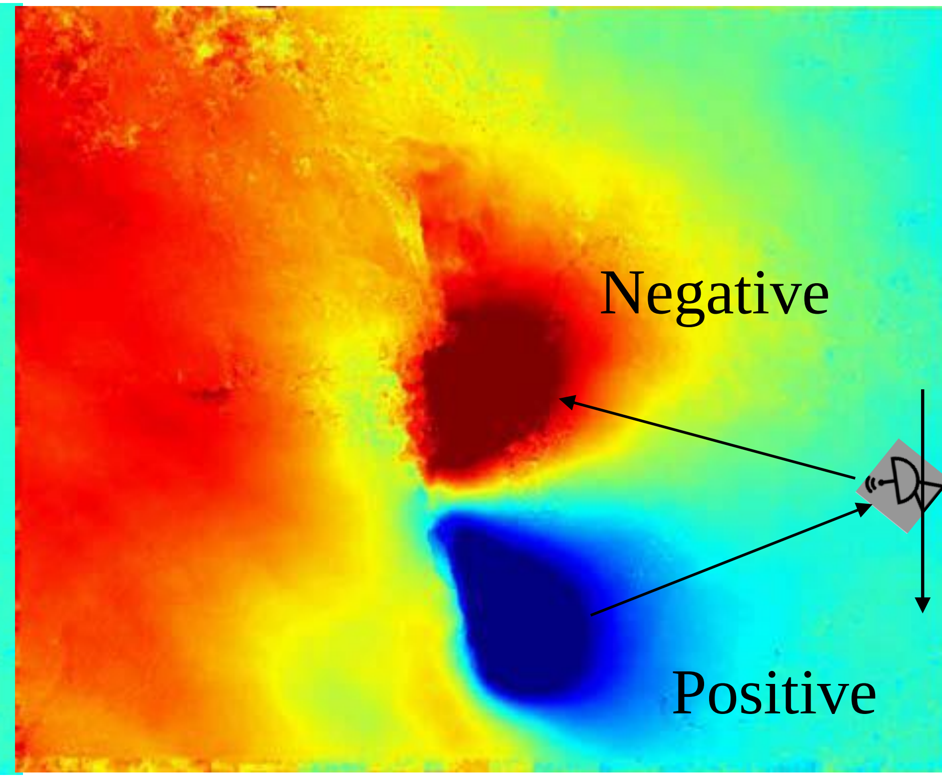

Unwrapped Phase (blue negative (towards) & red positive (away from radar)

30 cm moved towards (+ sign, blue) the radar and 18 cm away (- sign) from the radar (red)

defo_in_cm = - DinSAR_unwrapped_phase * 2.8/(2PI) in radar direction

Displacement towards and away from the Radar – Sign of the Phase (Downward motion)

First consider Time of the Images

We Generally take difference (Master – Slave) phase

Check $t_{Master} < t_{slave}$ Example: Dec. 3, 2003 Jan. 7, 2004 (Iran)

If Yes, Range Increase ($R_{t1} < R_{t2}$) Subsidence case

Phase decrease ($\phi_{t1} > \phi_{t2}$) due to $\phi = -4\pi R/\lambda$

Interferometric Phase Increase $\Delta\phi = \boldsymbol{\phi_{t1} - \phi_{t2}}$ **(positive)**

Displacement is negative $\Delta r = -\dfrac{\lambda}{4\pi}\Delta\phi$

i.e. object moved away from the radar

Sign for Upward Motion :

If range decrease, ($R_{t1} > R_{t2}$) Upward motion in second i.e slave image moved towards the radar.

Phase increase ($\phi_1 < \phi_2$) due to $\phi = -4\pi R/\lambda$

Interfermetric phase $\Delta\phi = \phi_1 - \phi_2$ (negative)

Displacement is positive $\Delta r = -\dfrac{\lambda}{4\pi}\Delta\phi$

i.e. object moved towards the radar

Suppose you interchanged master and slave (i.e. the condition is not met ($t_{master} < t_{slave}$) what will happen?

Example for Sign Convention

TerraSAR-X repeat pass : 10 GHz. = 3 cm
First pass : R1 = 718583.31294421m (before deformation)
Second pass ; R2 = 718583.61294421 m (after deformation)

$$\phi_1 = -\frac{4\pi}{\lambda} R_1 = \text{-}300999474.3$$

$$\phi_2 = -\frac{4\pi}{\lambda} R_2 = \text{-}300999599.9$$

$$R_2 = R_1 + \Delta r$$

$$\Delta\phi = \phi_1 - \phi_2 = +125.6637062 \text{ radians } = -\frac{4\pi}{\lambda} \Delta r$$

$$\Delta r = -\frac{\lambda}{4\pi} \Delta\phi = -0.3 \text{ m} = \text{-}30 \text{ cm subsidence}$$

Differential Interferogram obtained using 2-Pass Method

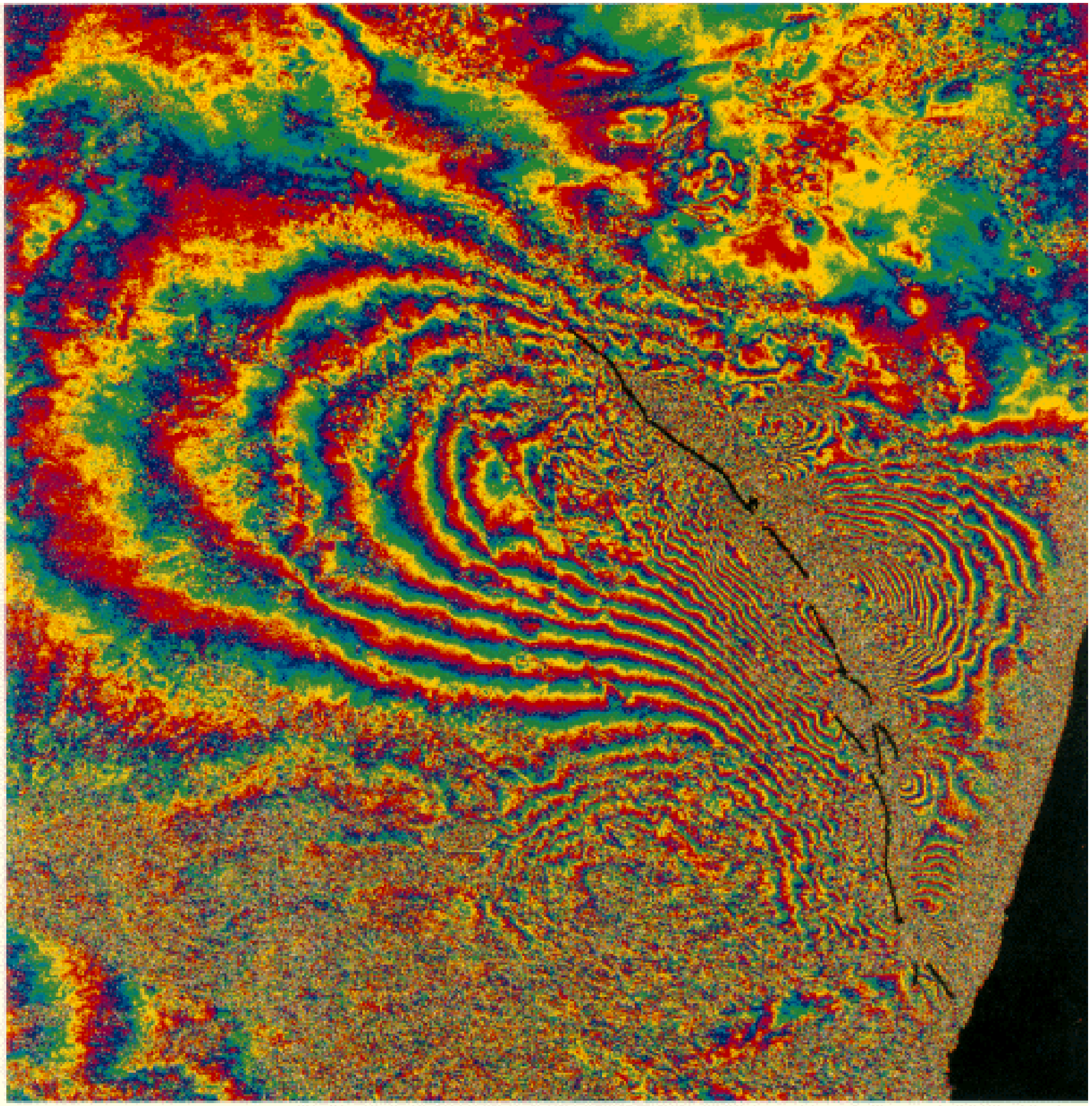

Fig. 3.3a. Compare this observed coseismic interferogram for the Landers earthquake [*Massonnet et al.*, 1993] with the synthetic interferogram in Fig. 3.3b. One cycle of color represents 28 mm of change in range. Black segments depict the fault geometry as mapped in the field. Both this image and Fig. 3.3b cover a 90-by-110-km area from April 24 to August 7, 1992.

ERS-1 SAR two scenes

April 24, 1992
June 18, 1993
DEM at 30m resolution

Earthquake $M_w = 7.3$
June 28, 1992

Surface rupture - 75 km

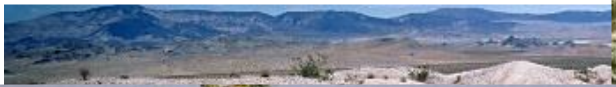

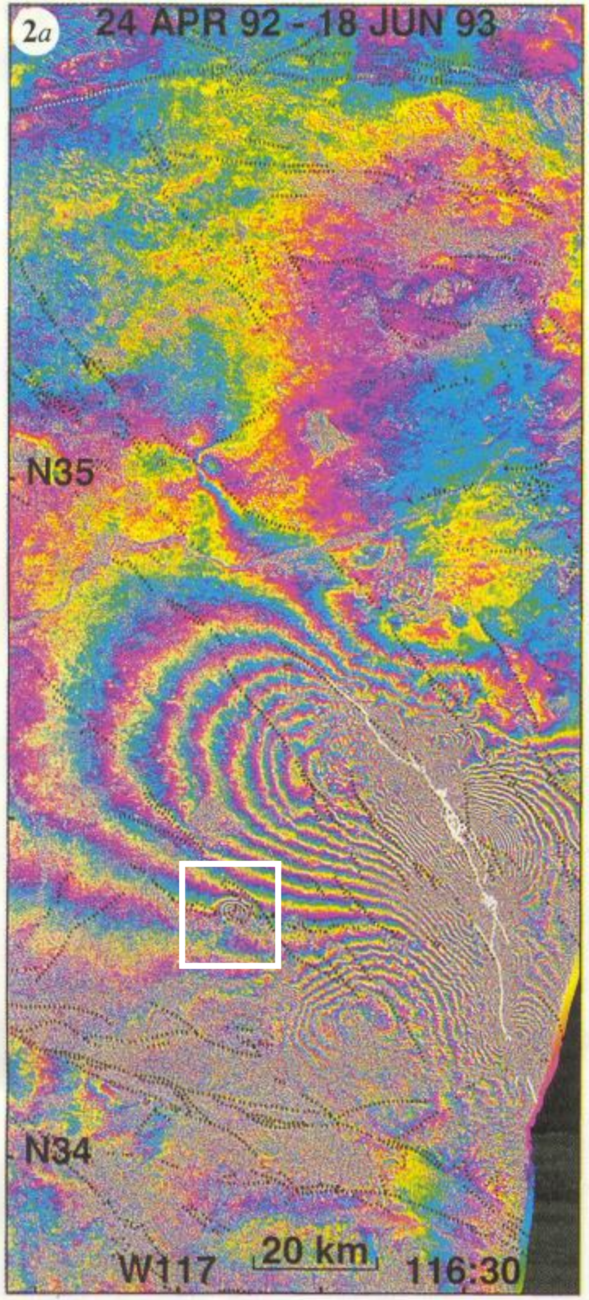

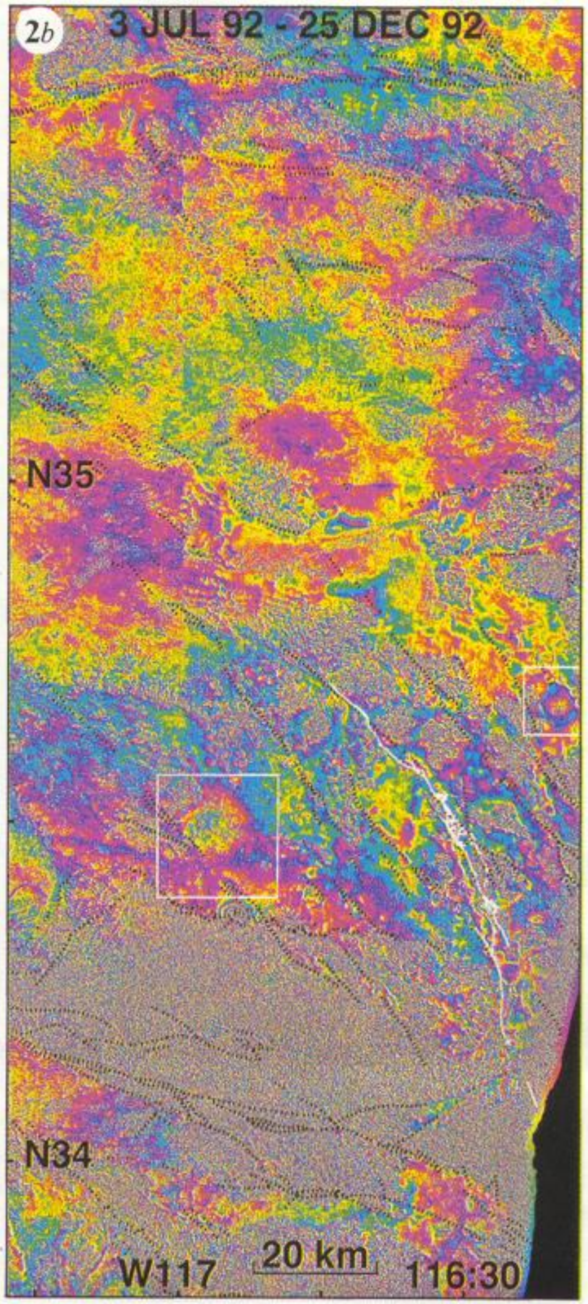

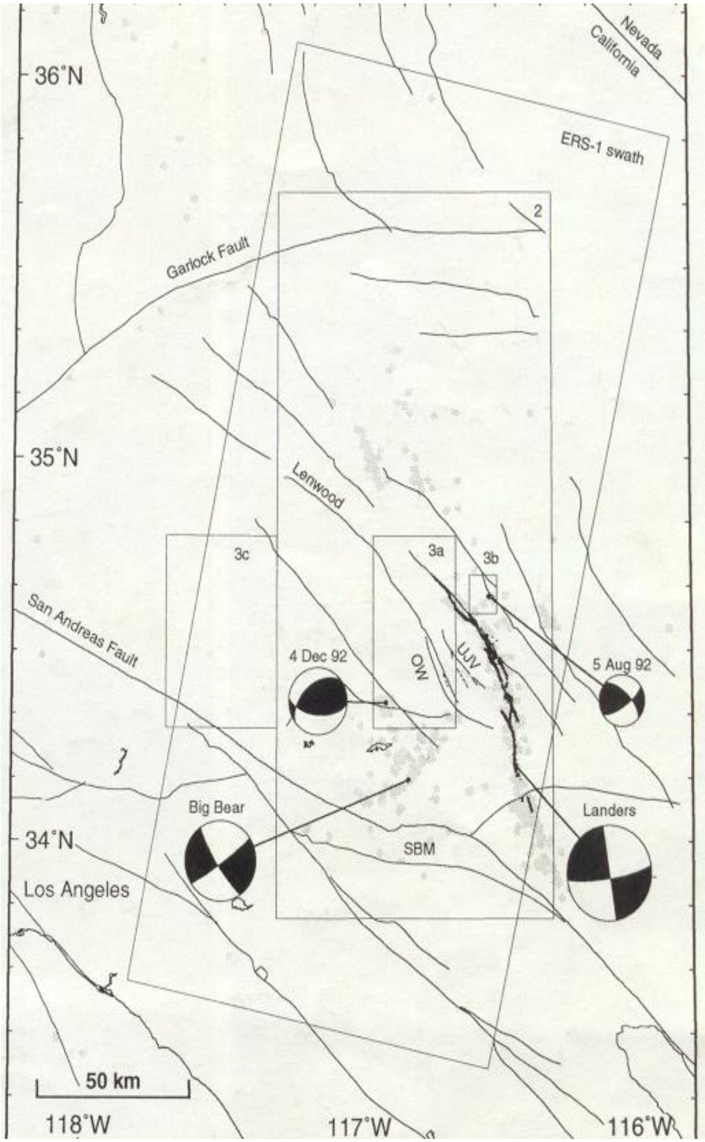

Coseismic

postseismic

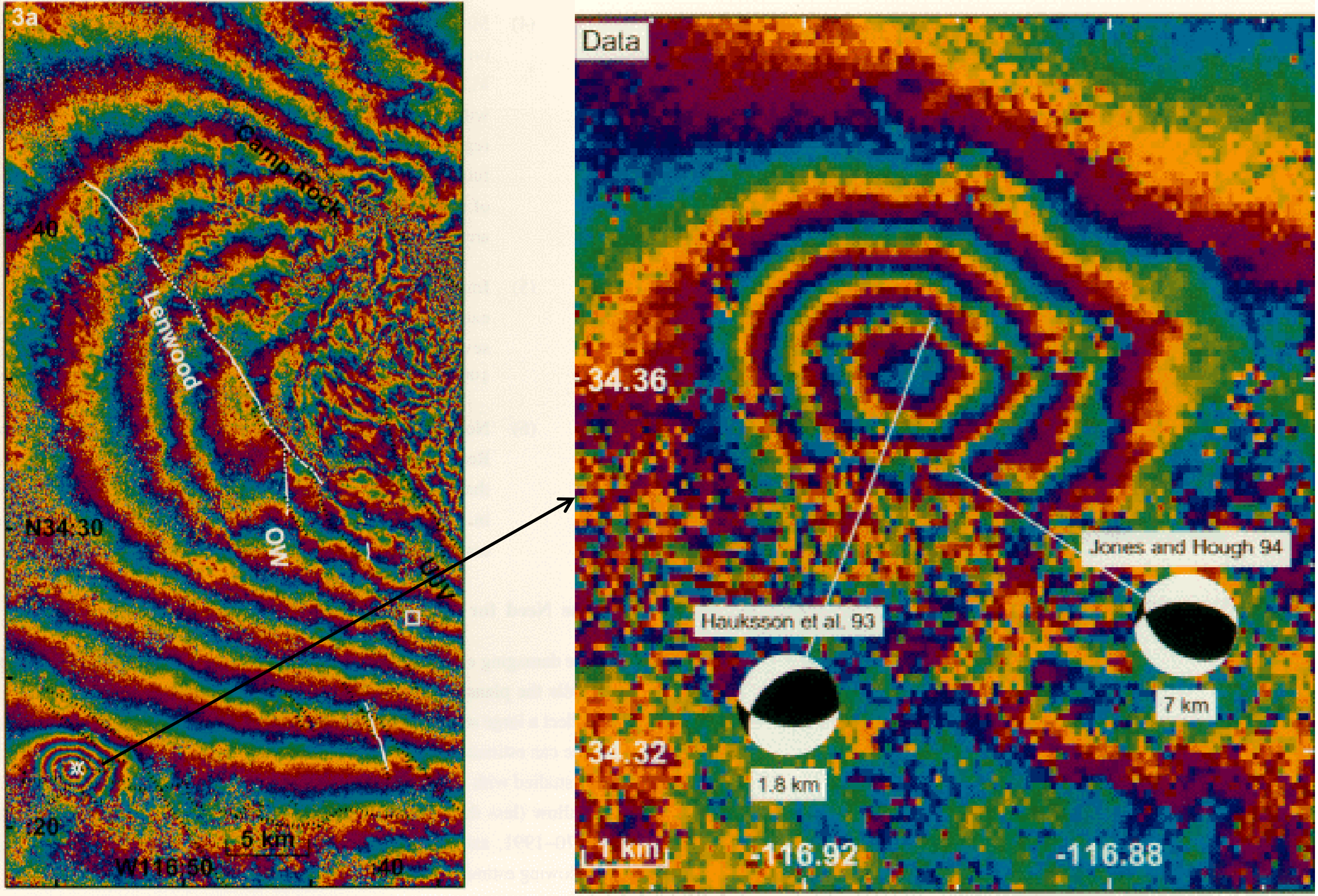

. Detail of a coseismic interferogram near Landers constructed from ERS-1 radar acquired on April 24, 1992 and June 18, 1993 [*Massonnet et al.*, 1994]. Note the osed fringes around the epicenter (star) of the December 4, 1992 magnitude 5.1 ock. Previously mapped faults are shown by dotted black lines; the rupture of the Rock fault segment mapped in the field is shown as a solid white line; Soggy Lake is square; and secondary faults with slip observed in the radar interferogram are as solid white lines. These secondary faults include segments of the Garlock, od, Old Woman (OW), and possibly the Upper Johnson Valley (UJV) faults. One epresents 28 mm of range change.

Dec. 4, 1992 M_w= 5.1

Comparison of displacements obtained using GPS and ERS-1 SAR DInSAR

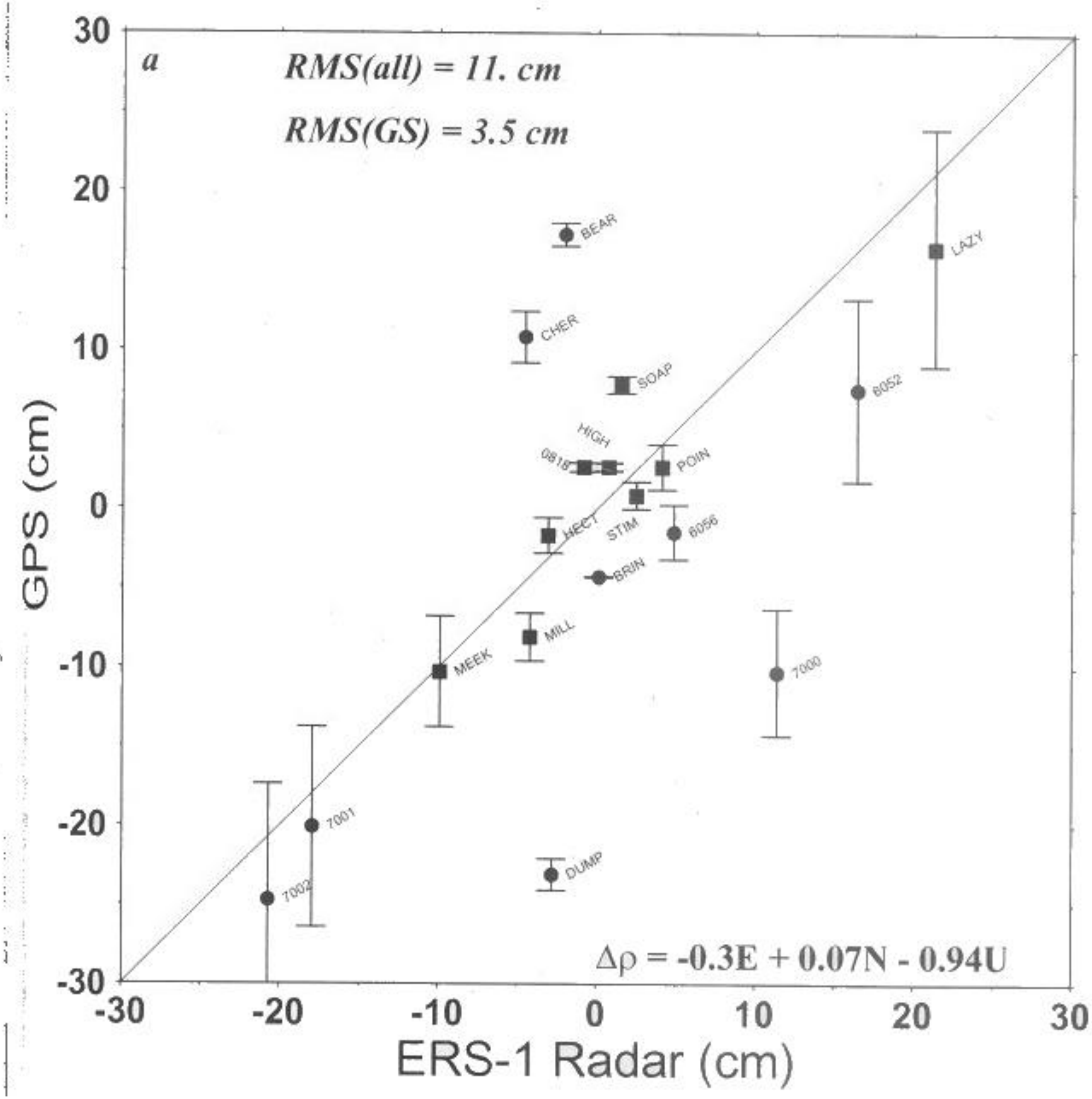

Comparison of displacements obtained using GPS and JERS-1 SAR DInSAR

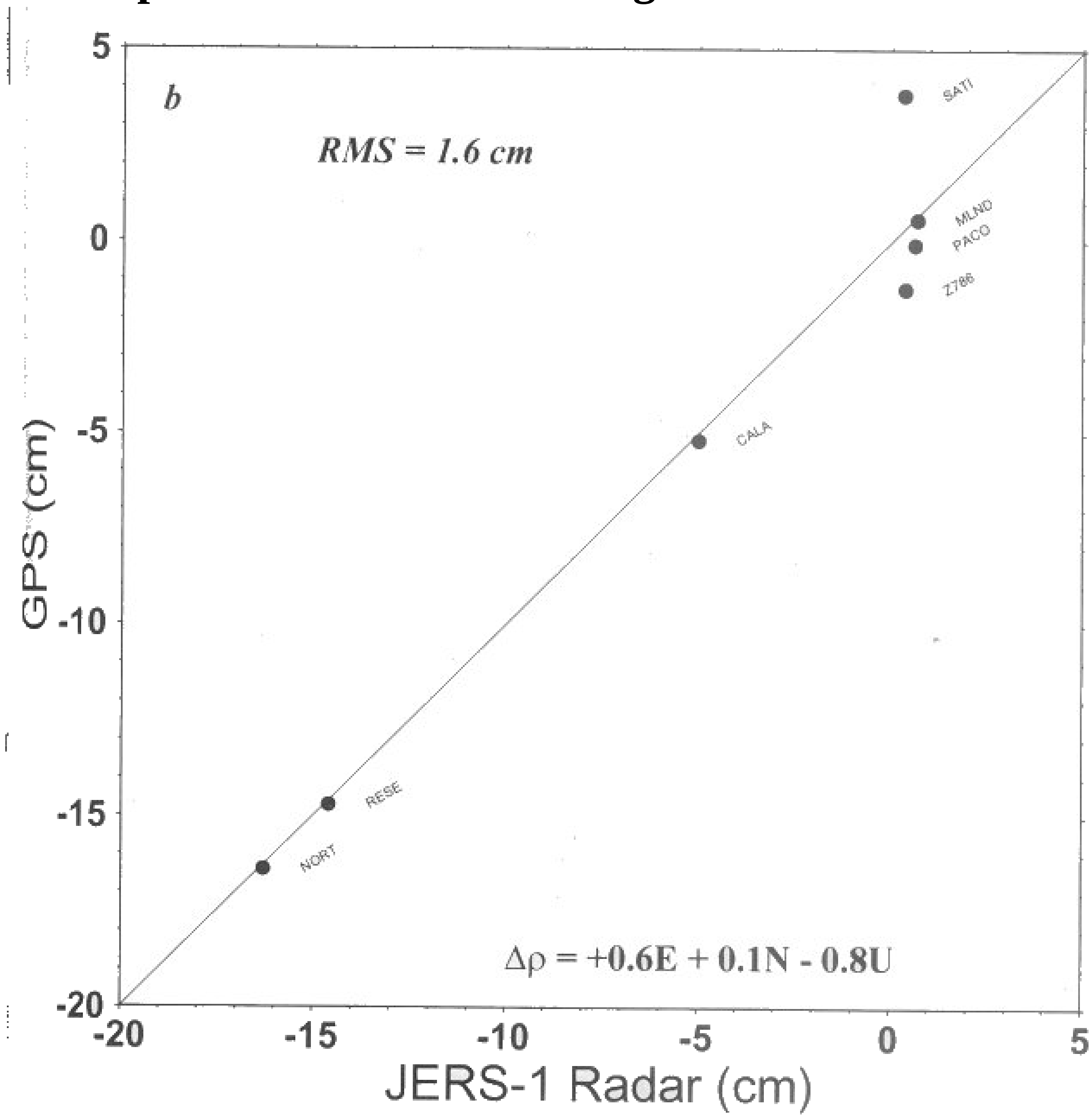

Simulation of Land Deformation

Geodetic Survey Displacements

Regional Strong Motions

Teleseismic Waveforms

Surface Offset Measurements

RNGCHN Software

Computes the Displacement due to dislocations using Okada's formula

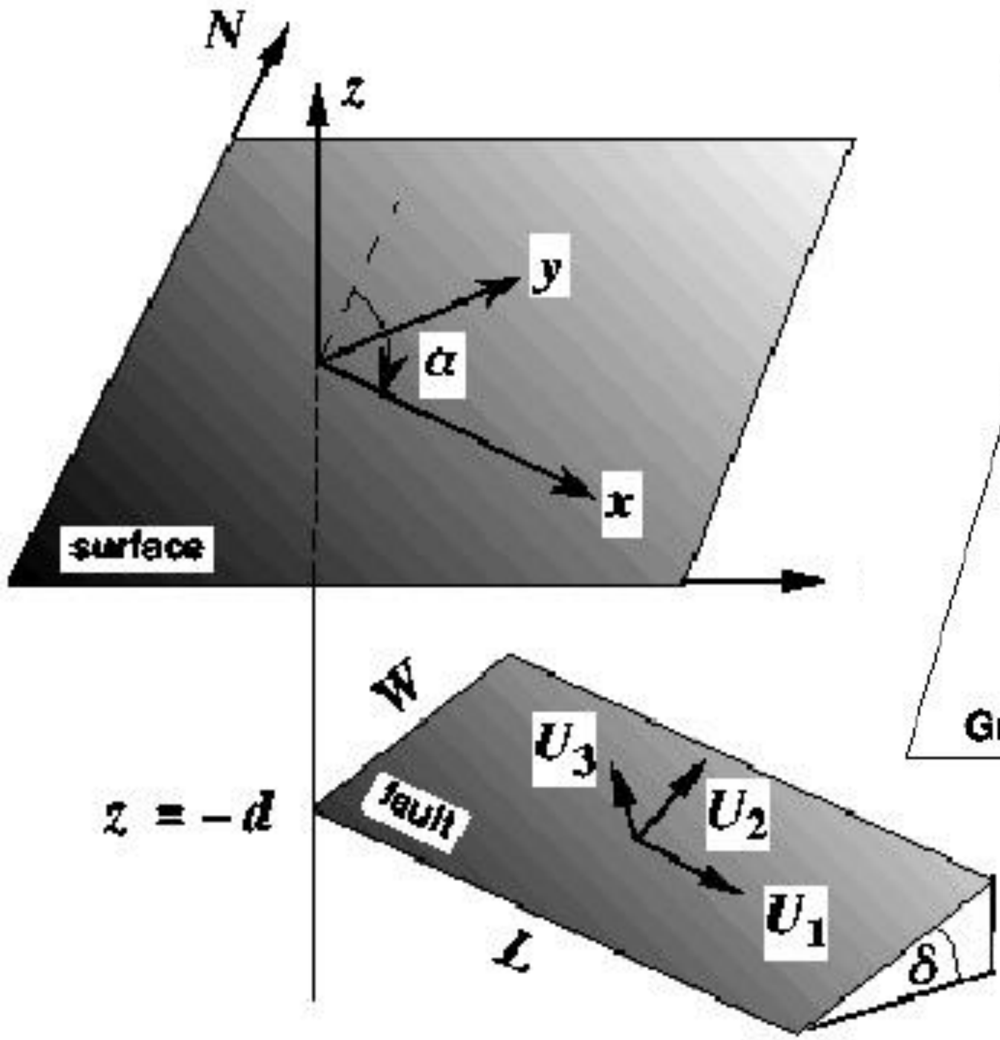

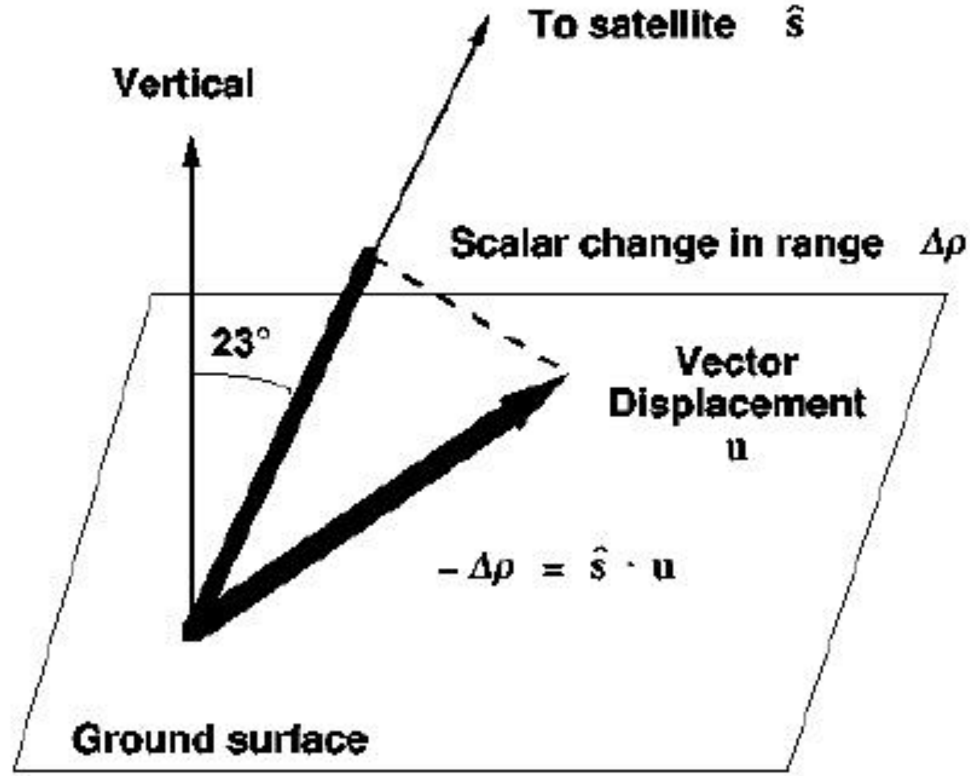

Strike is the orientation of fault measured from north.

Fault position, depth (z), Length (L), width (W), strike (α), dip(δ), and 3 components of slip (U_1, U_2, U_3).

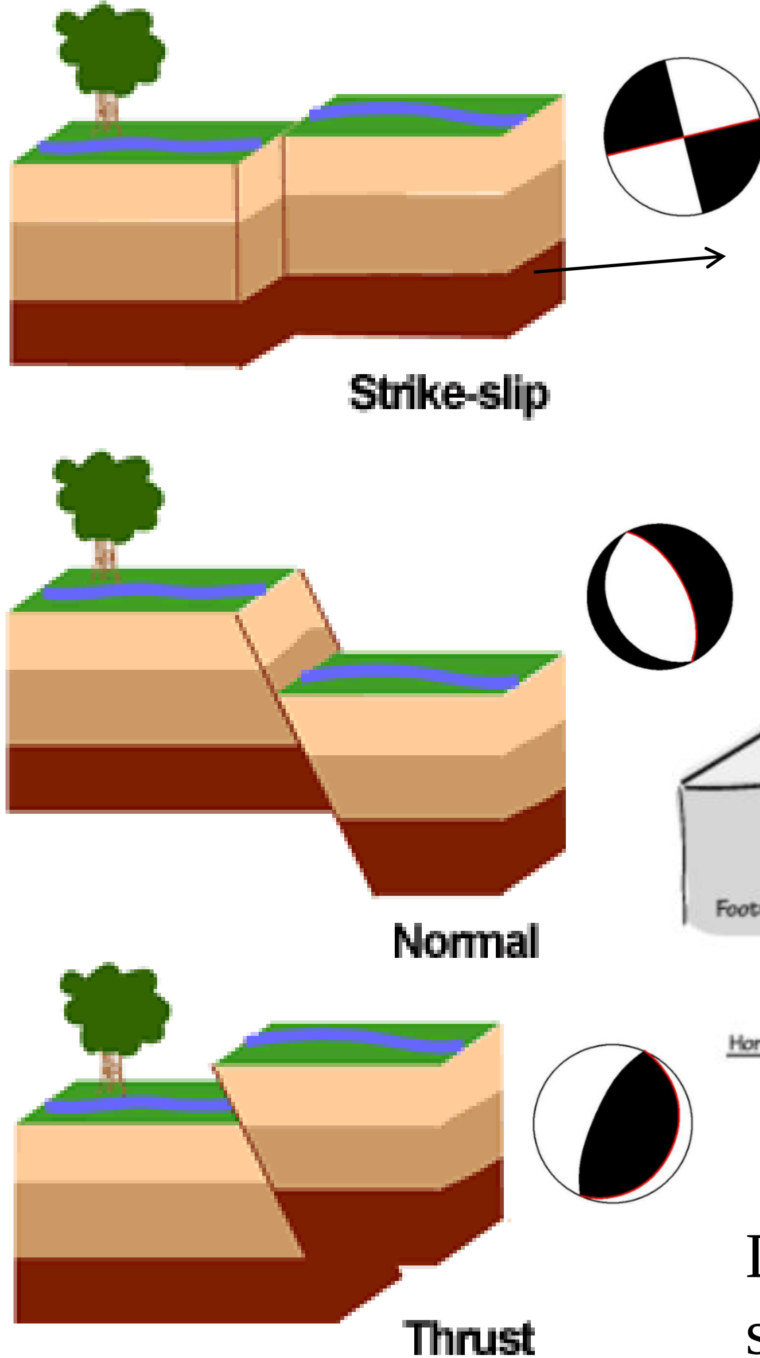

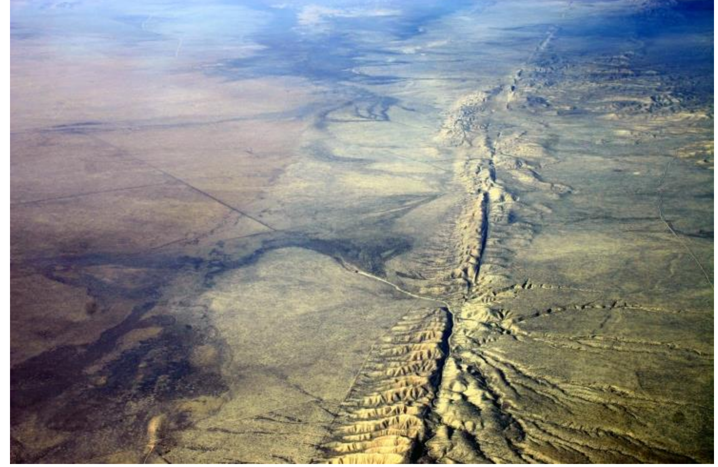

Aerial photo of the San Andreas Fault, North west of Los Angeles

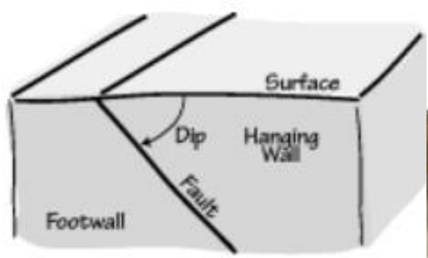

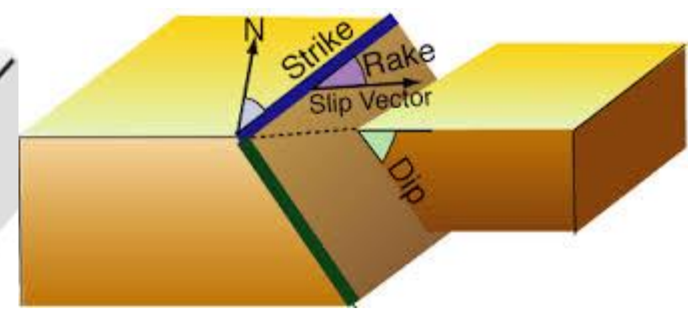

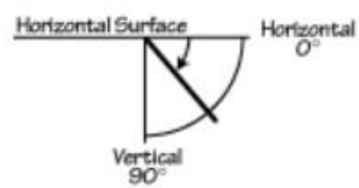

Dip is the angle that a planar geologic surface (for example, a fault) is inclined from the horizontal.

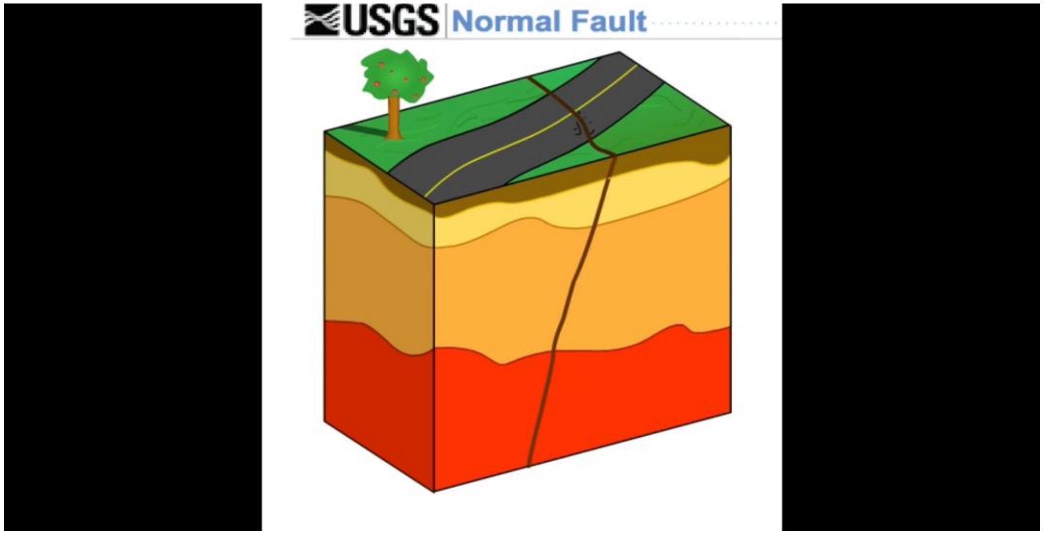
USGS Normal Fault

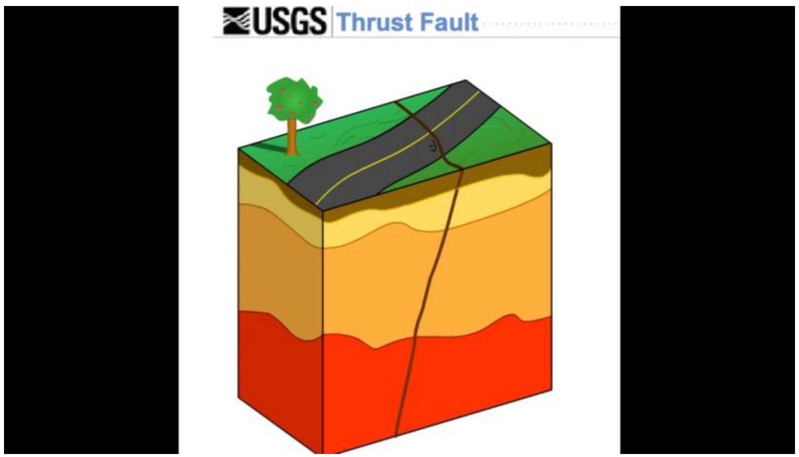
USGS Thrust Fault

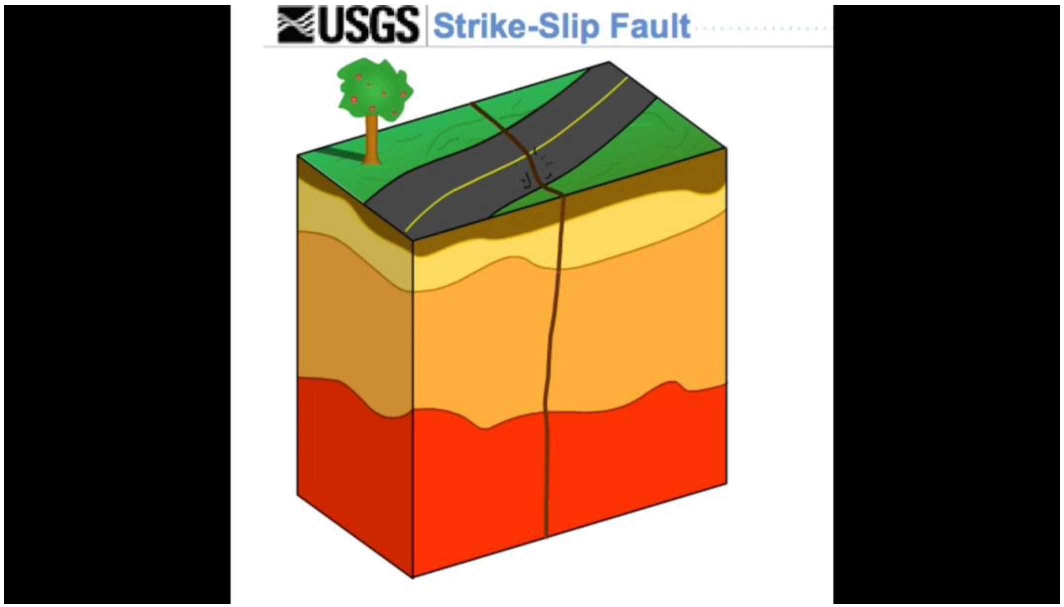
USGS Strike-Slip Fault

Observed

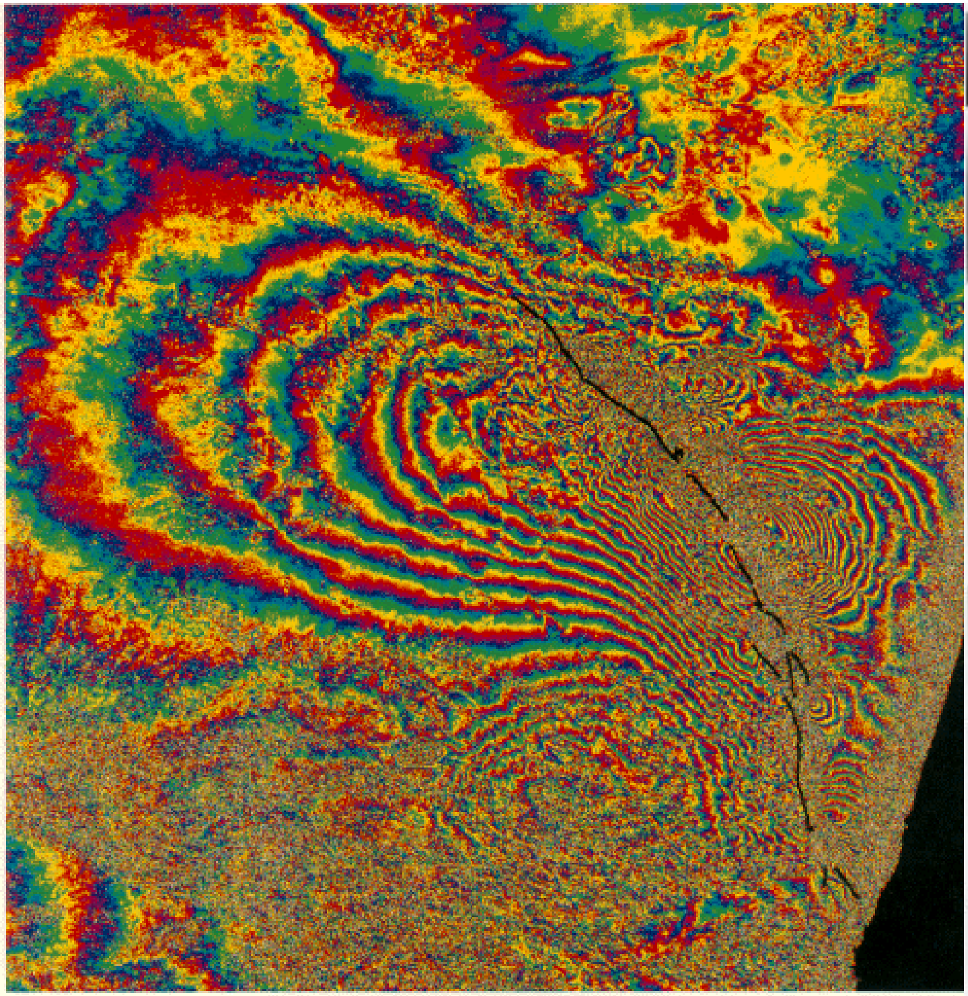

Fig. 3.3a. Compare this observed coseismic interferogram for the Landers earthquake [*Massonnet et al.*, 1993] with the synthetic interferogram in Fig. 3.3b. One cycle of color represents 28 mm of change in range. Black segments depict the fault geometry as mapped in the field. Both this image and Fig. 3.3b cover a 90-by-110-km area from April 24 to August 7, 1992.

Modeled

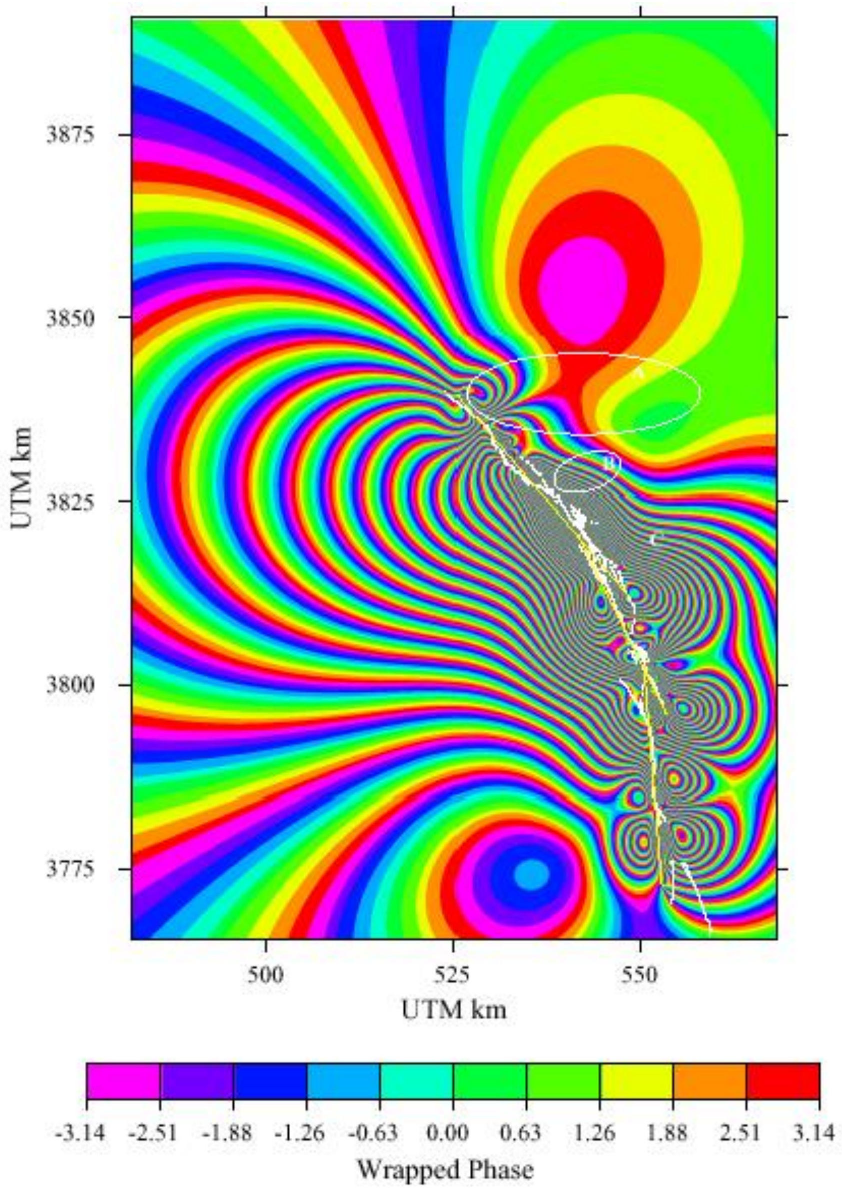

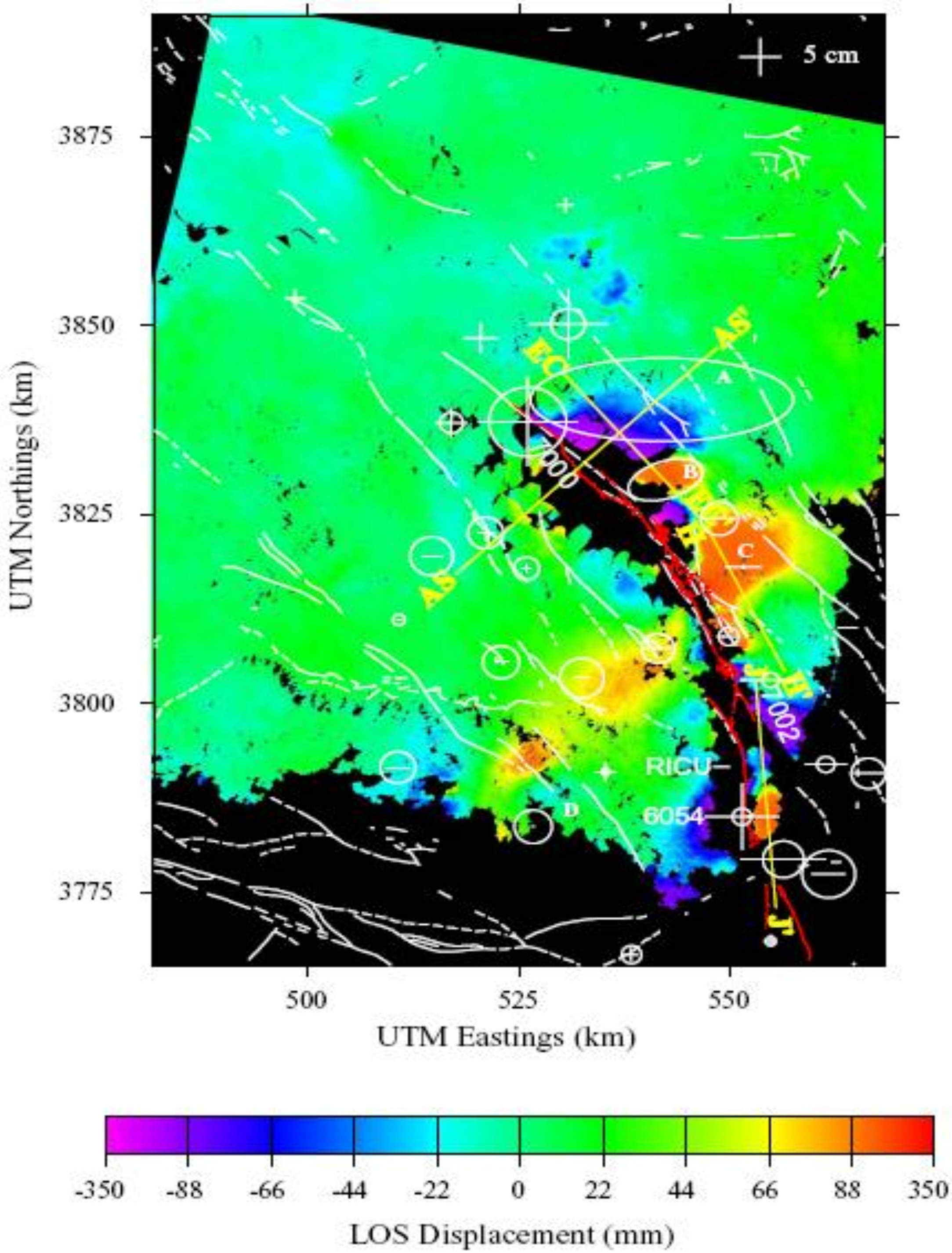

5 cm
3875
3850
3825
3800
3775
UTM Northings (km)
500
525
550
UTM Eastings (km)
A
B
C
D
EC
AS
AS'
RICU
6054
J'
-350
-88
-66
-44
-22
0
22
44
66
88
350
LOS Displacement (mm)

Observed Modeled

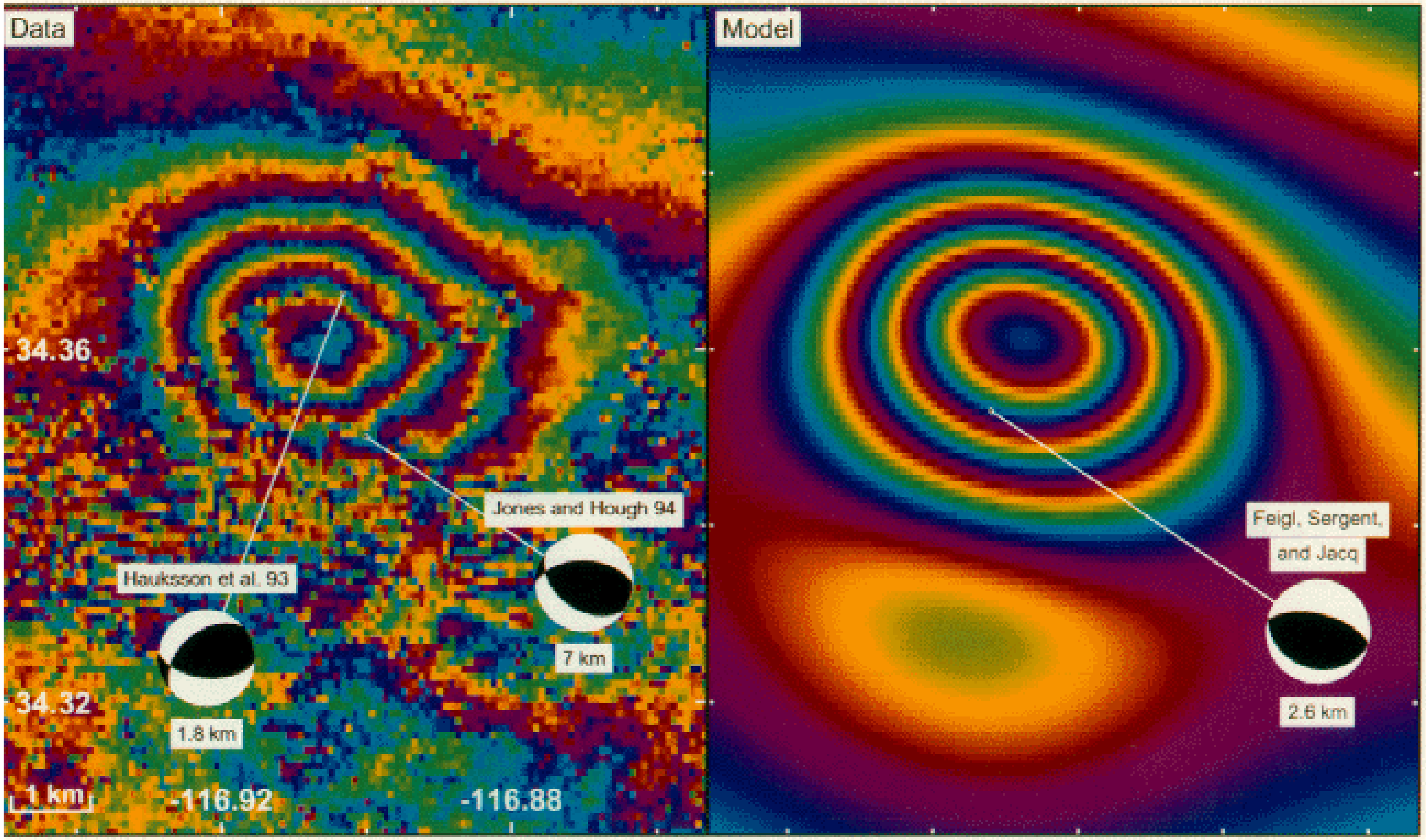

Fig. 3.4. Fringes produced by a small (M = 5.1) aftershock, as seen in an interferogram constructed from ERS-1 radar images acquired on April 24, 1992, and June 18, 1993 (left, [Massonnet et al., 1994]), and modeled using fault parameters estimated from the interferogram (right, [Feigl et al., 1994]). The interferometric signature is the sum of the main Landers shock (straight fringes in NE quadrant) and the aftershock (concentric fringes near center). One fringe represents 28 mm of range change.

Observed   Modeled

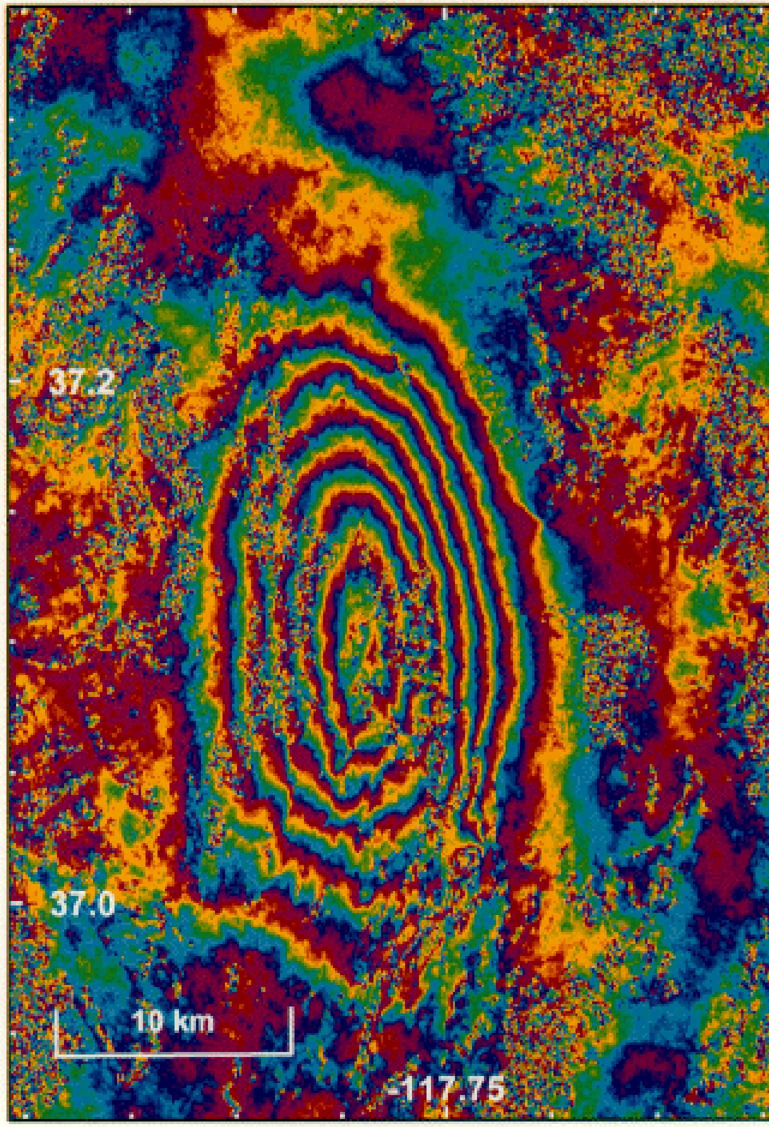

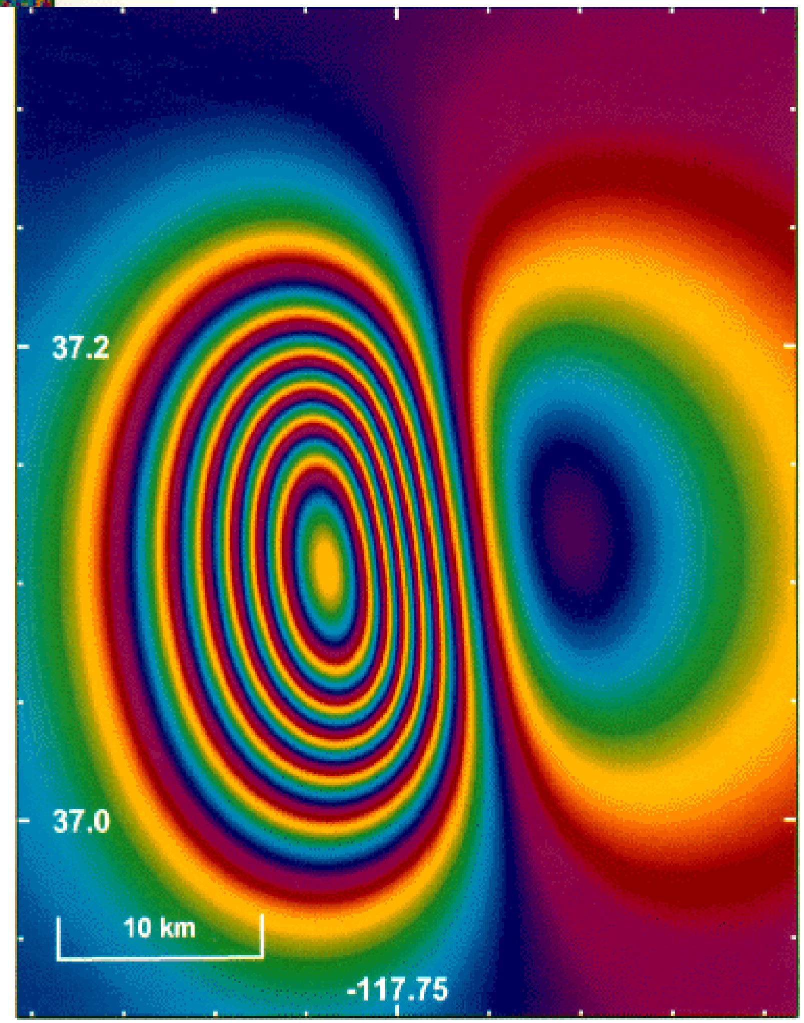

Fig. 3.8b. In this second image, a modeled interferogram shows the fringes calculated from the focal mechanism estimated from the observed fringes in Fig. 3.8a.

Fig. 3.8a. Composite interferograms may be produced by "stacking" two or more interferograms with unfavorable geometry. In this first of three images, observed fringes for the Eureka Valley earthquake are formed by stacking two interferograms; one fringe represents 14 mm of range change in all three panels because the stacking procedure doubles the earthquake signal.

Eureka Valley Earthquake fault parameters for Modeled Interferogram

	Units	Values	Remarks
East	Km	15.604	Coordinates of point on ground surface (east)
North	Km	20.179	Coordinates of point on ground surface (north)
Strike	Deg CW N	172.985	Strike of fault (azimuth taken clockwise from north)
F	0/1	1	0 for point and 1 for rectangular source
Depth	Km	12.966	Depth of the fault origin
Dip	Deg	54.341	Dip of fault (from horizontal)
λ	Pa.s	1	Elastic (Lamé) coefficient
μ	Pa.s	1	Elastic (Lamé) coefficient
U1	Mm	-54.649	Slip vector on fault (left-lateral)
U2	Mm	-469.730	Slip vector on fault (up-dip)
U3	Mm	0.0	Slip vector on fault (tensile)
Length	Km	16.172	Length of fault patch along strike
Width	Km	6.838	Width of fault patch along dip

Grid specification file used for generating model interferogram for the Eureka Valley earthquake is given below:

```
Z          11          -117.25  34.0
E          -116.28000    35.07000  -116.52000    34.18510  -28.4
G          -117.25   34.00000   0.00208333   0.002083333    480   480
                                                  118.25 W 35 N
```

Two-pass Diff. Interferogram **Modeled Interferogram**

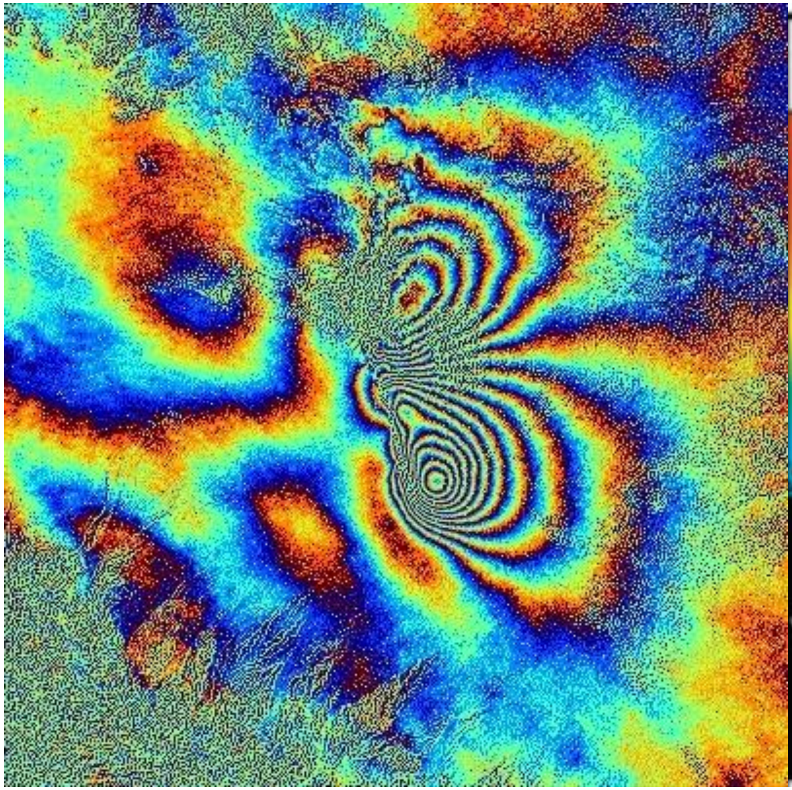

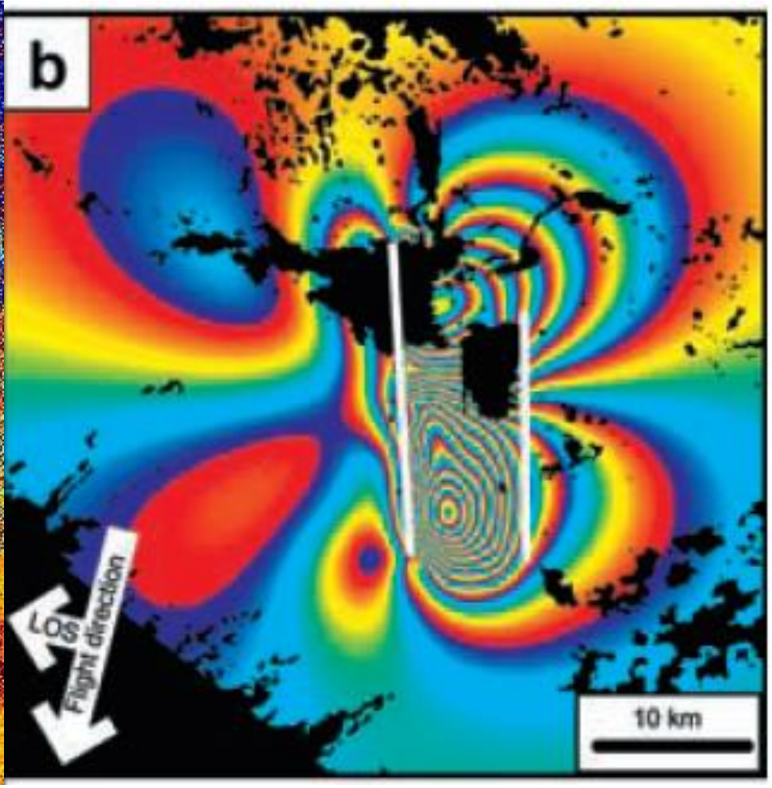

South-East Quadrant-30 cm (10 fringes) towards the radar (upliftment)

North-East Quadrant-17 cm (6 fringes) moved away from the radar (subsidence)

Strike, Dip and Rake for the main, strike-slip event (357, 88,166)

Long 12 km, wide 8 km, 2.5 m slip at the depth of 5 km. and 0.5 m in the upper 2 km.

Bhuj Earthquake M_w= 7.7, Jan. 26, 2001 – SAR Data Sets

S.NO	Satellite	Date of Acquisition	Orbit/Frame	Baseline (B‖)	Baseline (B_|_)	Elapsed Days
1	ERS-2	16-05-1996	5599/3141(Des)	0	0	0 (reference)
2	ERS-1	15-05-1996	25272/3141(Des)	73	150	1
3	ERS-2	10-06-1999	21631/3141(Des)	-99	-350	1120
4	ERS-1	10-04-1996	24711/3141(Des)	7	119	36
5	ERS-2	11-04-1996	5098/3141(Des)	-38	21	35
6	ERS-2	01-03-2001	30649/3141(Des)	1857	5006	----
7	ERS-2	14-02-2002	35659/3141(Des.)	-90	11	2100
1	ERS-2	11-04-1996	5098/3141 (Des)	0	0	0
2	ERS-1	10-04-1996	24711/3141(Des)	45	95	1
3	ERS-2	10-06-1999	21631/3141(Des)	-61	-287	1155

SAR Intensity Image

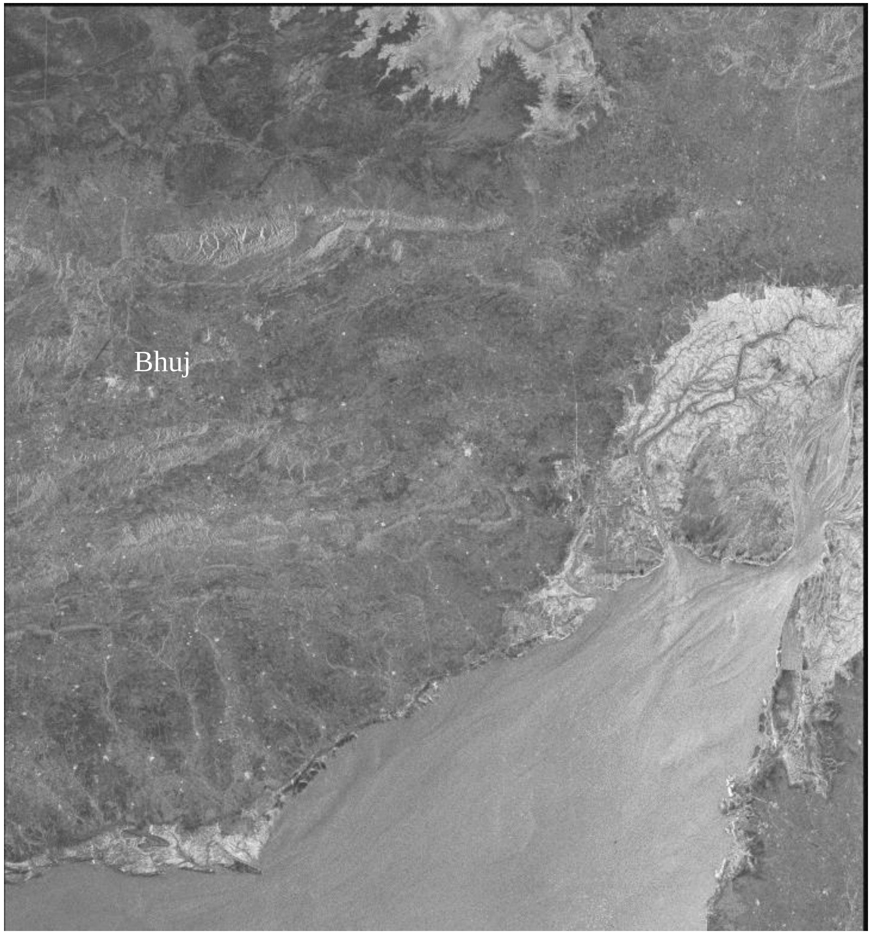

May 16, 1996

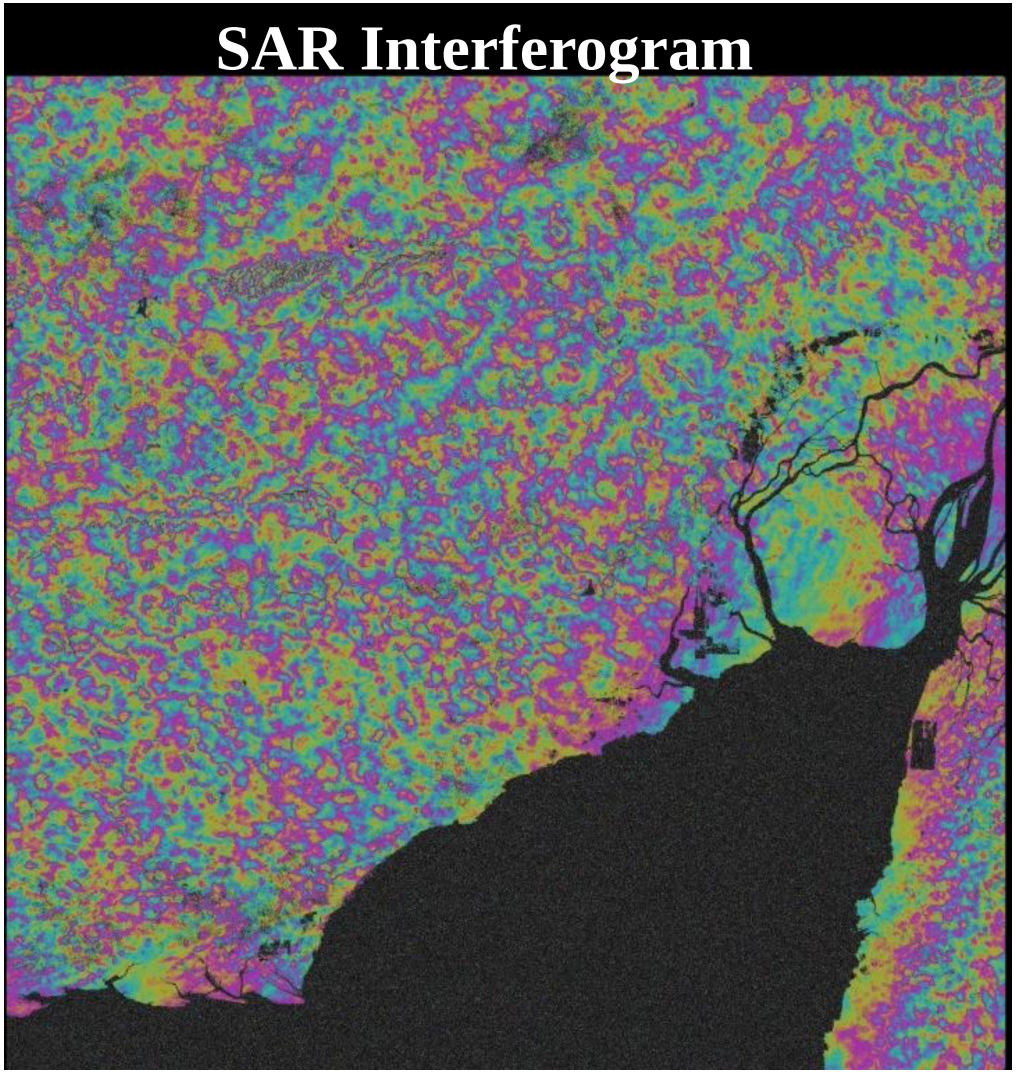

May 16 & 15, 1996 B=160 m

Coherence

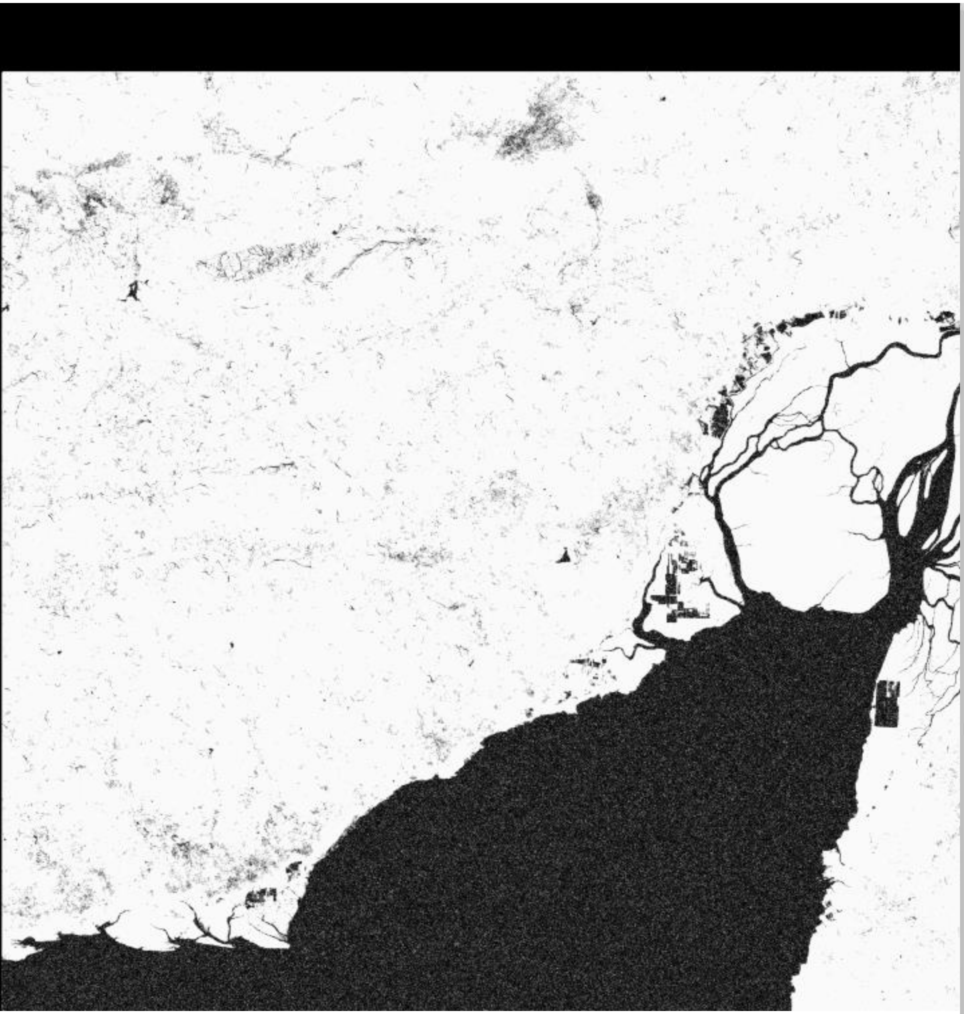

Elevation Map

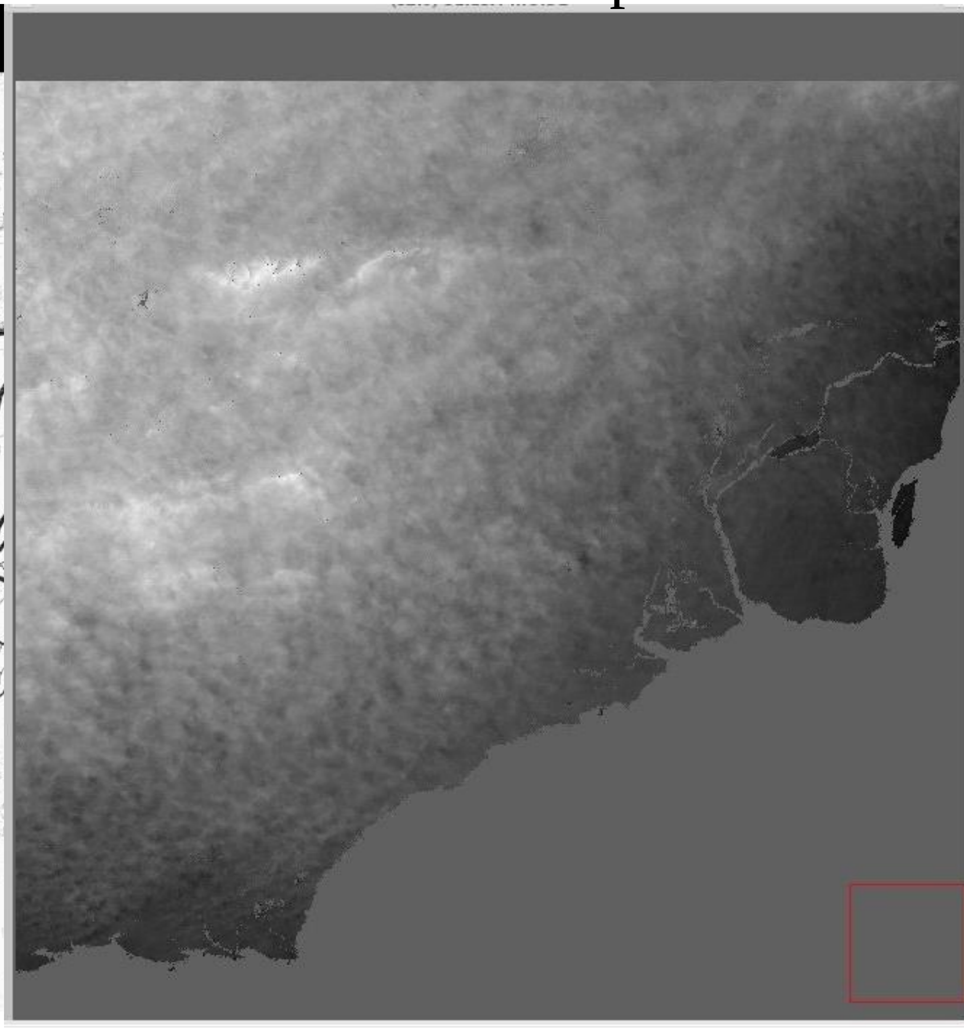

May 16 & 15, 1996

Interferogram

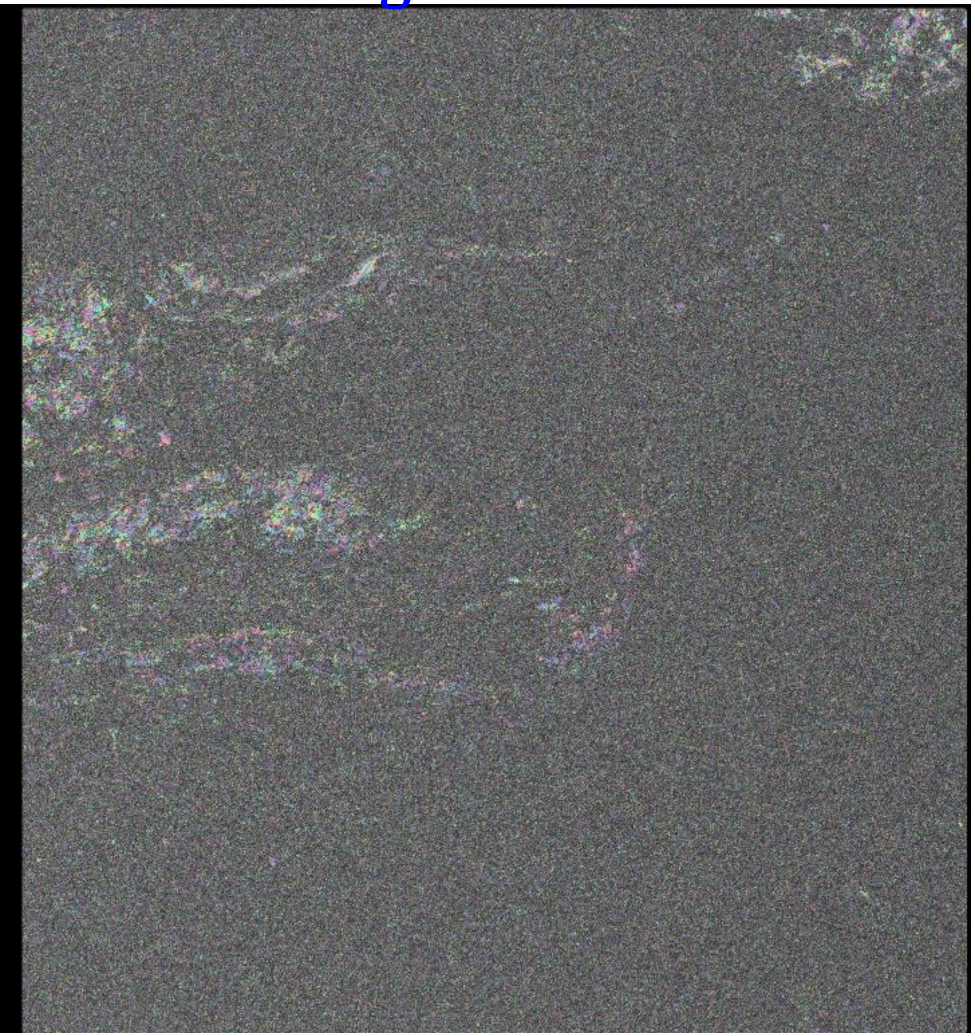

Coherence

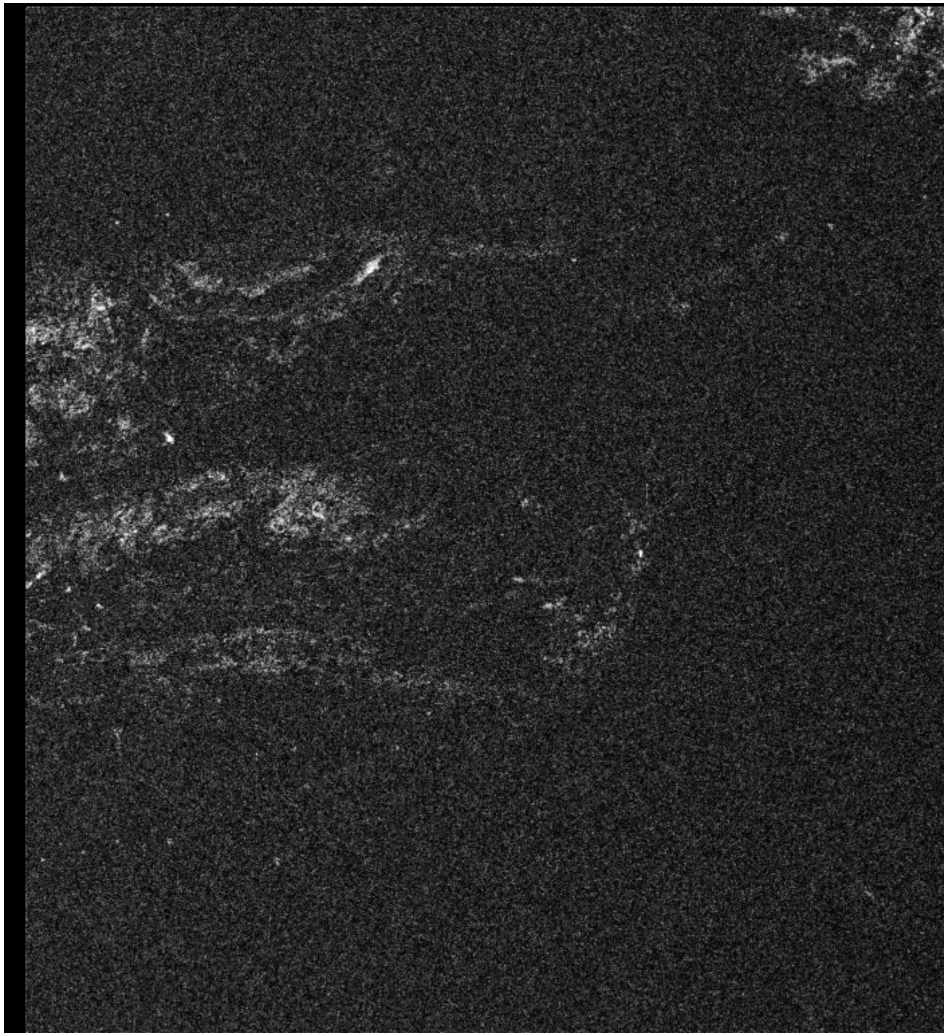

Apr. 11, 1996 & June 10. 1999 (1155 days gap)

Displacement Map over Bhuj between Apr. 11, 1996 – June 10, 1999, 2-Pass DInSAR

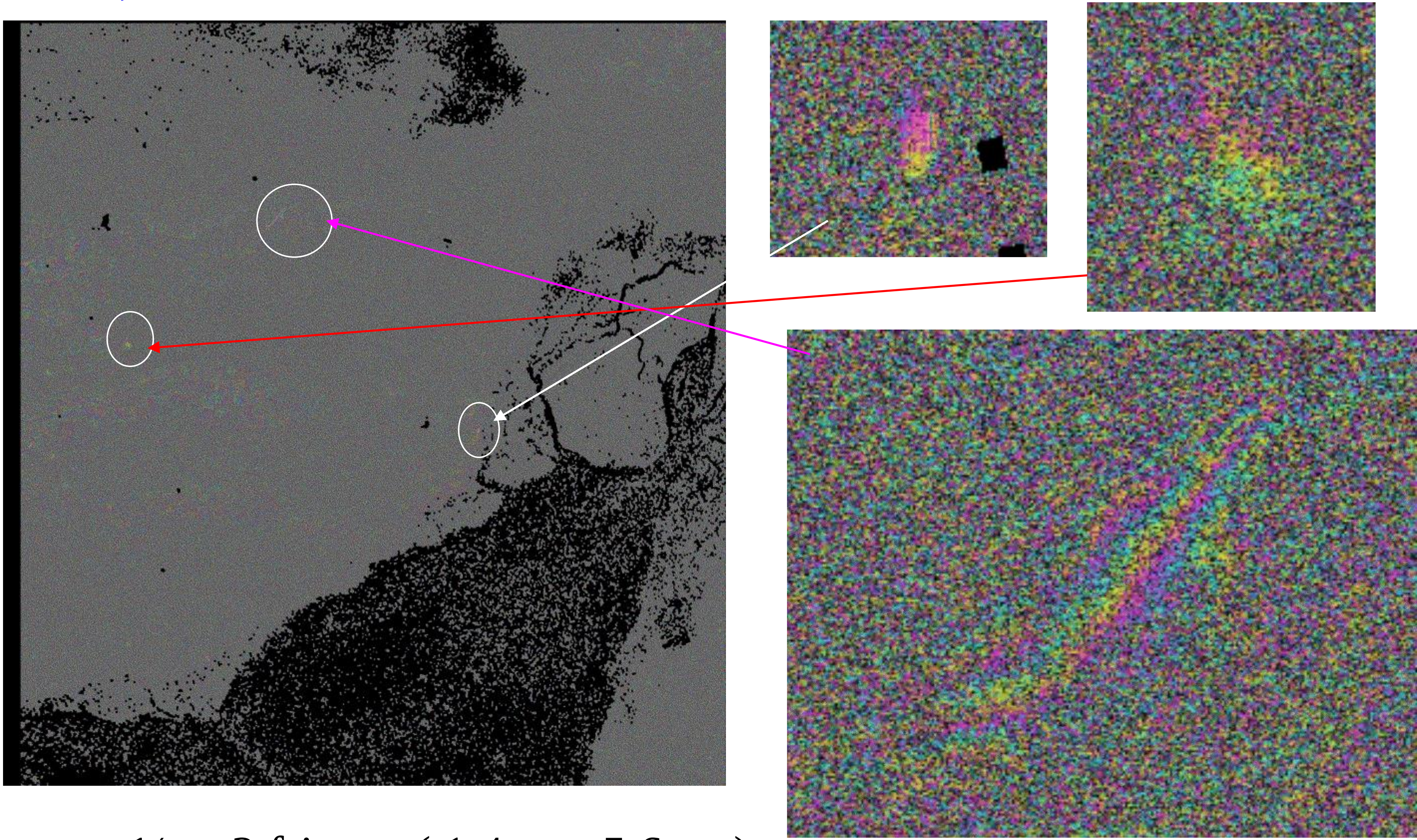

½ to 2 fringes (1.4 to – 5.6 cm)

Bhuj ERS-1/2 InSAR Data sets, **Bhuj Earthquake M_w= 7.7, Jan. 26, 2001** (Burgmann, Uni. of Berkeley)

A.	Master 1996-04-11 (Desc.)	B(normal baseline)	Day
	Slave 2002-02-14	9 m	5y, 10m, 3d
B.	Master 2000-05-06 (Desc.)		
	Slave 2002-09-28	310 m	2y, 4m, 22d
C.	Master 1998-08-27 (Asc.)		
	Slave 2002-09-01	30 m	4y, 0m, 5d

Bhuj Earthquake (Jan. 26, 2001) Displacement Map Results, Burgmann et al., Geophysical Research Letters (2006)

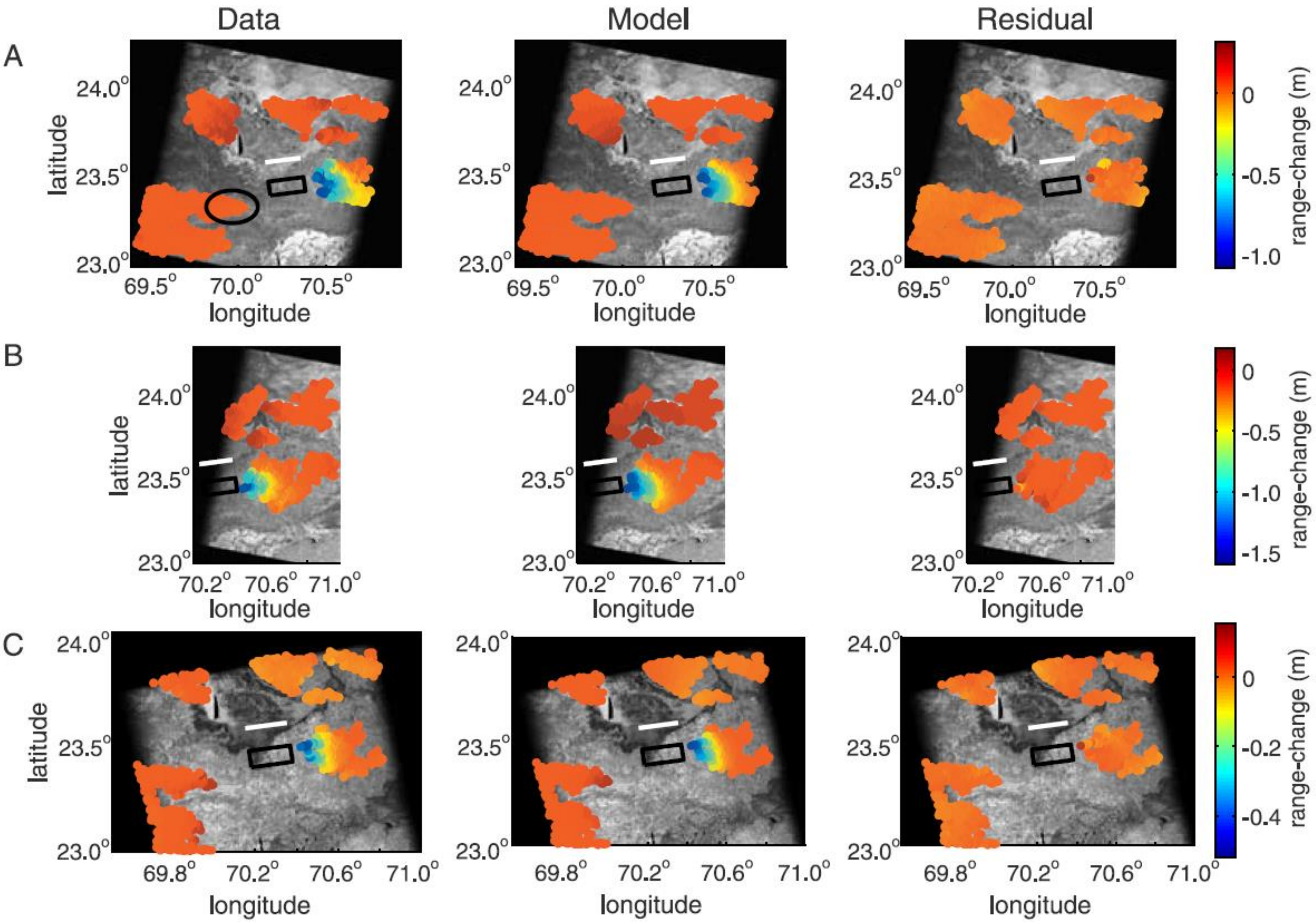

DInSAR **Modeled** **Difference**

Latur Earthquake (6.3 Richter), Sept. 30, 1993 – SAR Data Sets

S.NO	Satellite	Date of acquisition	Orbit/Frame	Baseline (B‖)	Baseline (B_⊥_)	Elapsed Days
1	ERS-1	23-02-1993	8409/3249(Des)	0	0	0 (reference)
2	ERS-1	26-10-1993	11916/3249(Des)	22	18	245
3	ERS-1	28-07-1992	5403/3249(Des)	31	43	-210
4	ERS-1	23-07-1992	5403/3249(Des)	0	0	0 (reference)
5	ERS-1	26-10-1993	11916/3249(Des)	-9	-25	455

Lature Earthqauke Displacement Map (Satyabala GPR, 2006)

Master : 23-02-1993 and Slave : 30-11-1993, Bperp = 49 m, interval = 280

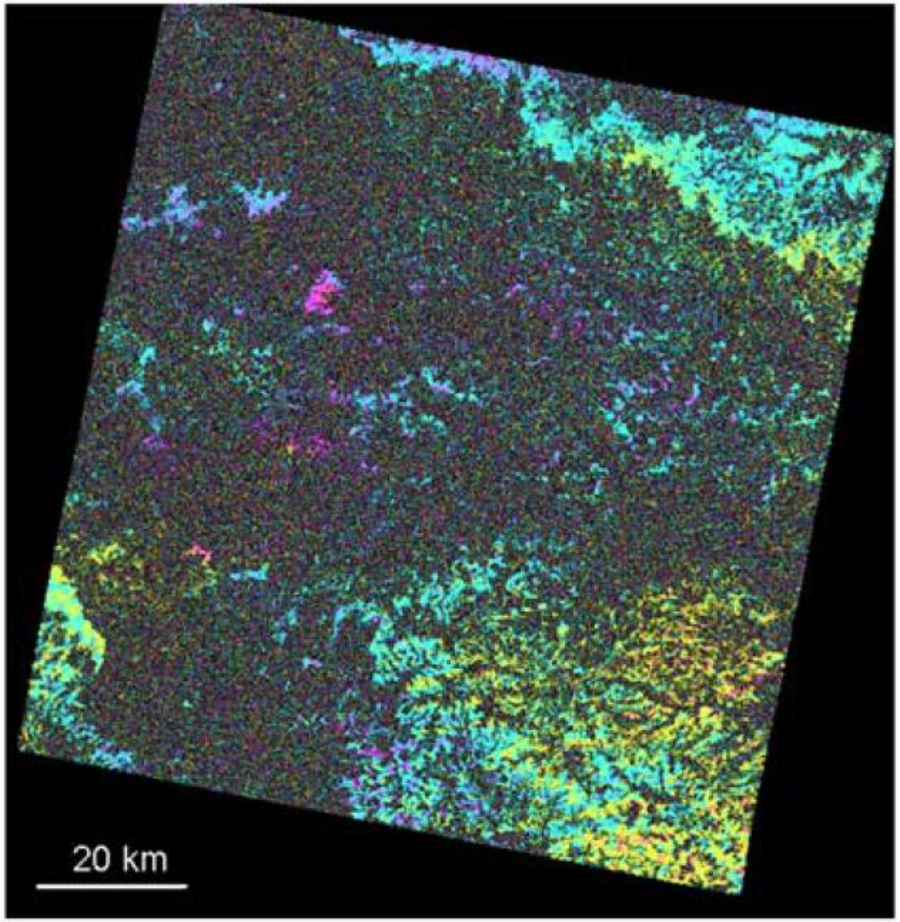

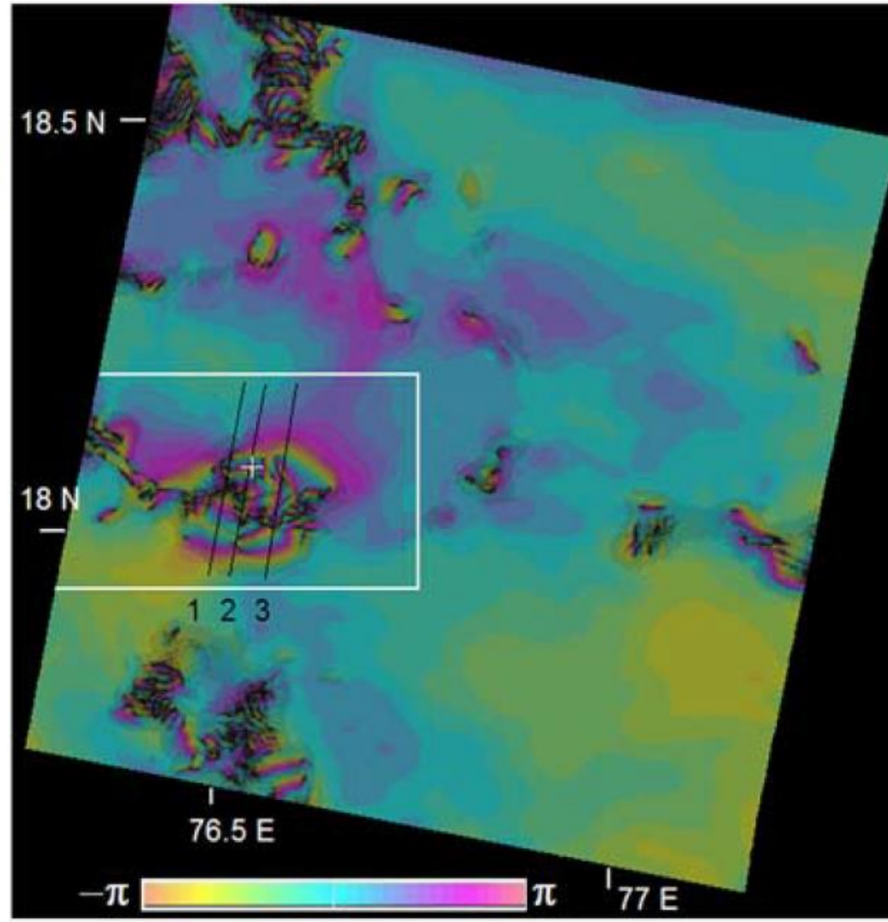

DInSAR interferogram

DInSAR interferogram after filtering

Chamoli Earthquake (6.8 Richter), Mar. 29, 1999

S.NO	Satellite	Date of acquisition	Orbit/Frame	Baseline (B‖)	Baseline (B_|_)	Elapsed Days
1	ERS-1	16-05-1996	25286/2997(Des)	0	0	0 (master)
2	ERS-2	17-05-1996	5613/2997 (Des)	-63	-121	1
3	ERS-1	11-04-1996	24785/2997(Des)	-43	-42	35
4	ERS-1	12-04-1996	5112/2997(Des)	-90	-62	34
1	ERS-1	25-03-1996	24549/603 (Asc)	0	0	0 (master)
2	ERS-2	26-03-1996	4876/603 (Asc)	45	95	1
3	ERS-2	07-09-1999	22913/603 (Asc)	-274	-715	1261
4	ERS-1	28-09-1998			10	344 (with 1999)

Chamoli SAR Image

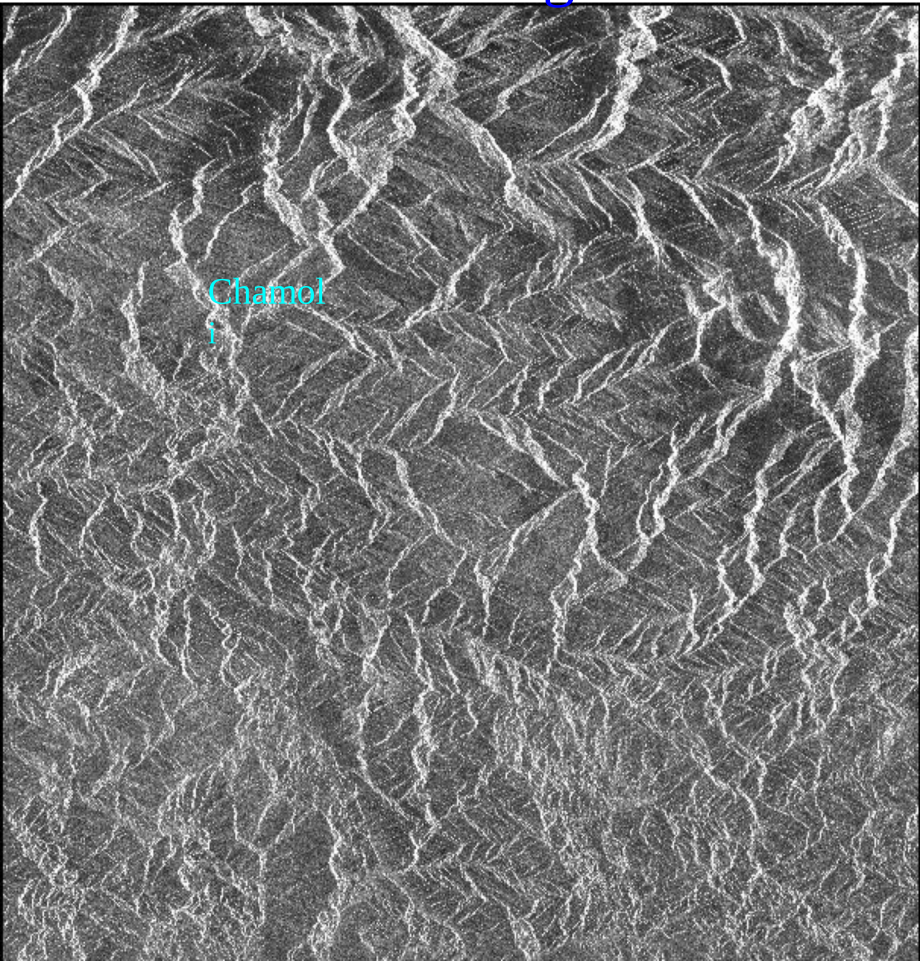

May 16, 1996

Interferogram

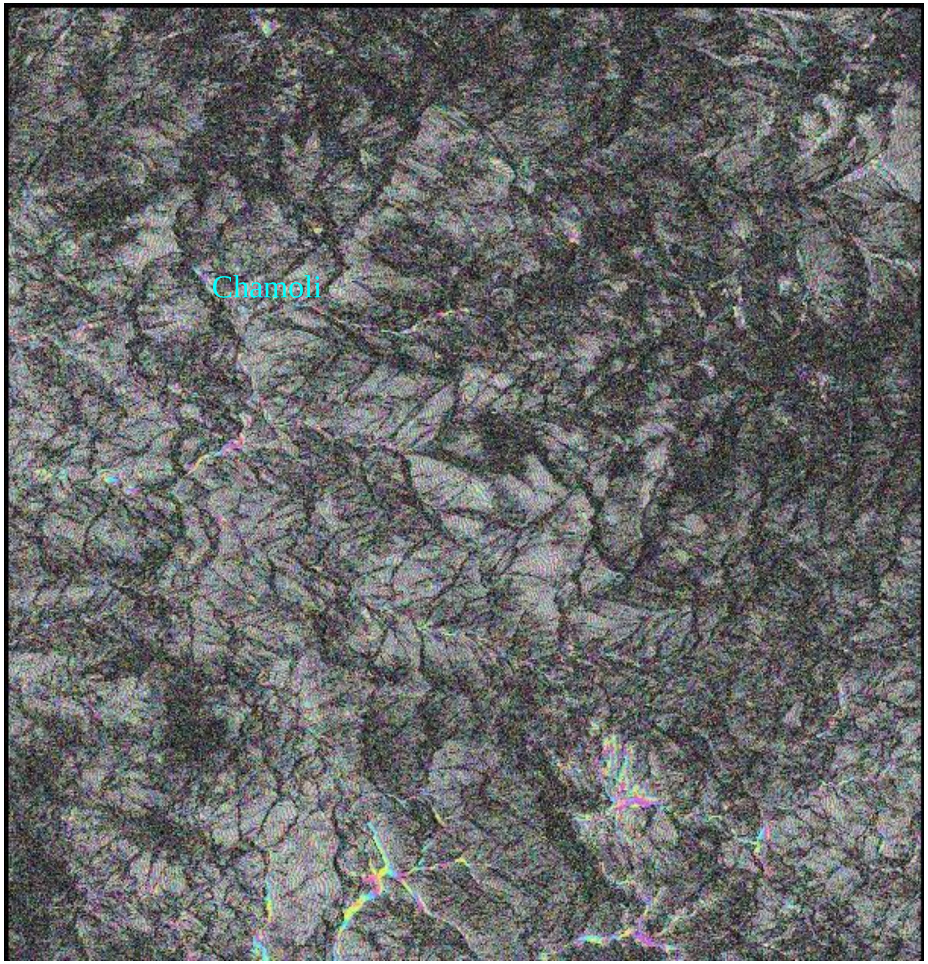

May 16 & 17, 1996

Chamoli Earthquake M_w=6.2, March 28, 1999

InSAR Pair : Sept. 21, 1998 and Sept. 7, 1999 (344 days gap)

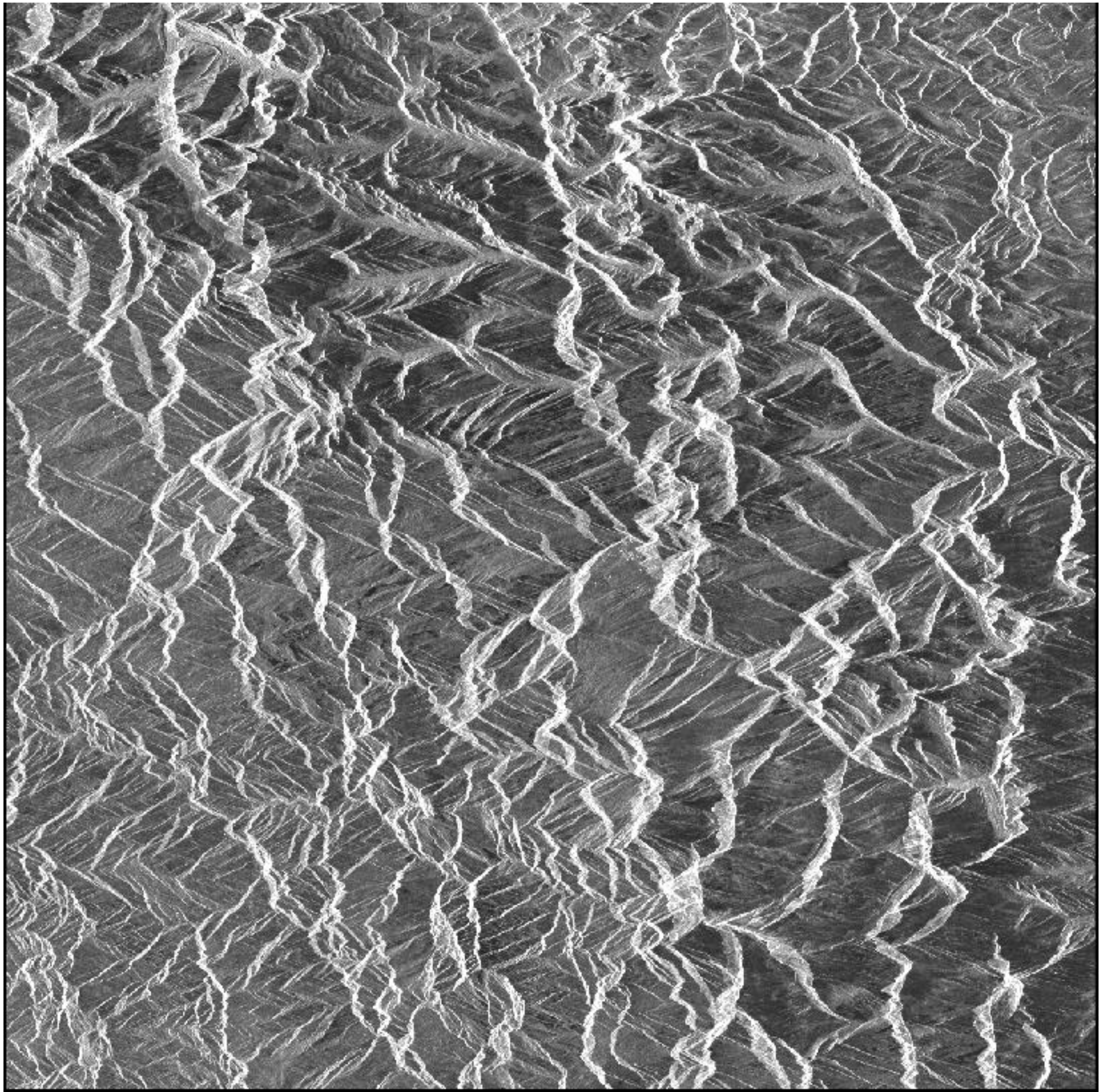

Chamoli Earthquake Area

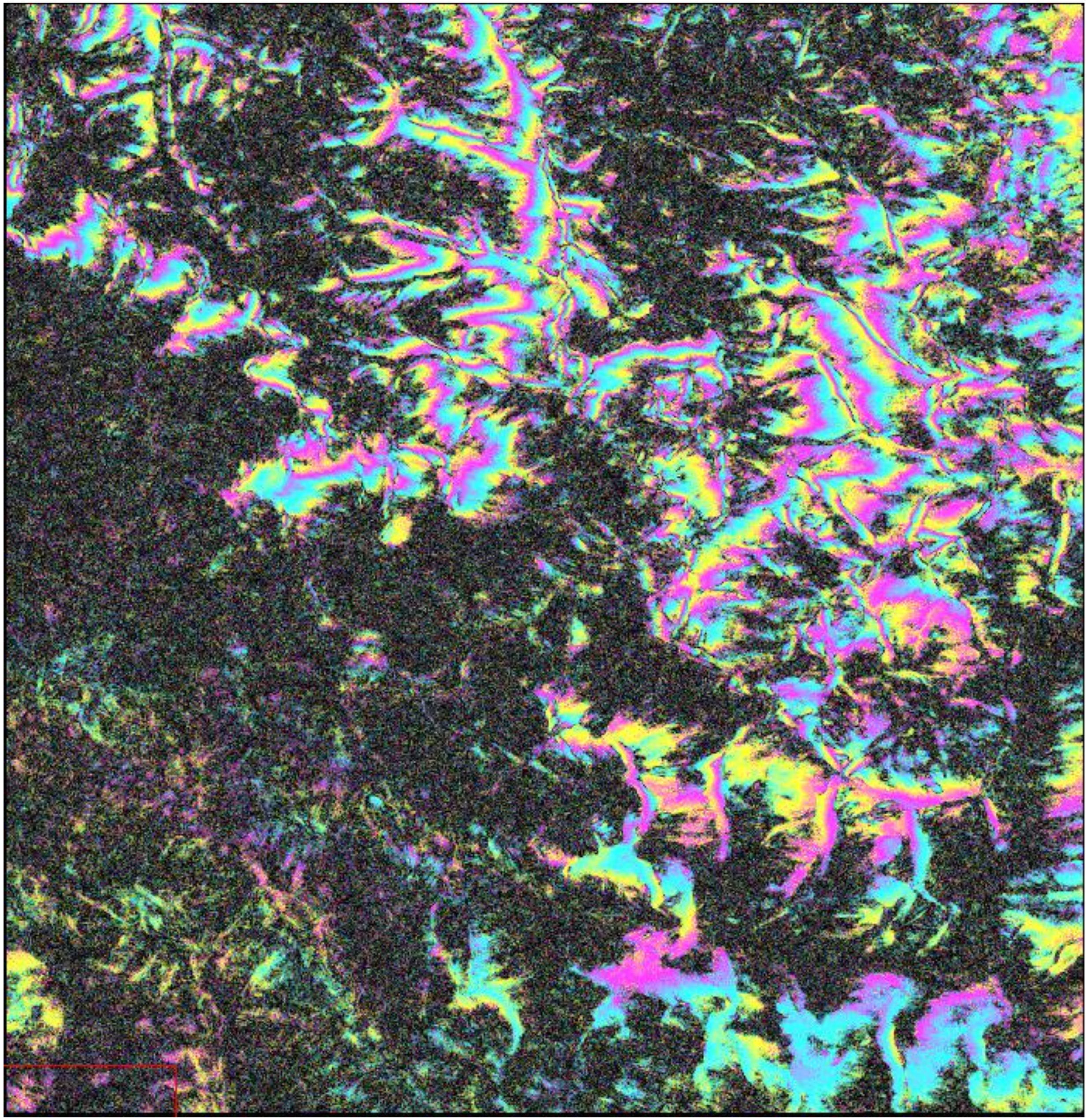

Interferogram with Baseline of 10m (contains topography and displacement

Chamoli Earthquake Area

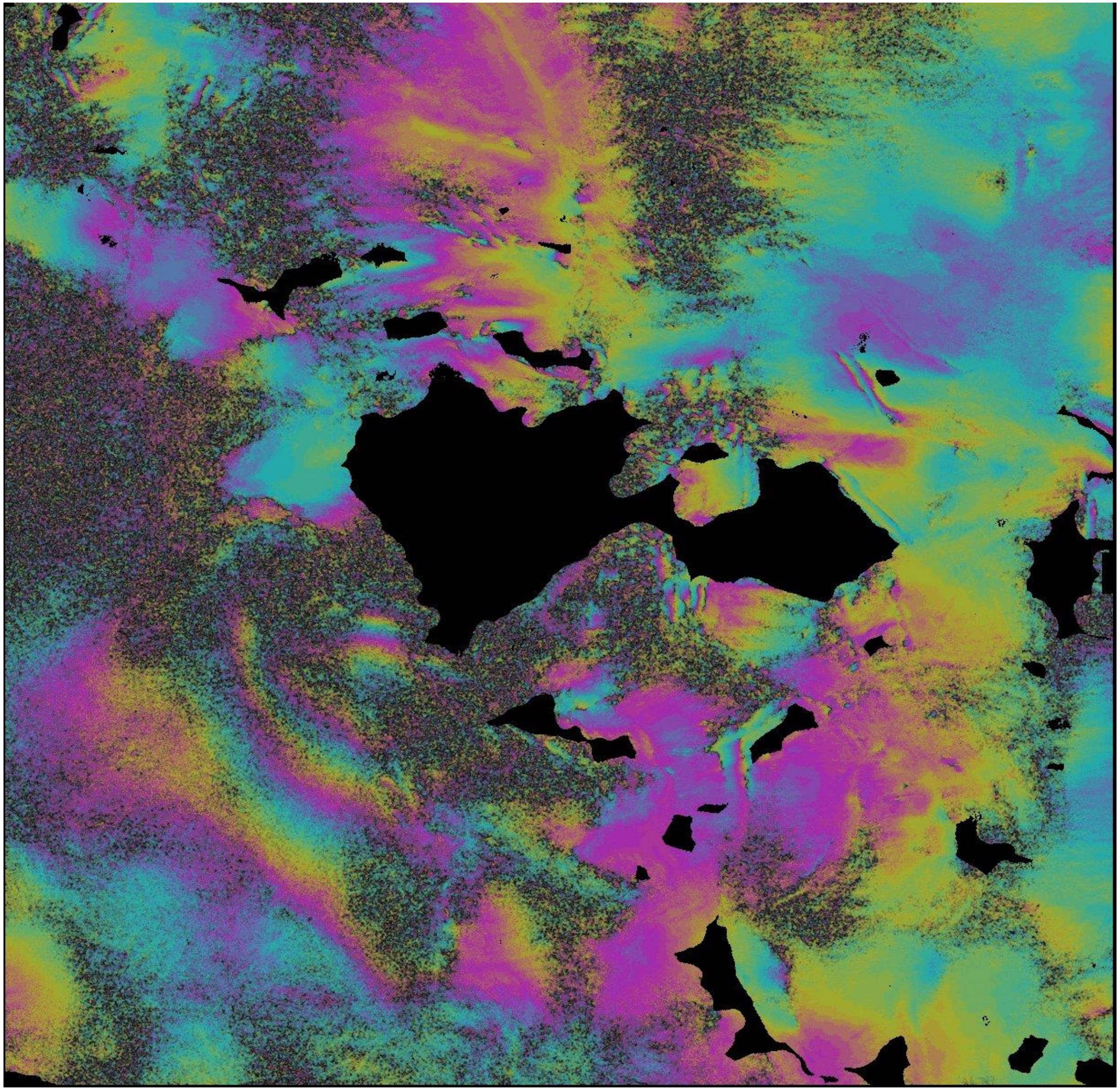

Differential Interferogram

(after removing topography fringes)

Chamoli Earthquake Area

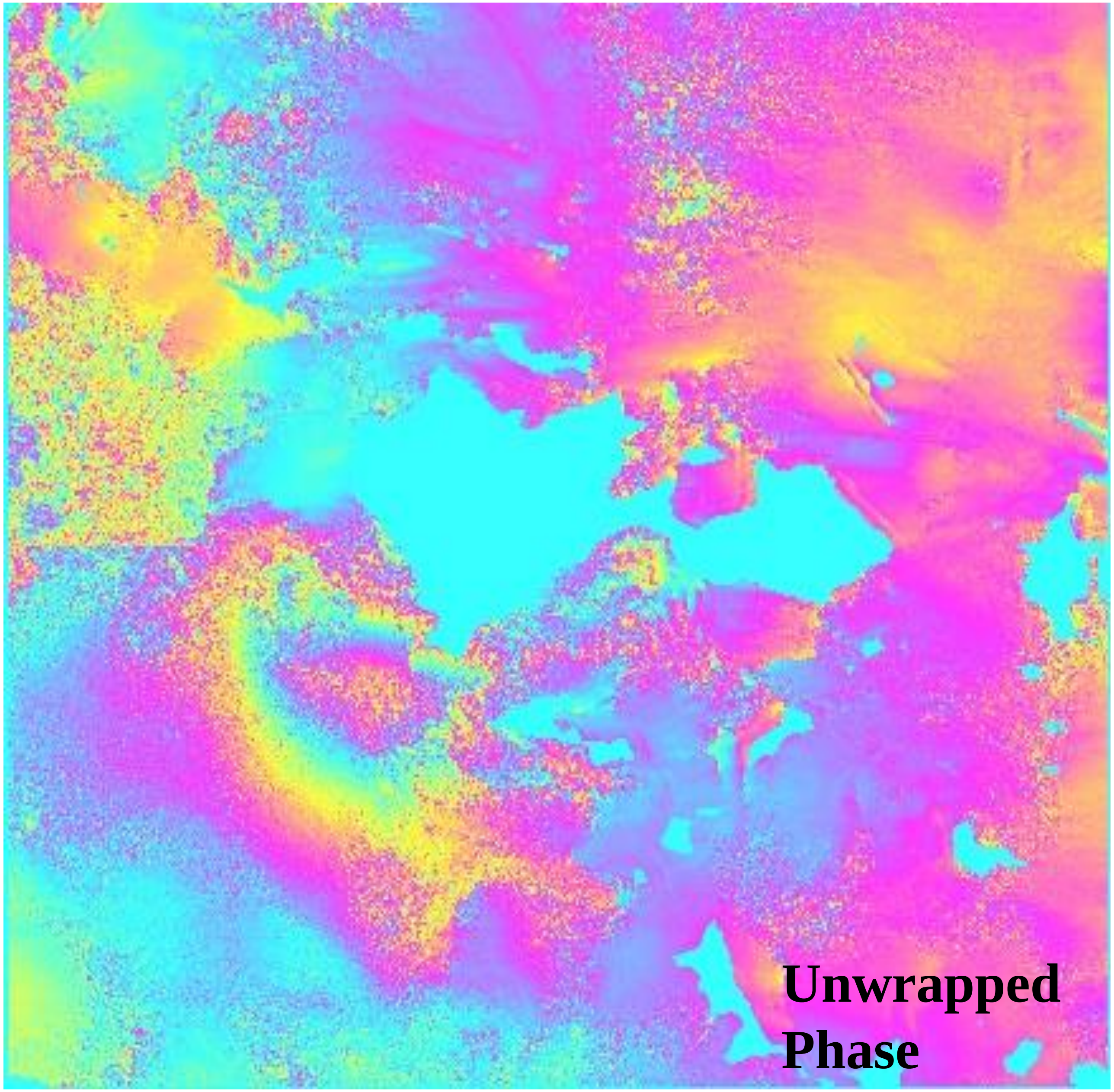

Chamoli Earthquake Area

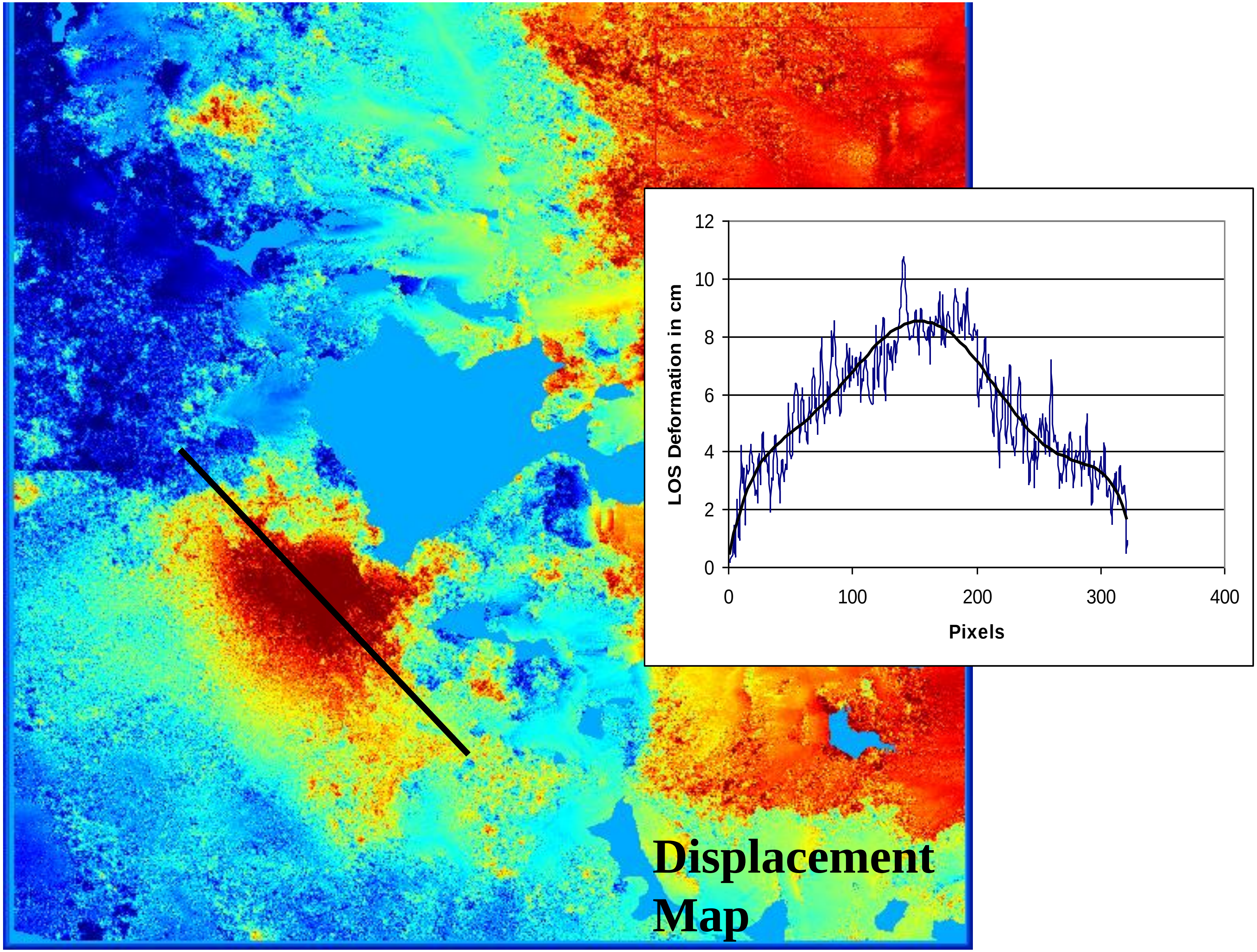

Land Subsidence

Conventional InSAR: deformation

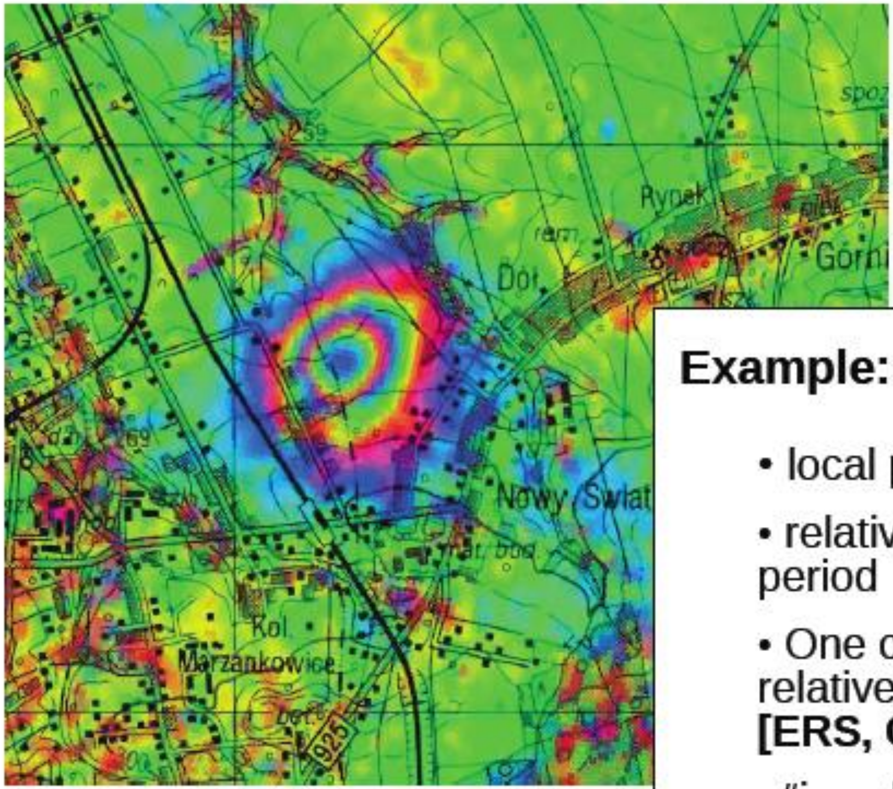

Example: Mining induced subsidence

- local phenomenon
- relatively large displacement in short time period
- One color cycle (fringe) corresponds with relative deformation of 2.8cm in satellite LOS **[ERS, C-band]**
- "in coherent interferograms relative deformation can be determined by counting fringes"

Deformation Map using ERS-1, Spet-Nov, 1992

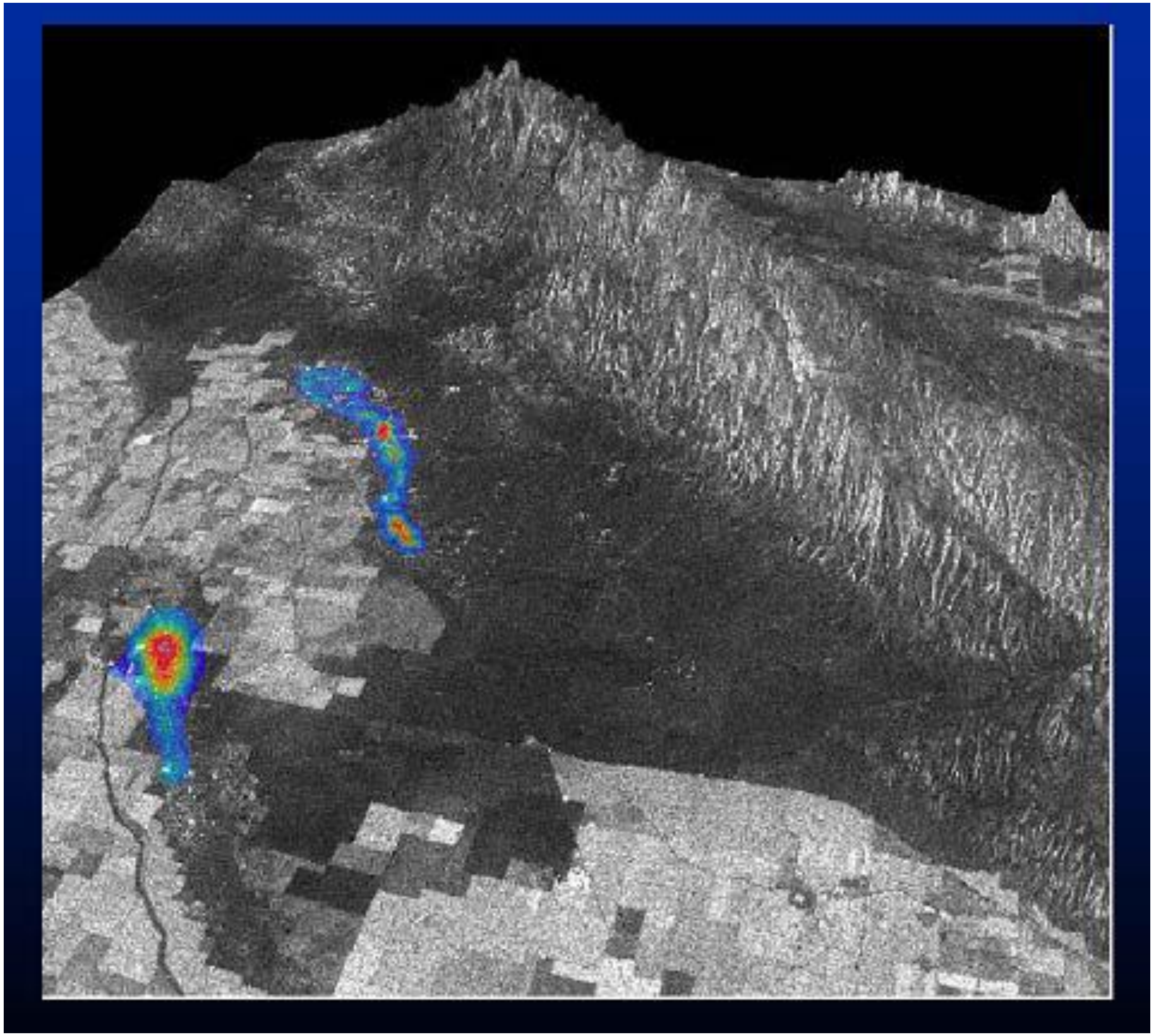

Land Subsidence due to Oil Extraction in California

Deformation map of Belridge, California has been draped with a RADARSAT image and illustrates the occurrence of land subsidence due to oil extraction. The colours in the map depict a major land shift, which in this case caused due to oil extraction. Absence of colour (grey) would indicate no deformation at all.

4-Pass Differential InSAR - Belridge and Lost Hills Oil Fields, California

DEM: ERS 1/2 Tandem + Differential InSAR: ERS-1 92/09/17 and 92/11/26

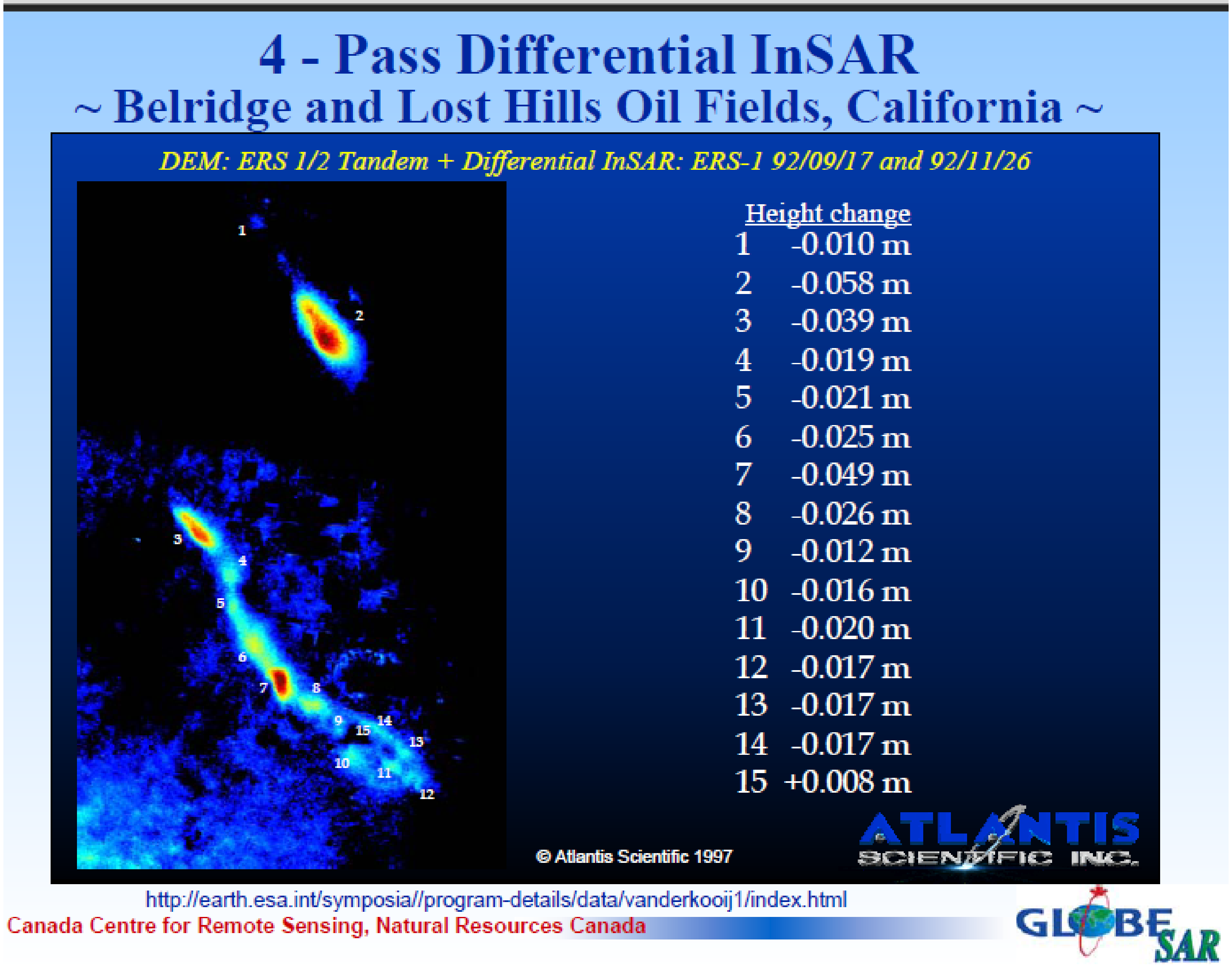

70 days

Subsidence due to Oil Extraction

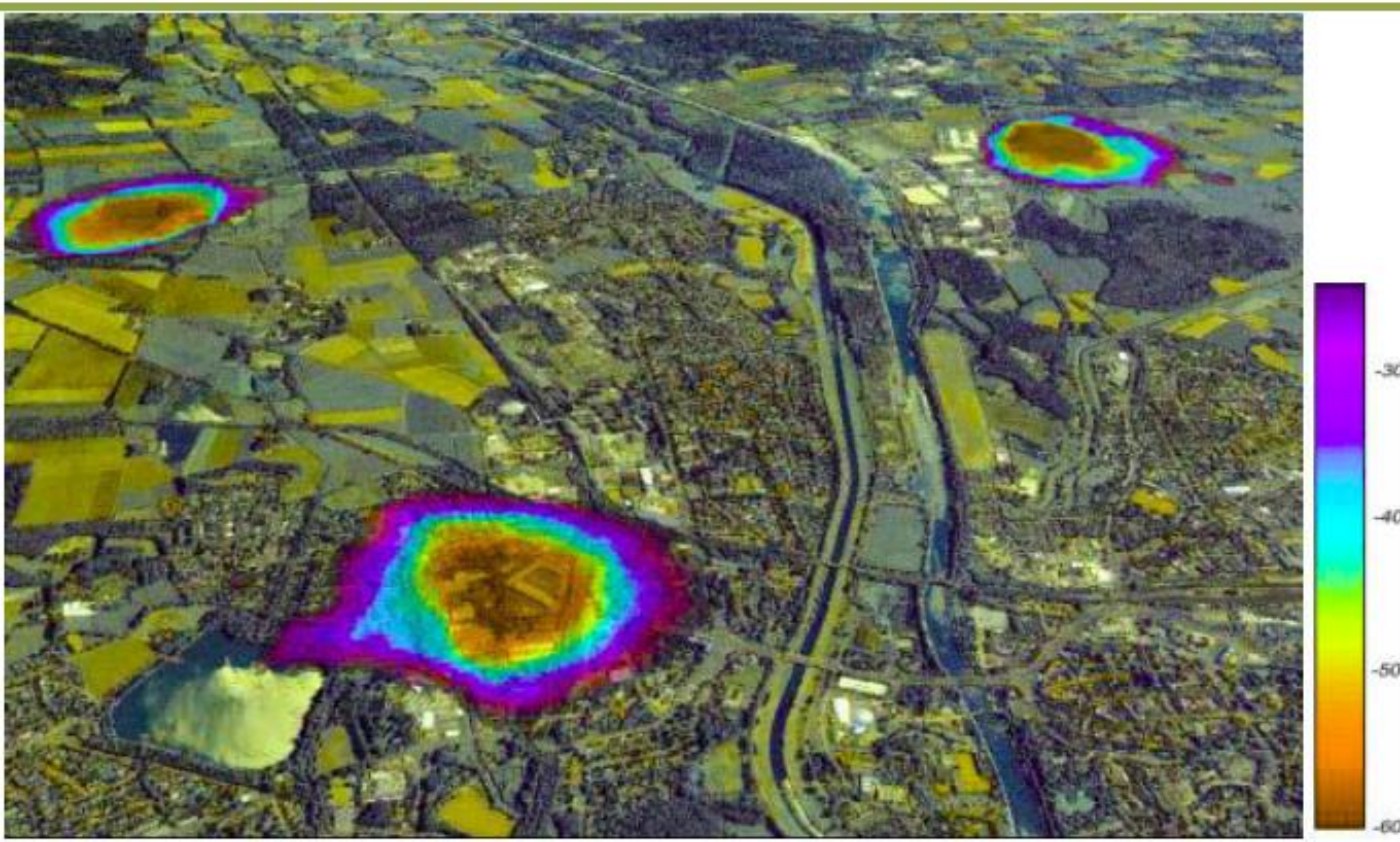

Figure 3-43 Deformation map showing rapid mining subsidence over a pipeline network in in Dorsten, Germany. The interferometric colour cycles are overlain on IKONOS imagery. The color bar shows subsidence levels in mm over 35 days. (Riedmann and Haynes, 2005)

Germany, Dorsten

Two ERS SAR Data, 35 days interval, Land subsidence 6 cm

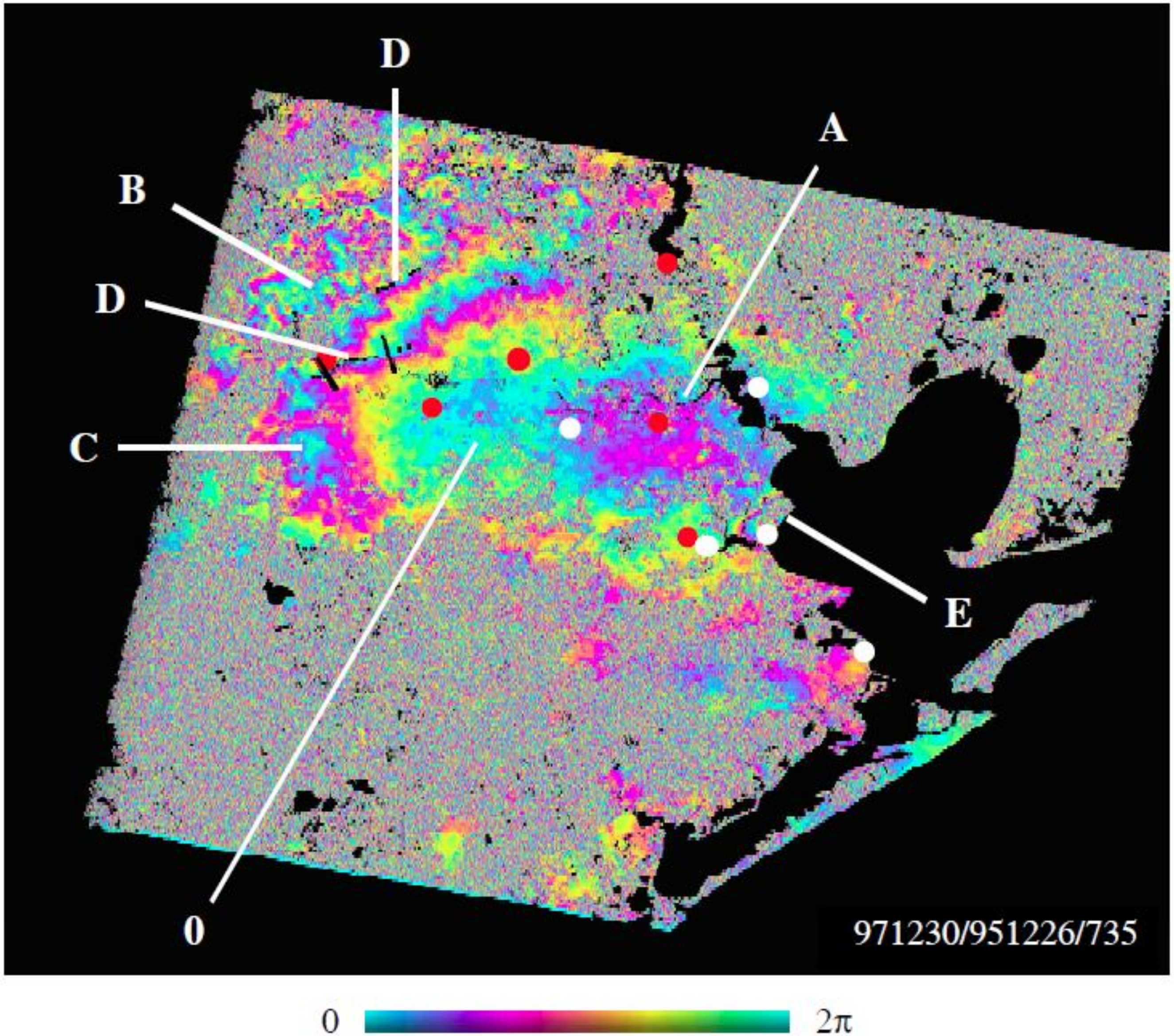

ERS SAR Interferogram with 2 year interval
About 5 cm subsidence in 2 years period

Land subsidence in and around Houston city due to drinking water extraction

Prati et al., Politechnic of Milano

Landslides detection and monitoring

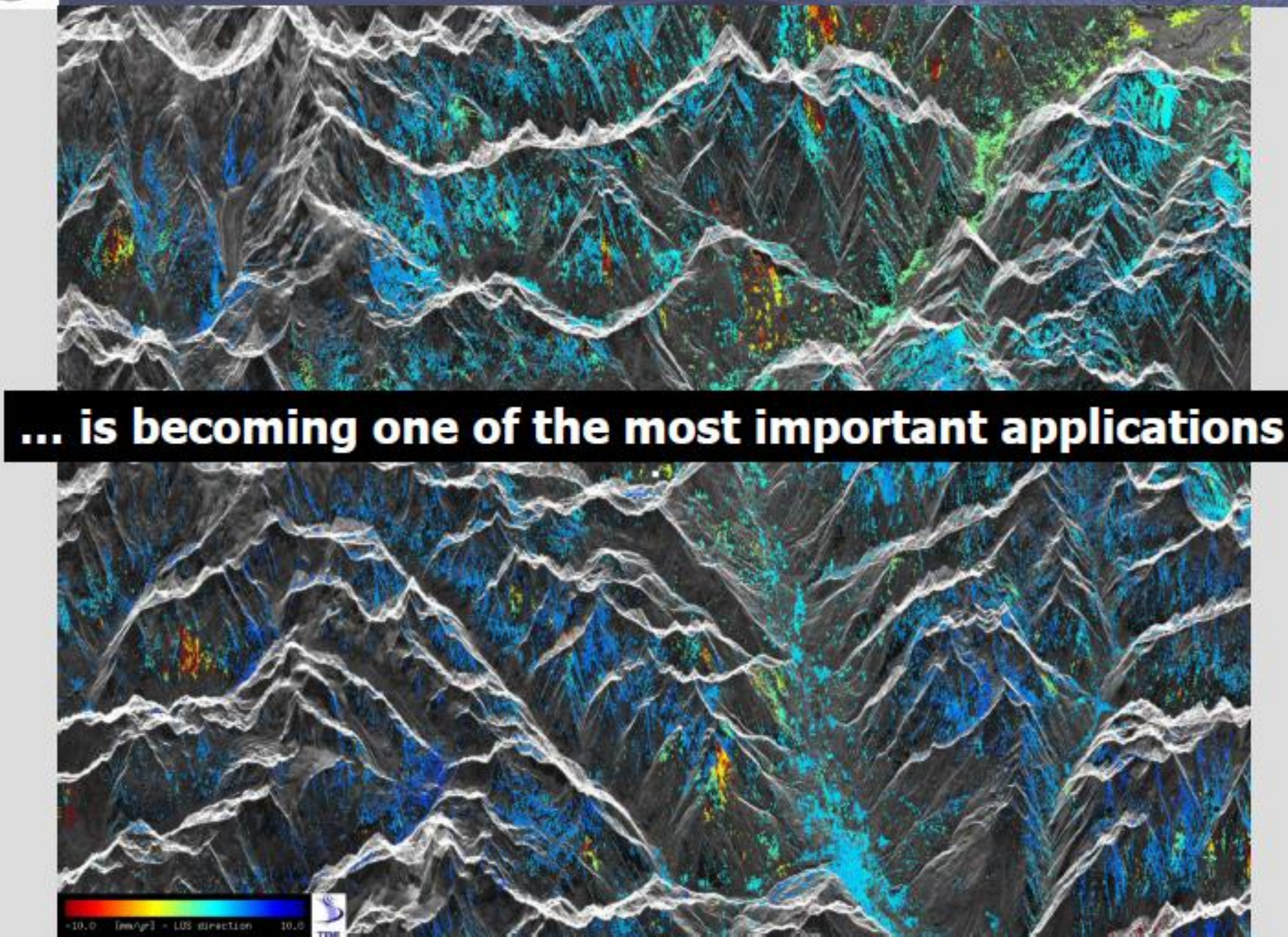

Landslide Monitoring

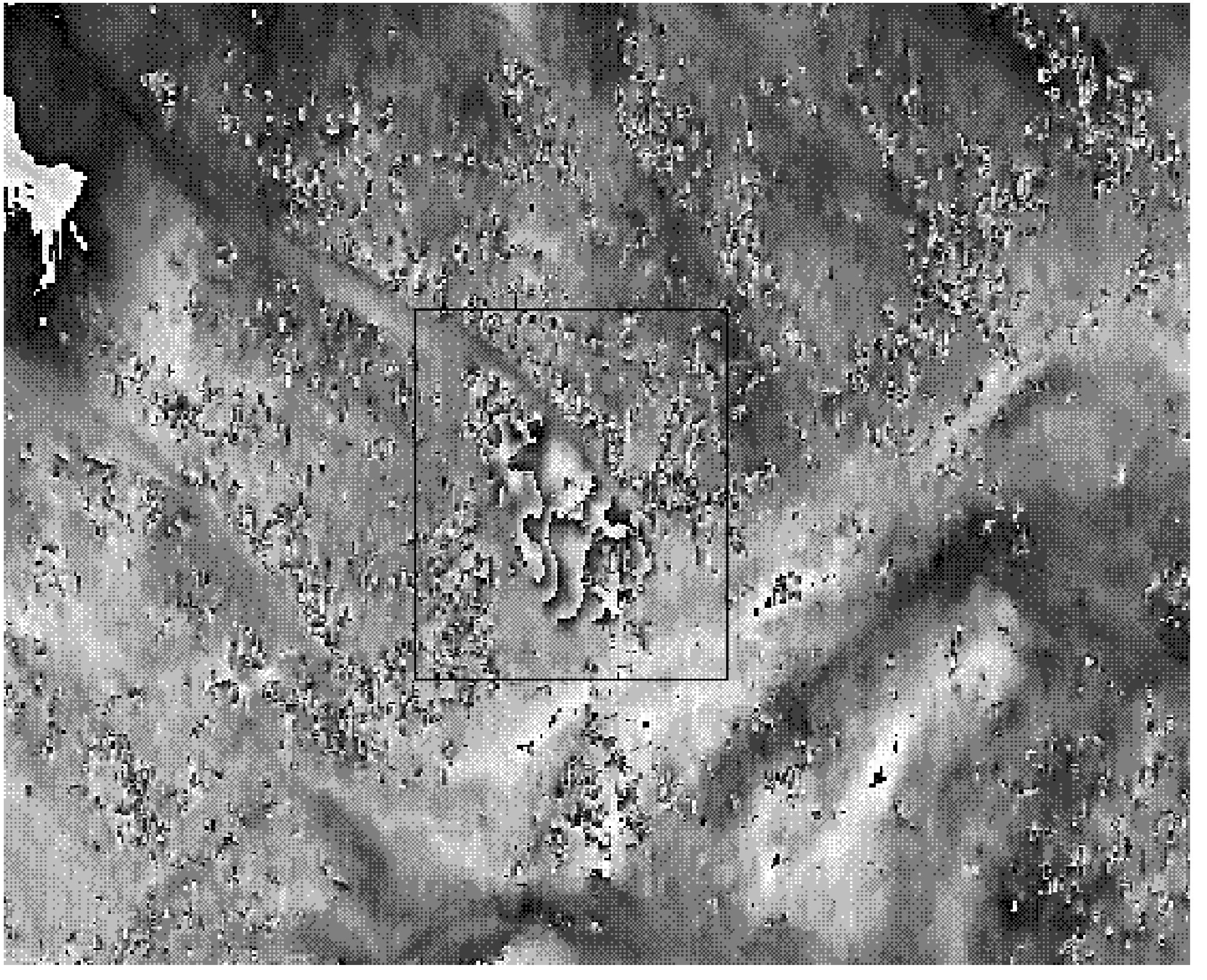

Two ERS-1 SAR Images with 9 days gap give Landslide motion. Landslide is moving 1cm/day Baseline = 10 m

Landslide Monitoring in France with DInSAR

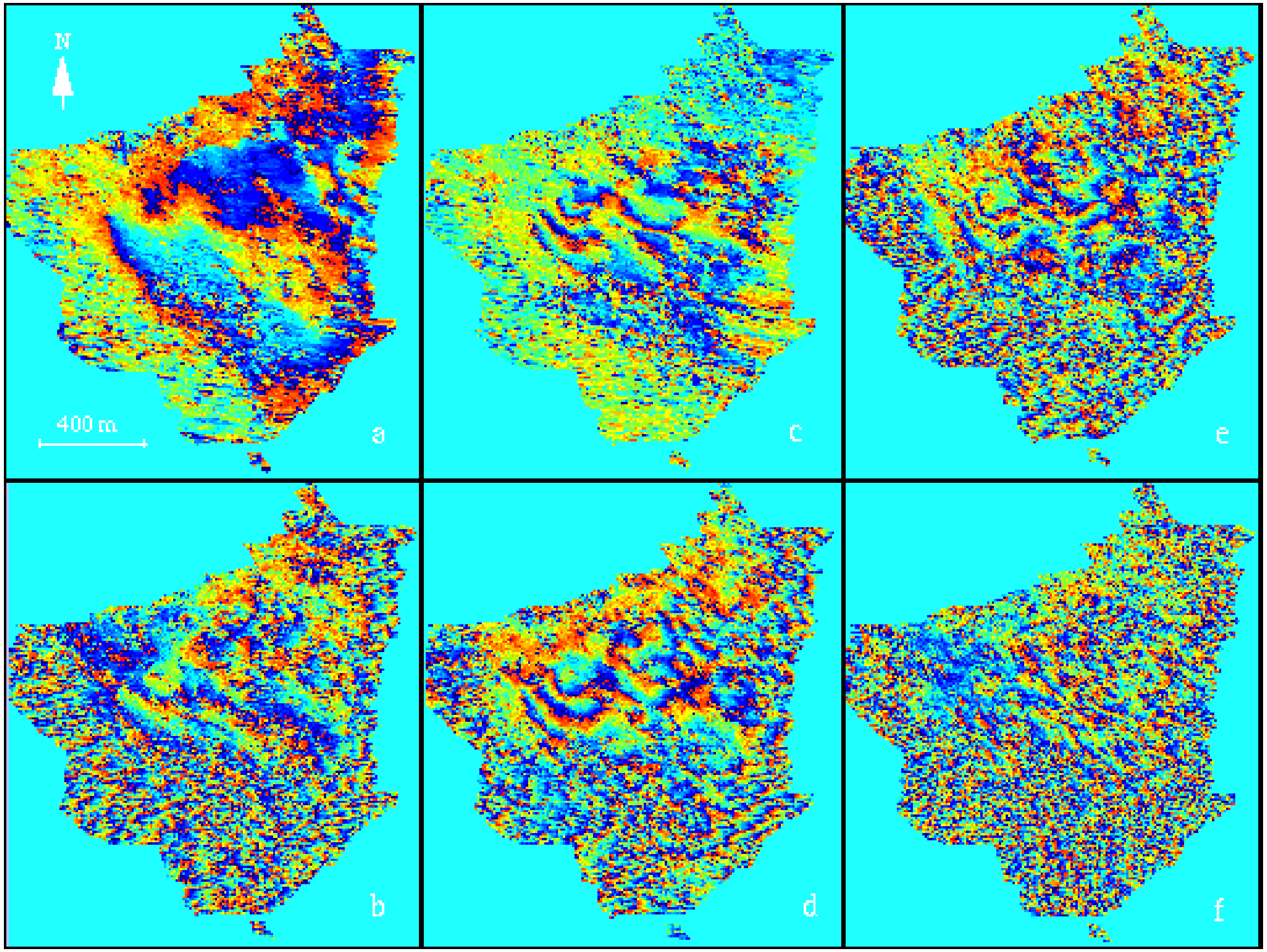

August 20, 23, 26, 29 and September 4, 1991.

*Geocoded differential interferograms. **(a)** 23-26 pair (3 days). Bperp= 43 m. **(b)** 26-04 pair (6 days). Bperp= -298 m. **(c)** 20-29 pair (9 days). Bperp= -4 m. **(d)** 26-04 pair (9 days). Bperp= 248 m. **(e)** 23-04 pair. Bperp= 291 m. **(f)** 20-04 pair. Bperp= -301 m*

http://earth.esa.int/workshops/fringe_1996/benedict/

Joshimath Landslide *Dec. 31, 2022 and Jan. 2, 2023*

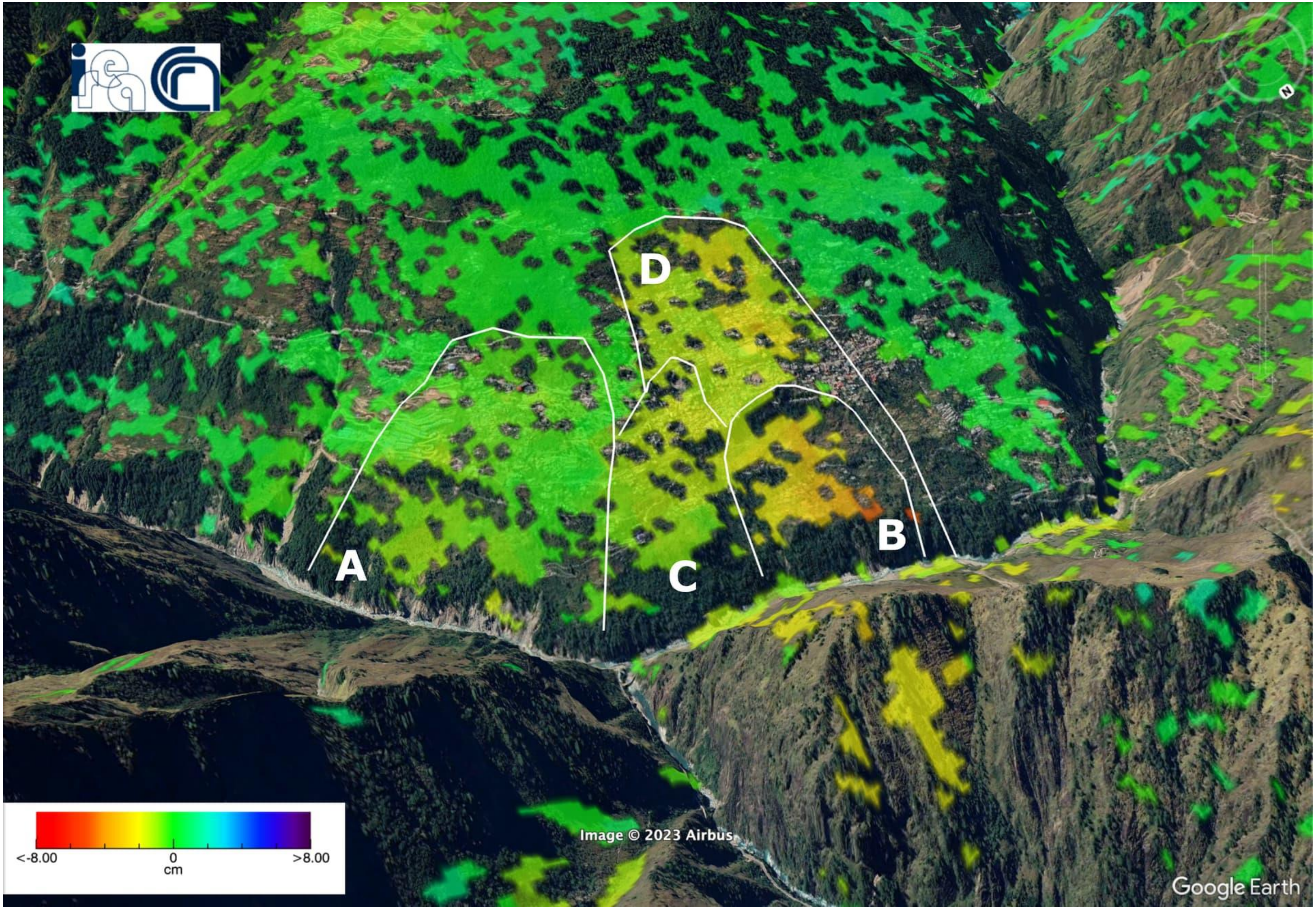

Gangotri Glacier

The remnants of lateral moraines, rocky debris pushed along by the glacier, can be seen on both sides of the valley up to Gangotri town.

Gangotri Glacier Motion

Gangotri glacier area

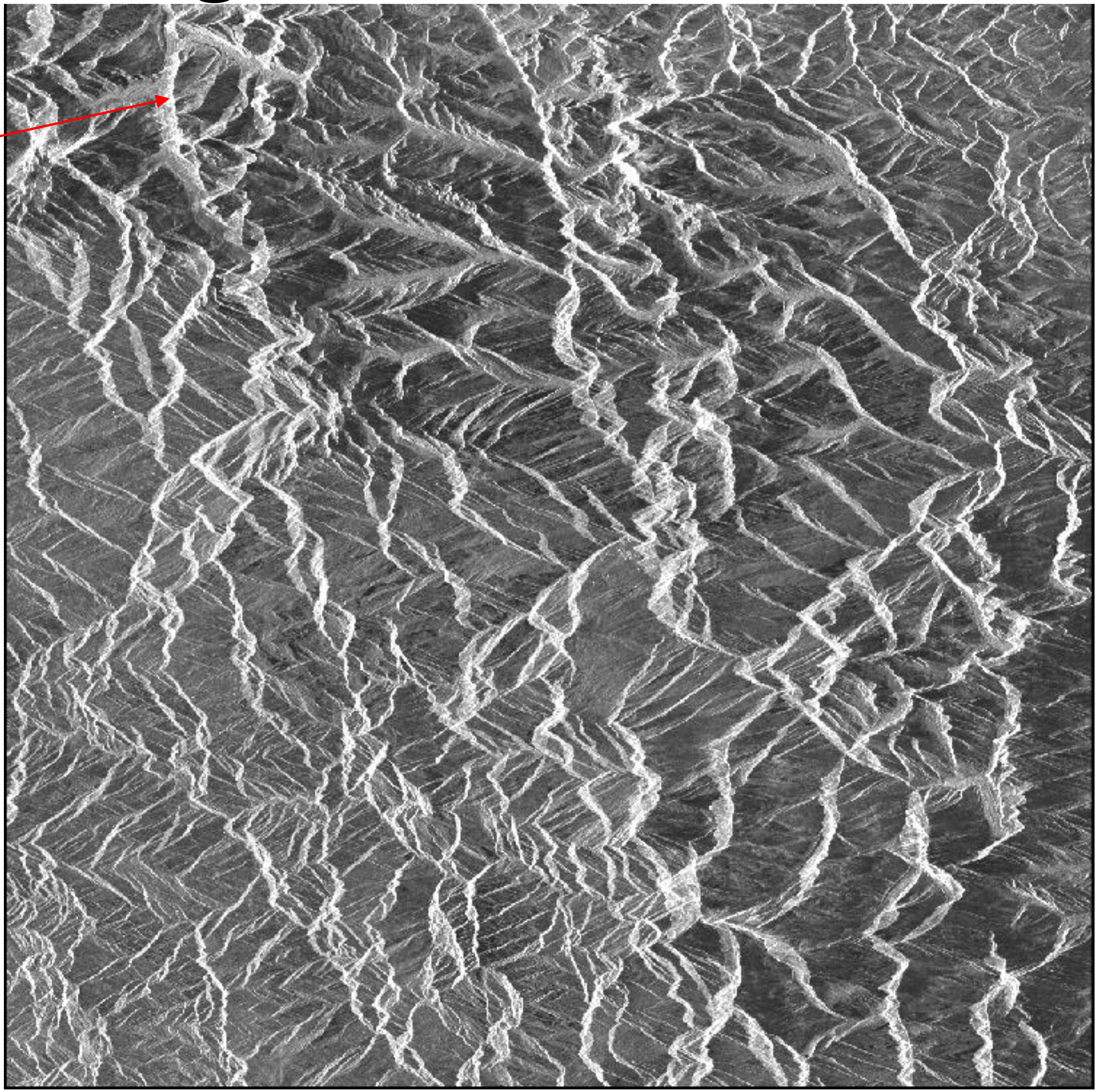

Ascending pass Image.

Gangotri Interferogram showing topography

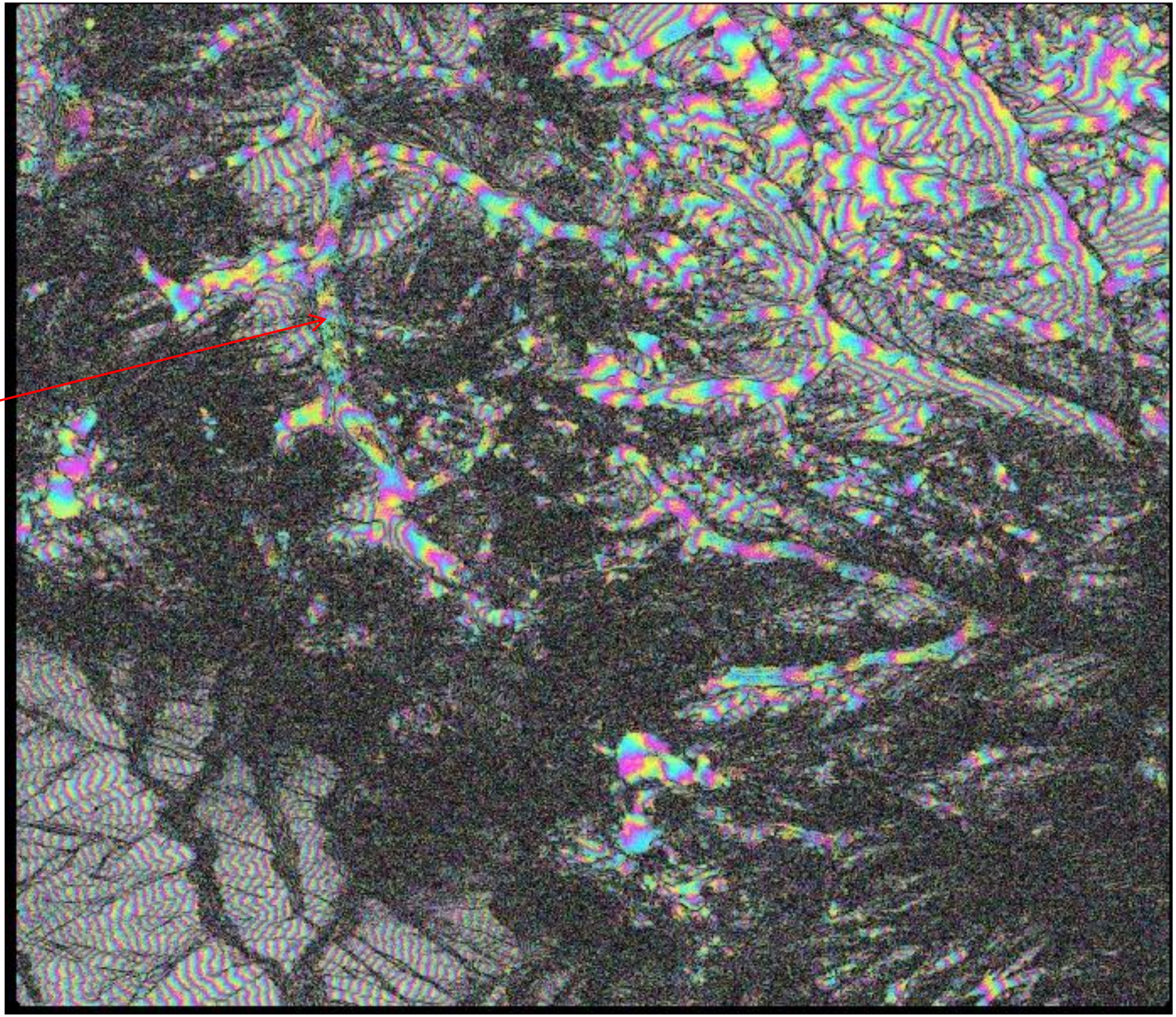

Differential Interferogram of Gangotri Glacier after removing topography

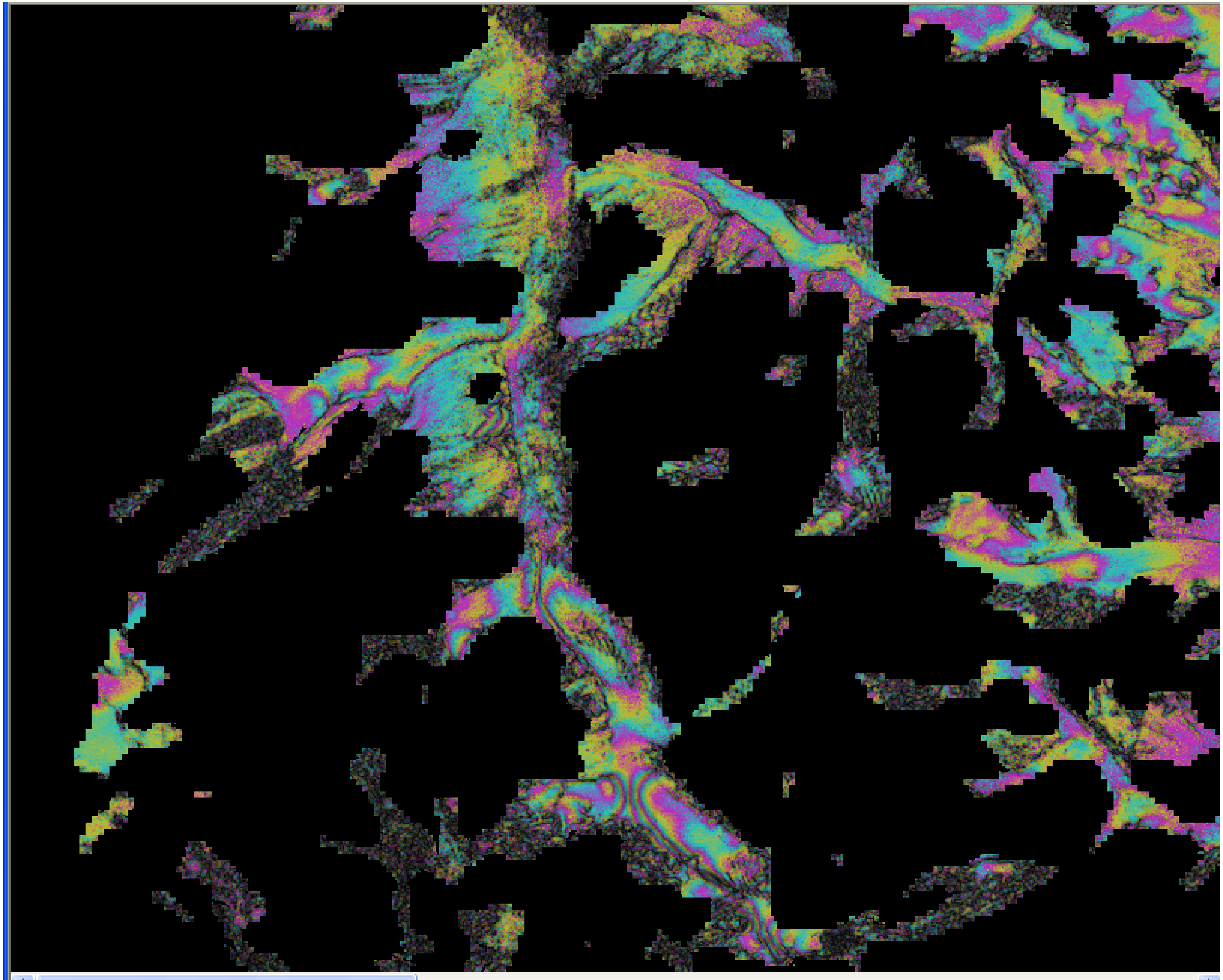

Glacier Velocity Map

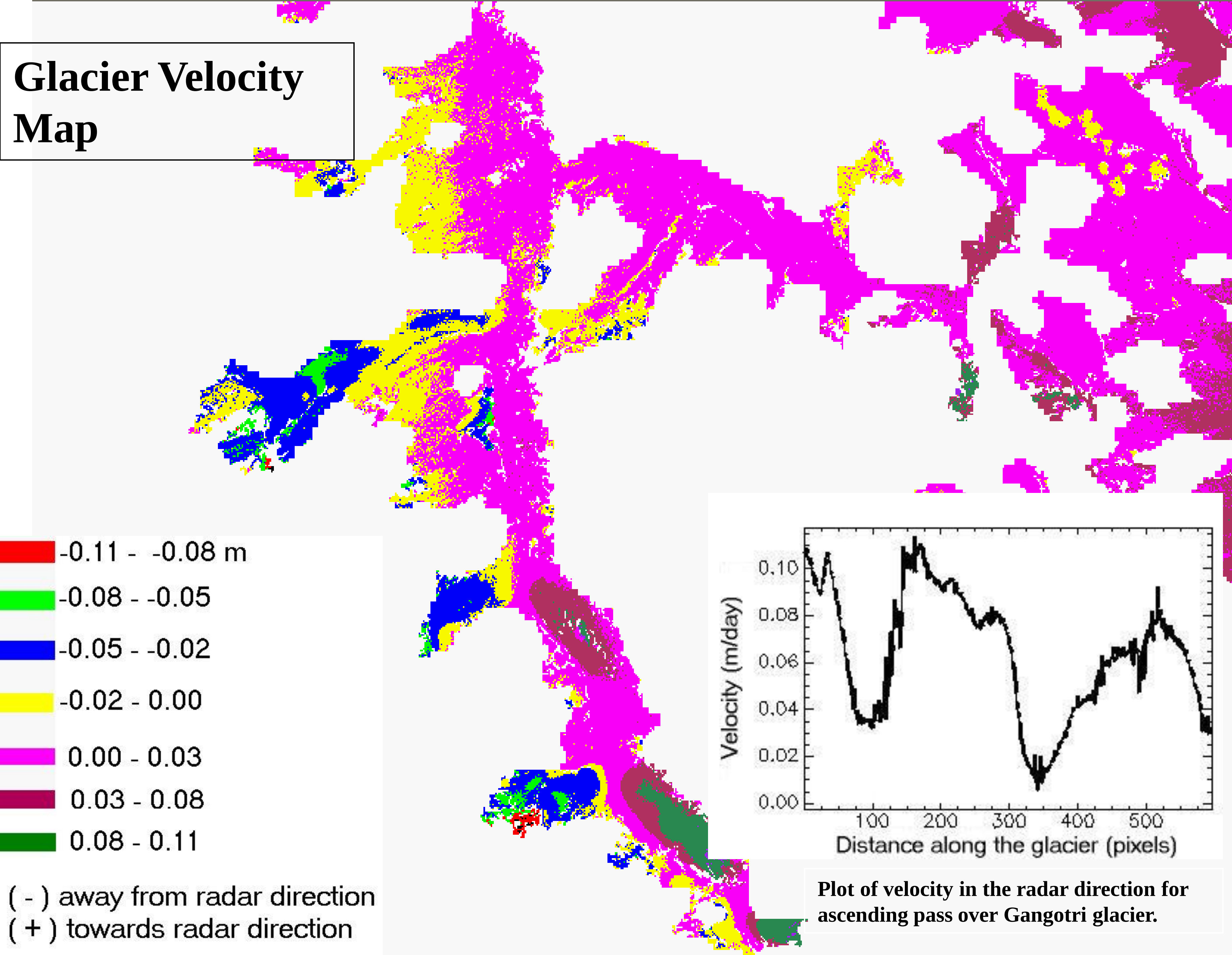

Plot of velocity in the radar direction for ascending pass over Gangotri glacier.

Glacier Movement Map for Siachen (April 1&2, 1996)

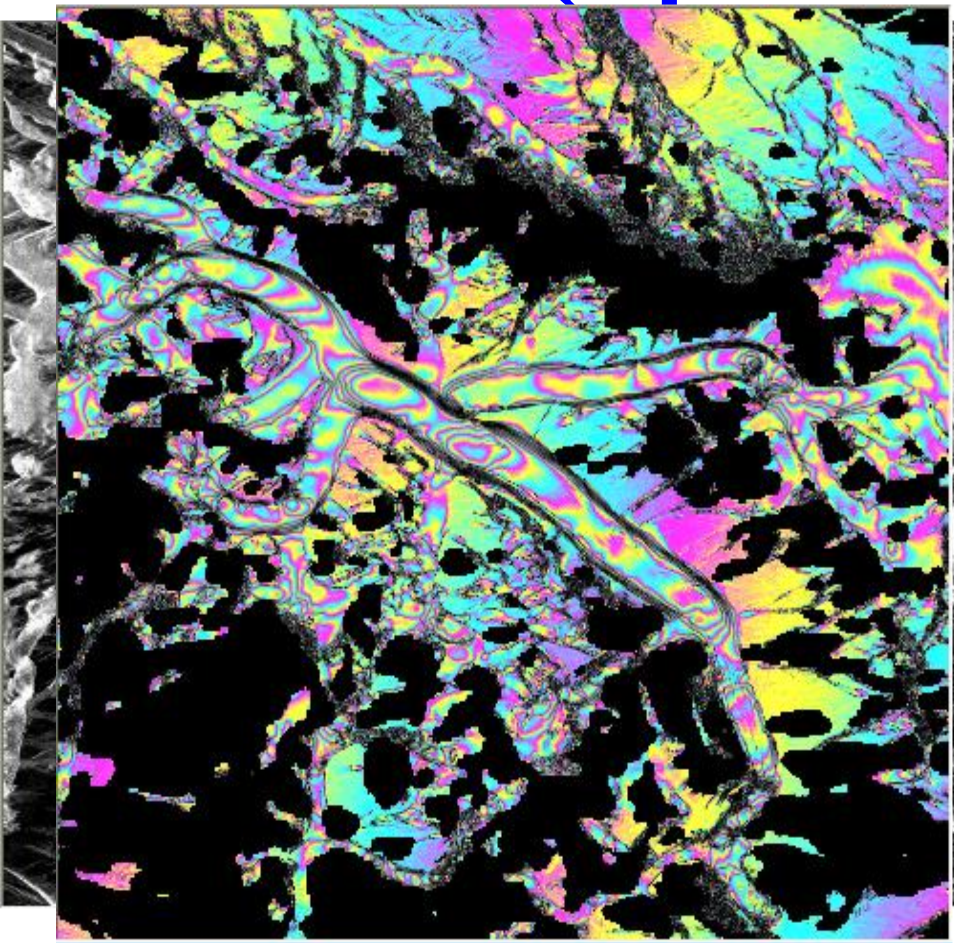

Intensity

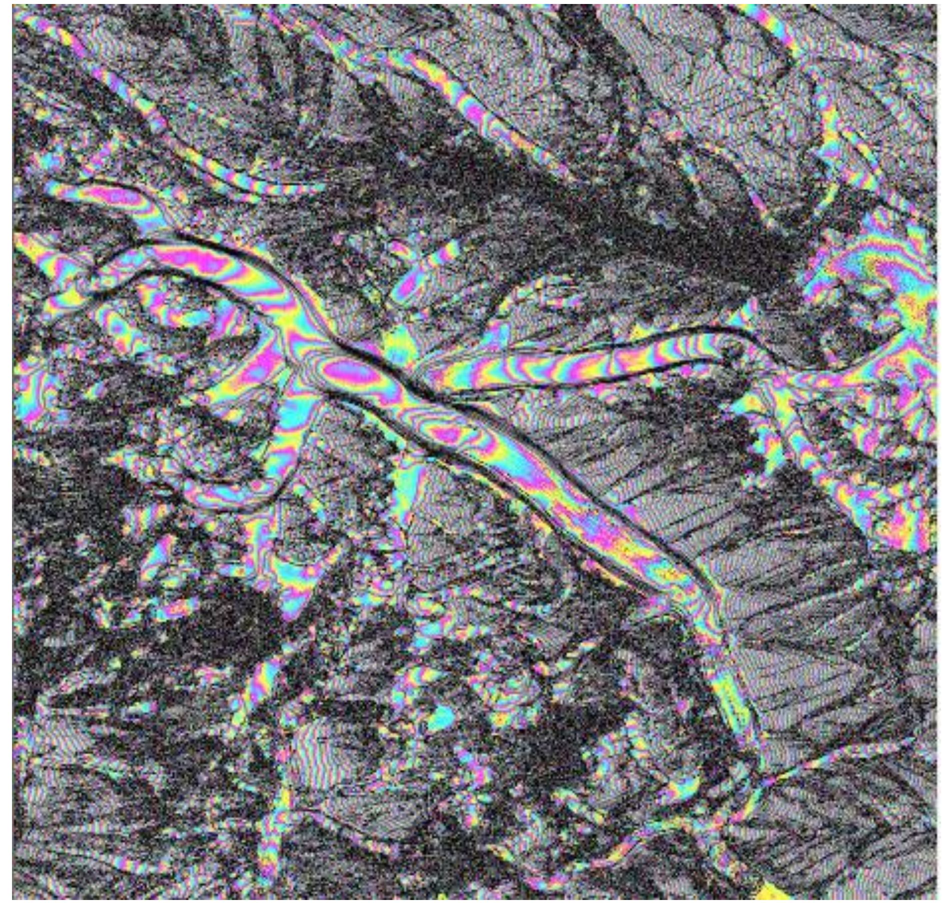

Interferogram,
One fringe = 86 m in height

Siachen Glacier Movement Map (Des. Pass) (April 1&2, 1996)

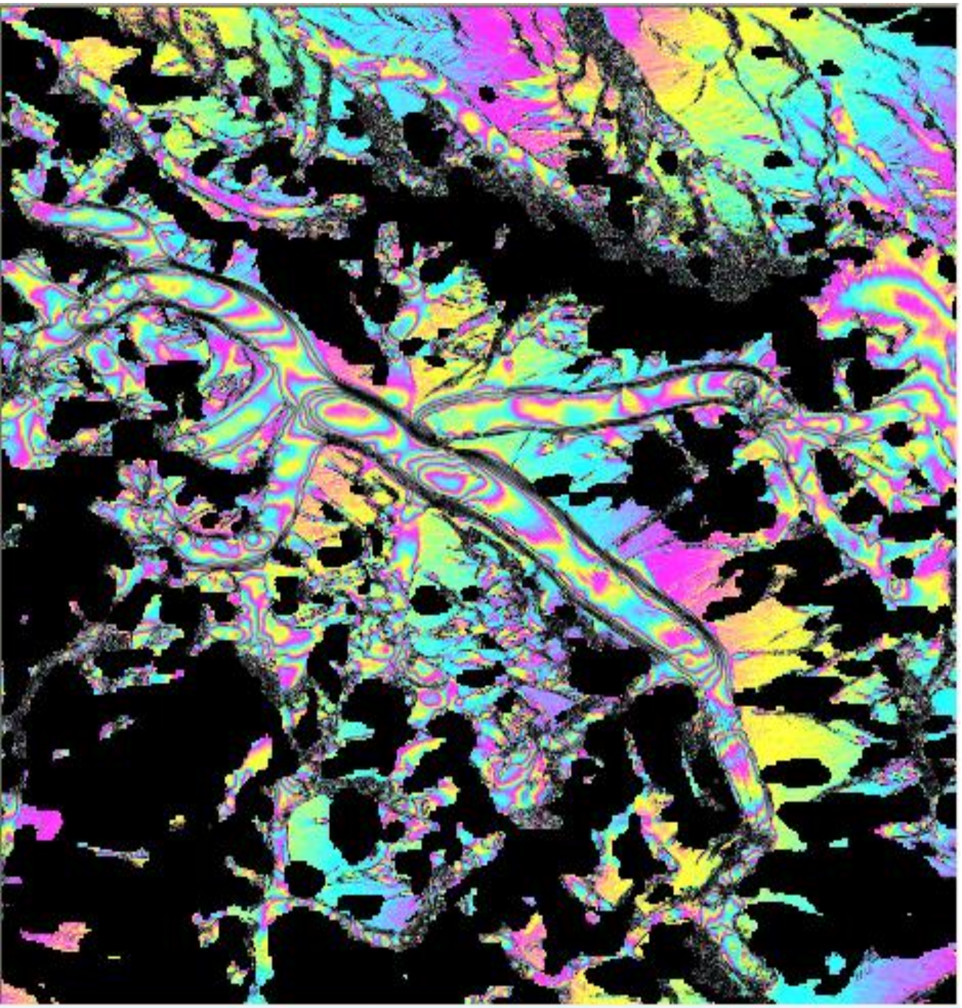

Differential Interferogram

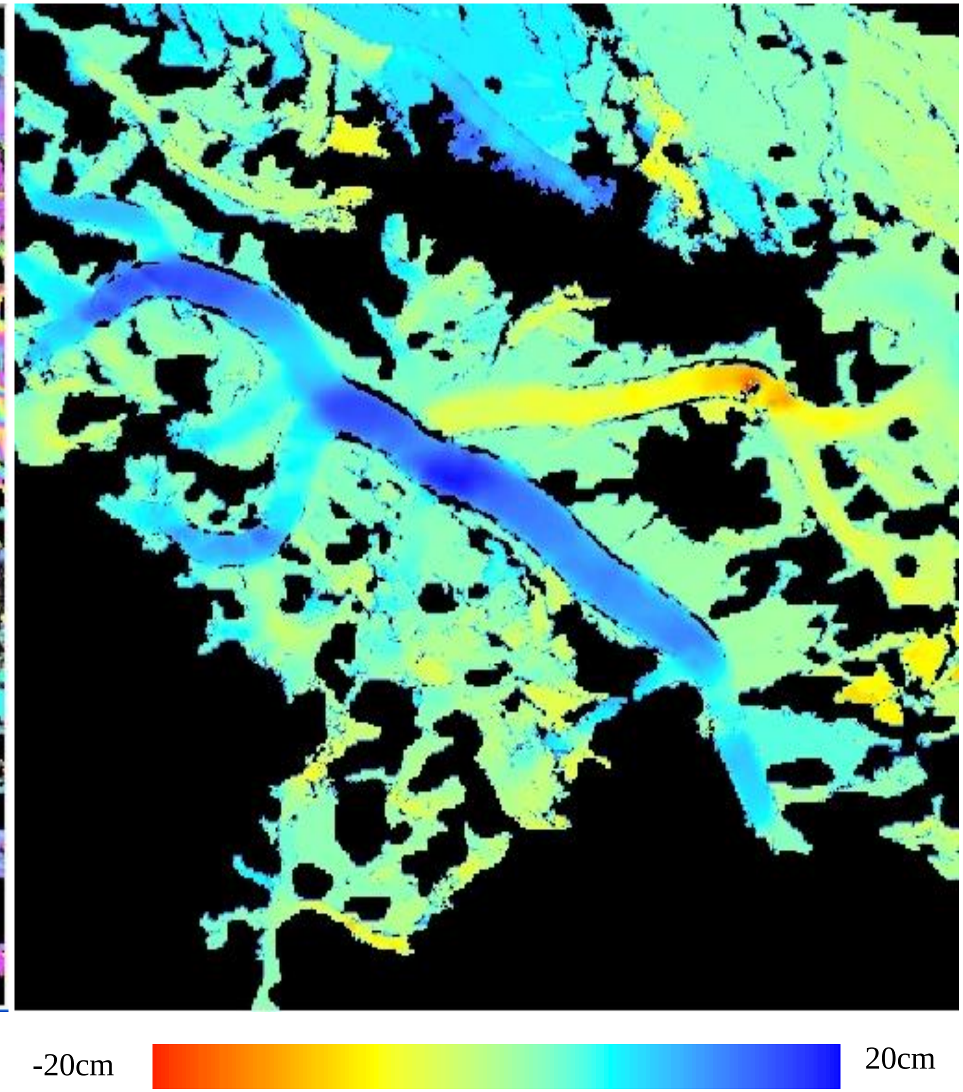

Glacier Velocity Map per day

Siachen Glacier Movement Map (Asc. Pass) May 1996

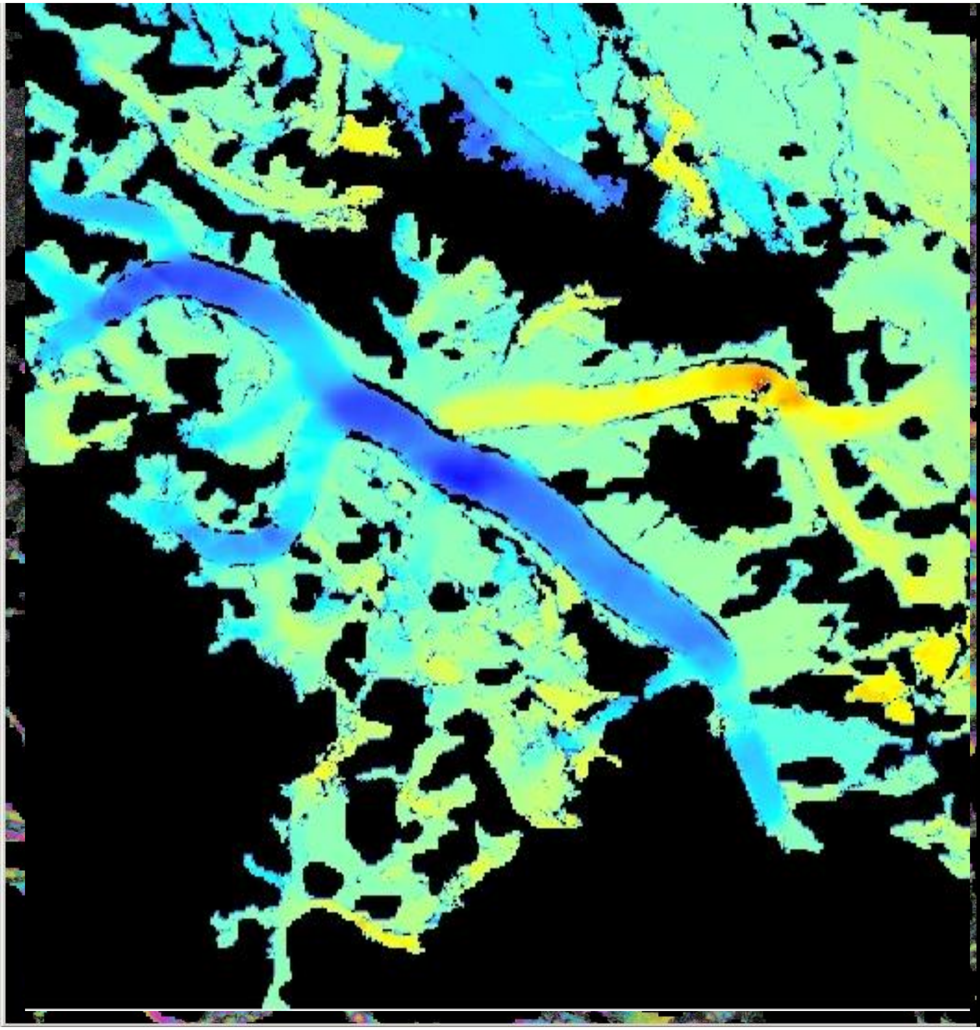

Differential Interferogram

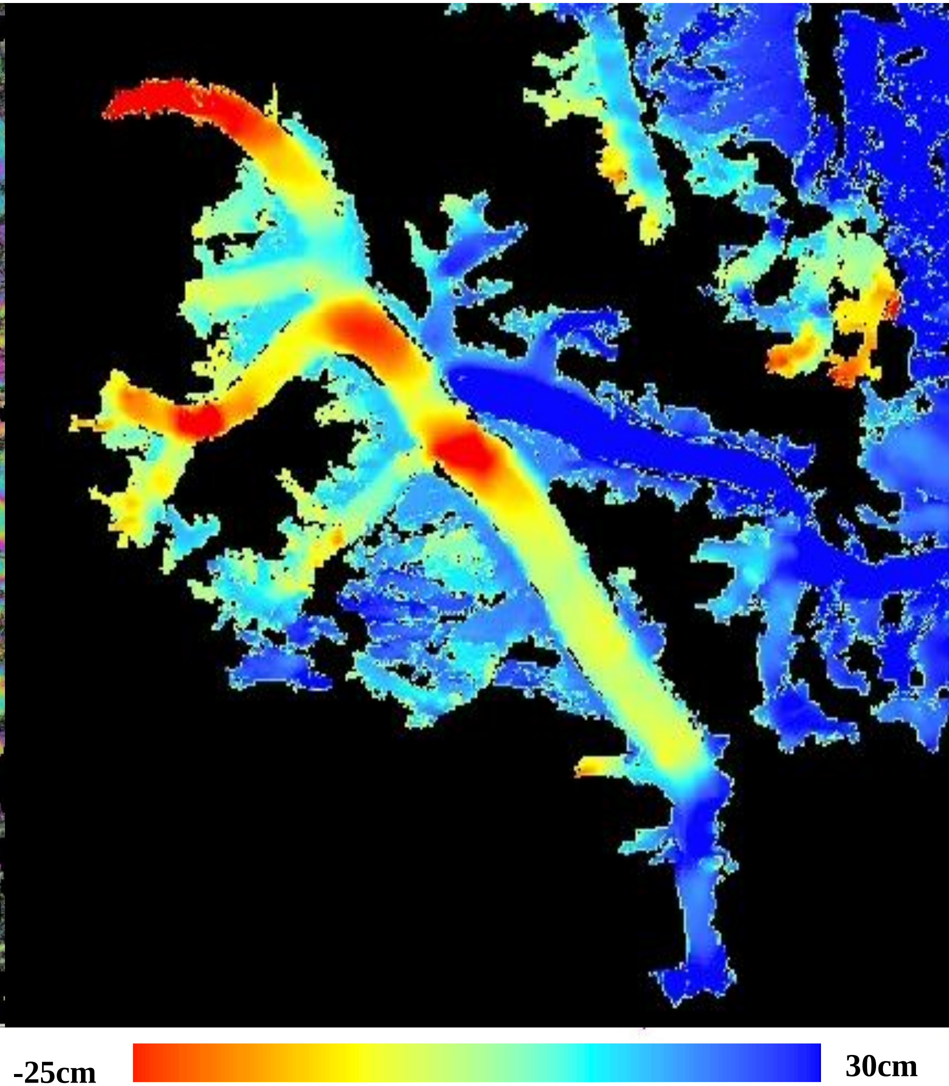

Velocity Map

Glacier Motion along the Middle part of the Siachen Glacier

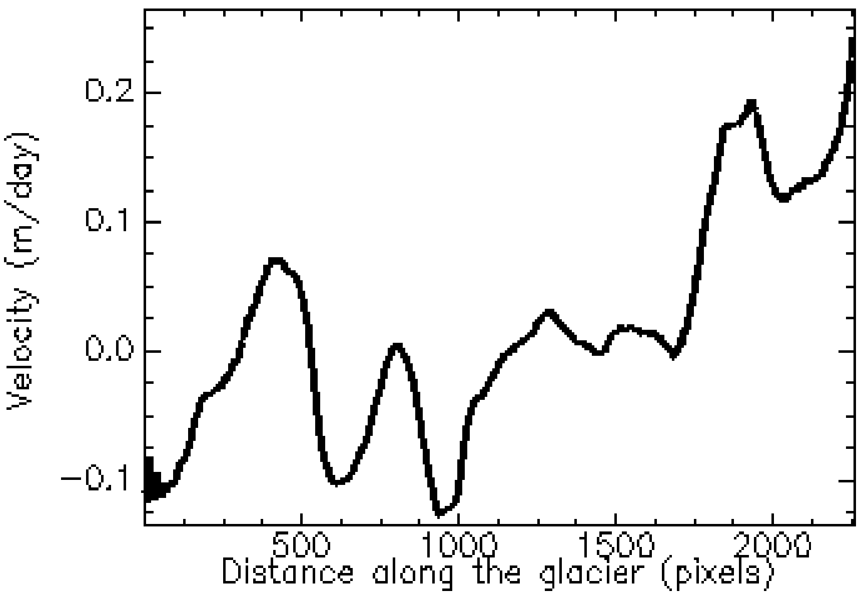

Descending

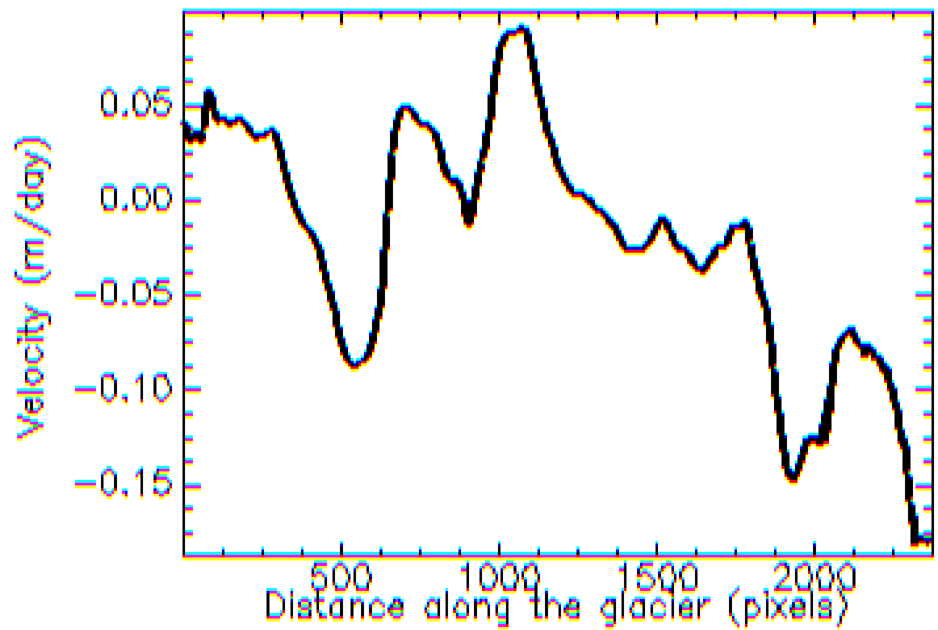

Ascending

Antarctic Glacier Motion

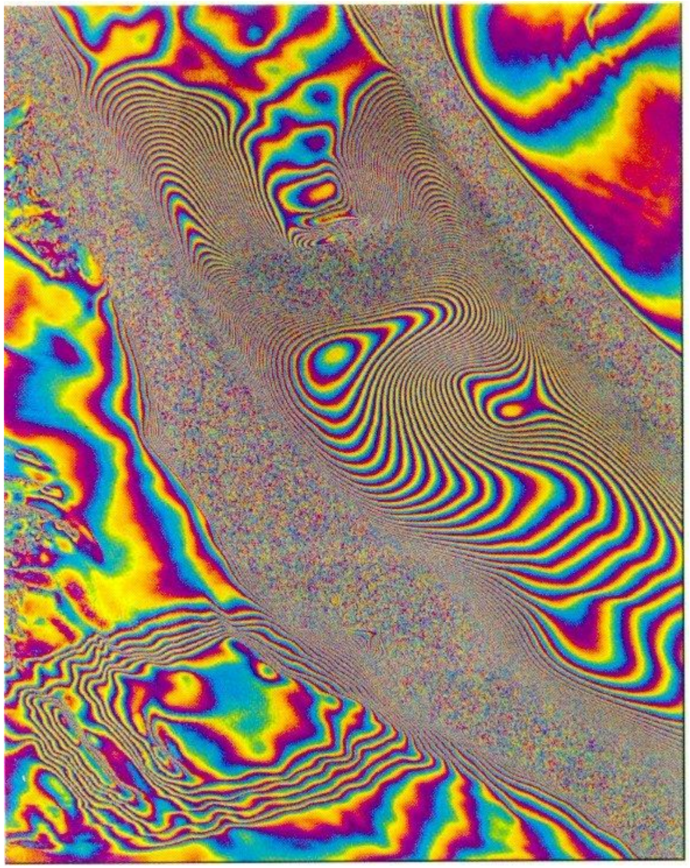

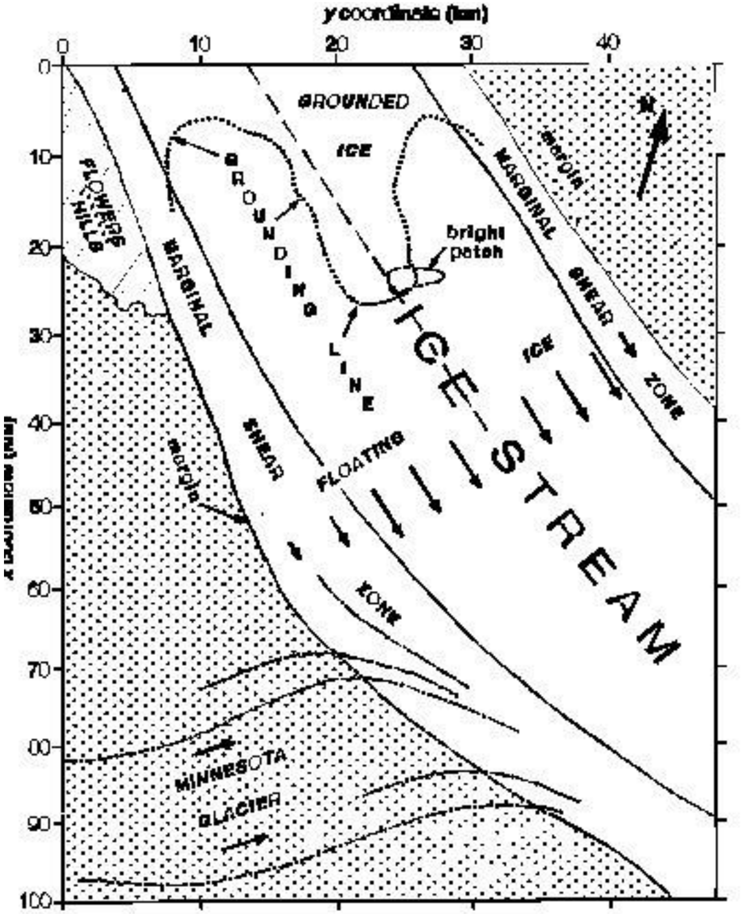

Barren Island in Andaman Showing Volcano area

February 2003

Observed and Modeled Fringe Patterns

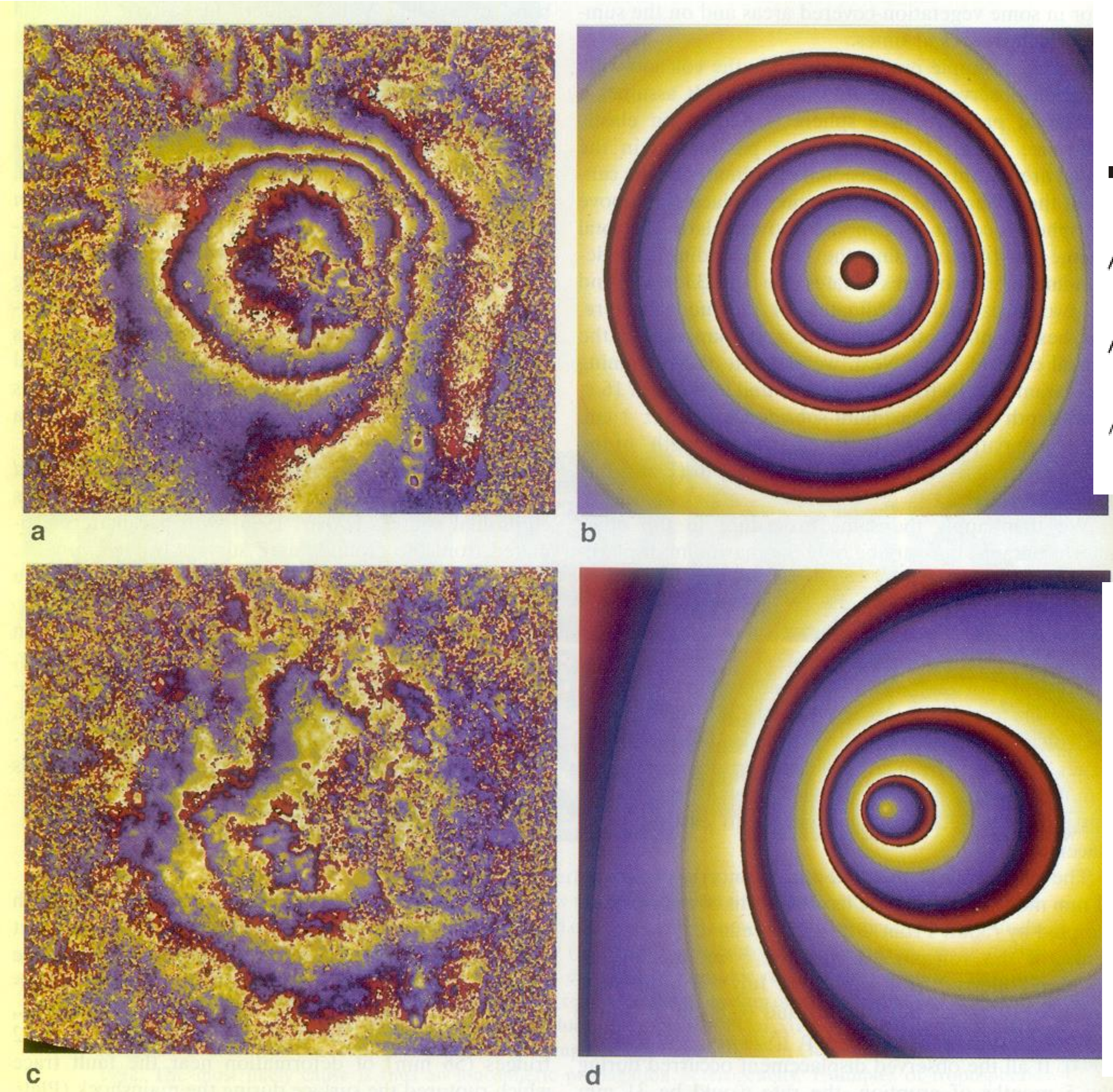

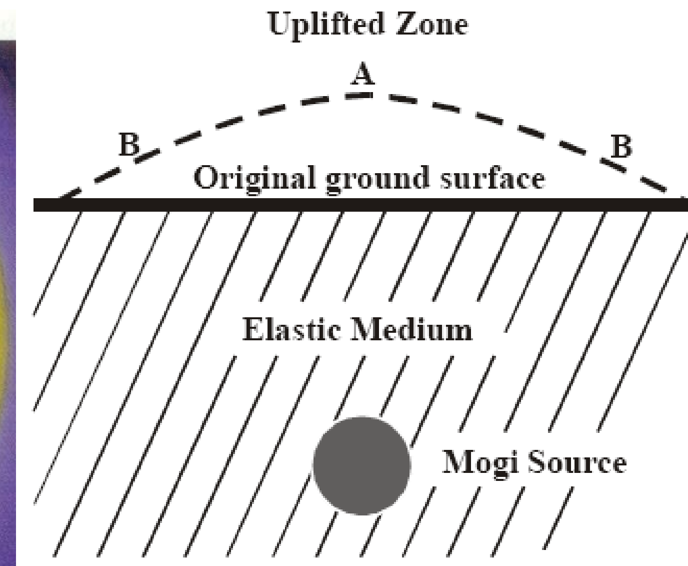

Mogi's Model

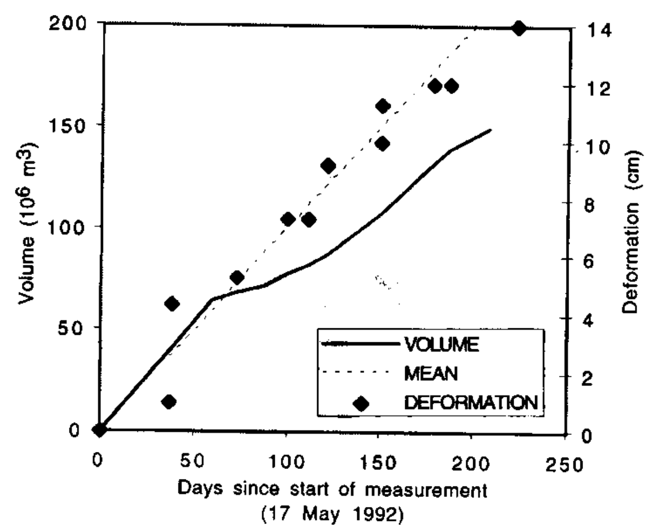

April 4 and May 9, 1996 InSAR Pair

CR No.	Actual height (cm)	Estimated Height (cm)	Difference (cm)
CR1	2.0	1.77	0.23
CR2	4.1	4.21	0.11
CR3	5.9	5.92	0.03

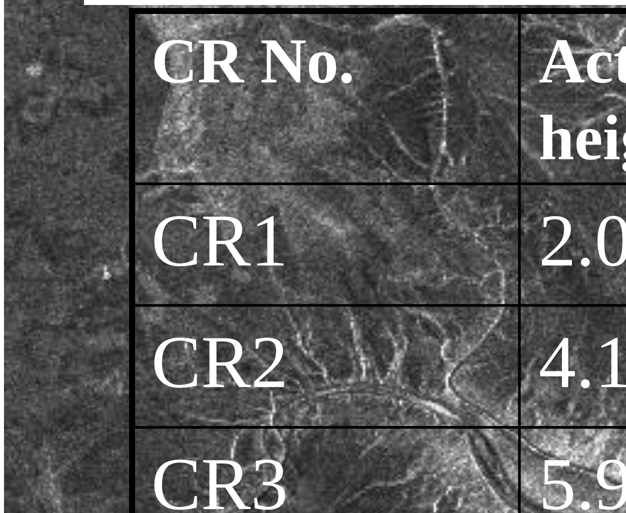

April 4, 1996

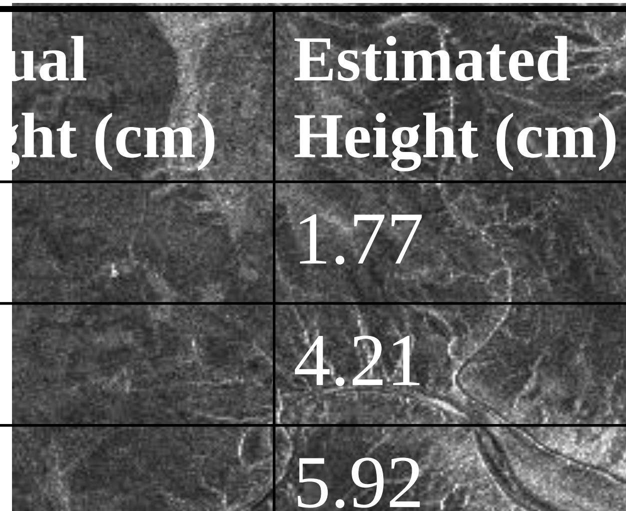

April 5, 1996

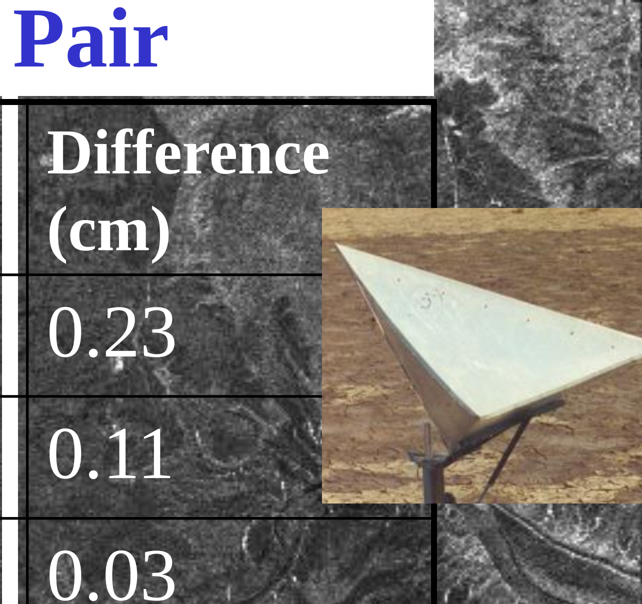

May 9, 1996

Bhavnagar Experiment Corner Reflector Experiment

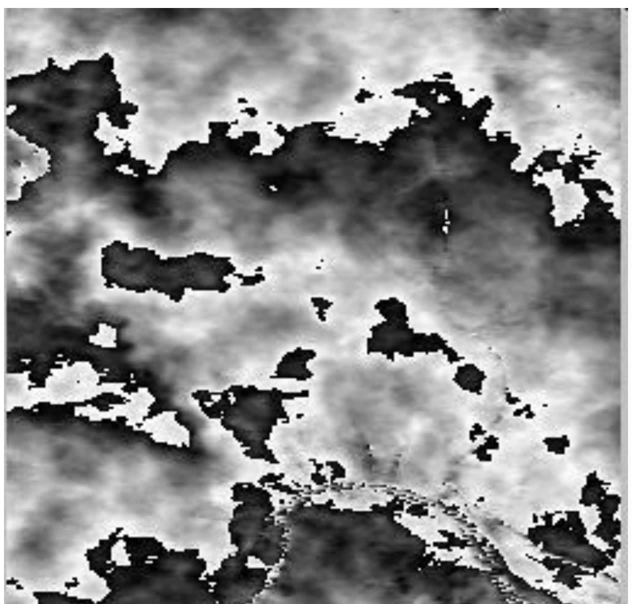

Fringes (April 4 -5)

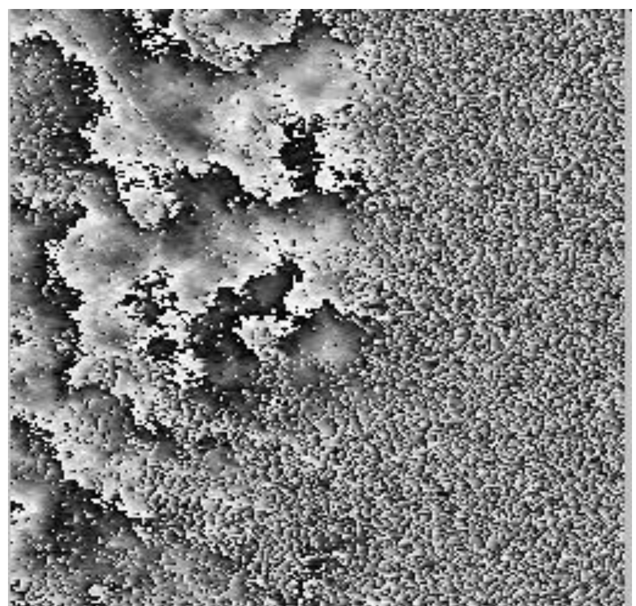

Fringes (April 4 -May 9)

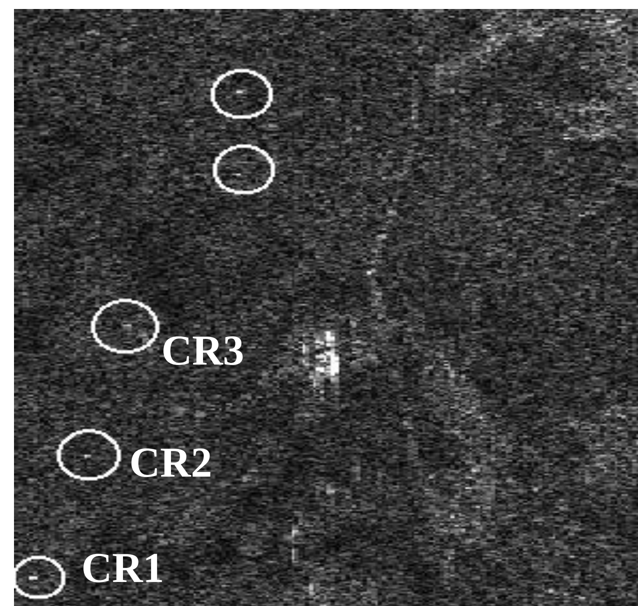

CRs in intensity image

Land Use/Land Cover Change Analysis

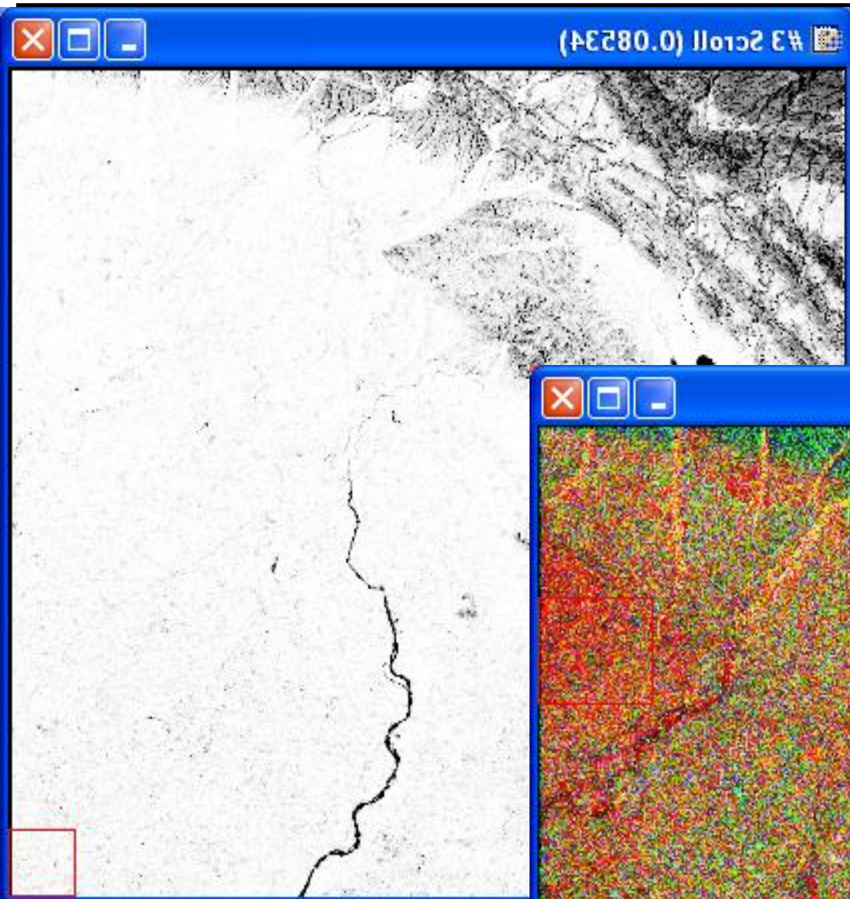

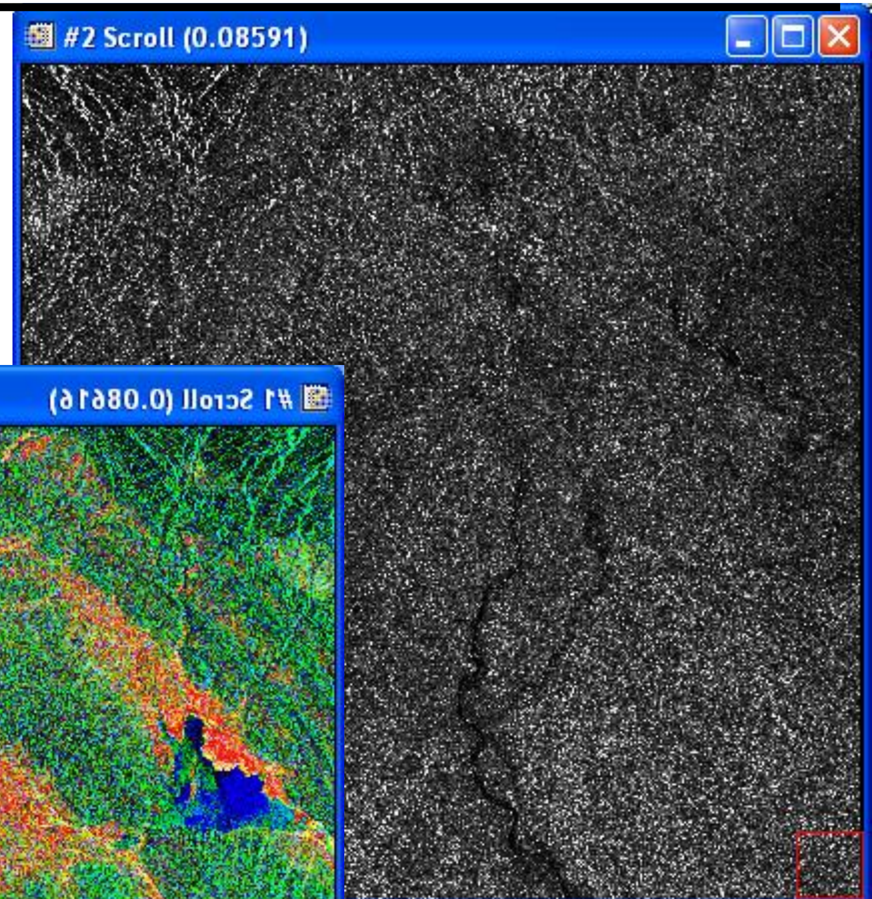

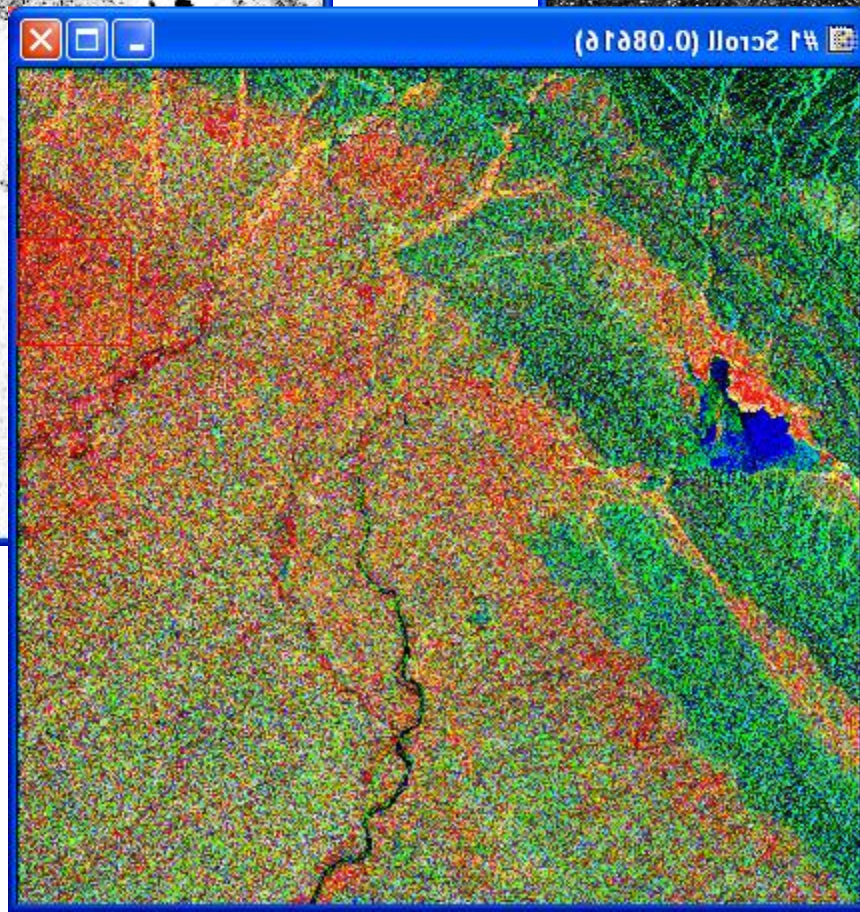

Coherence

Intensity

B= Master - Slave

Gurdaspur area

R(Coh) G(Int) B(diff)

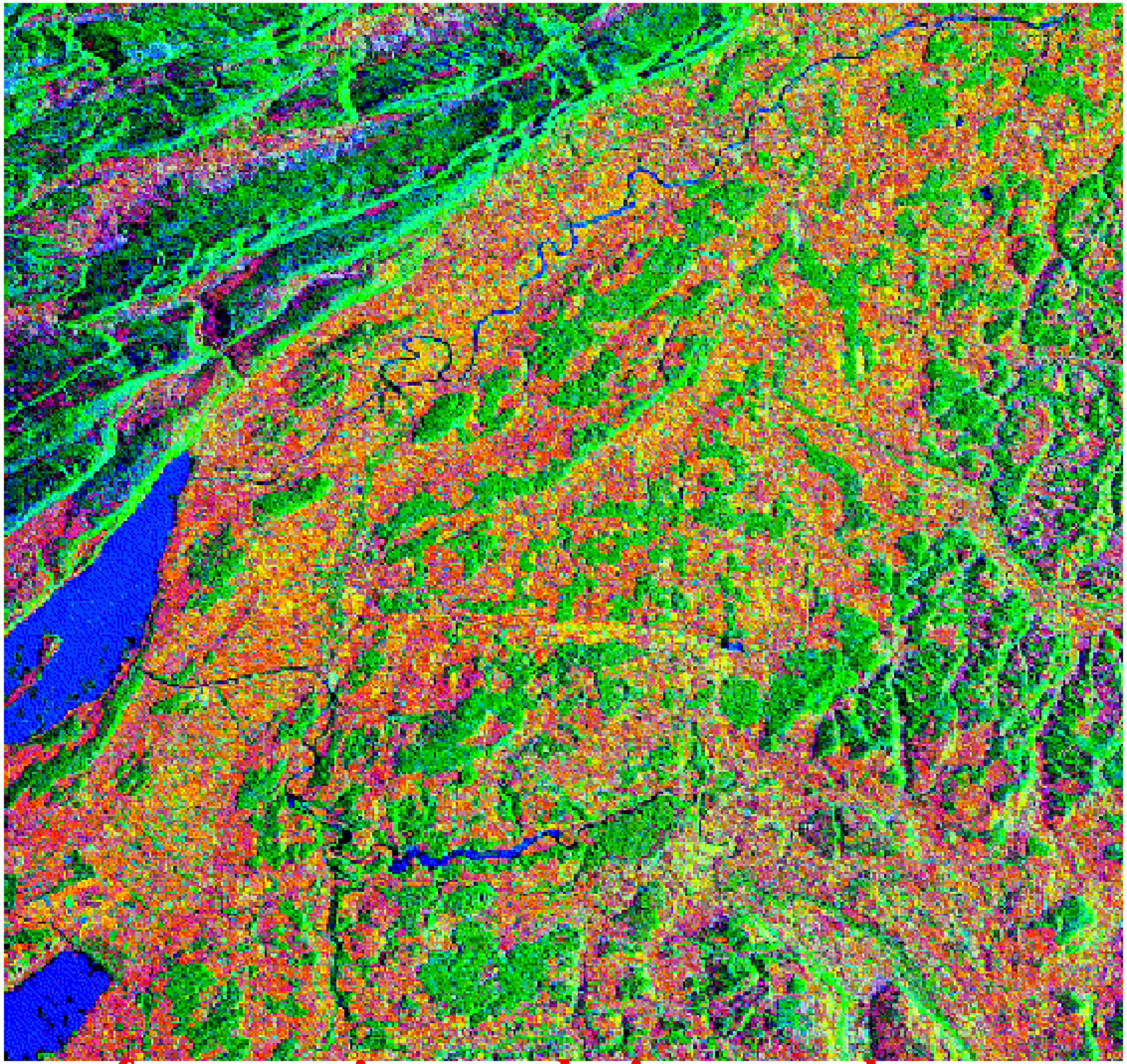

red = **interferometric correlation or coherence;**

green = backscatter intensity on 24 November;

blue = backscatter intensity change between 24 and 27 November

THE INTERFEROMETRIC « CARTWHEEL » SYSTEM

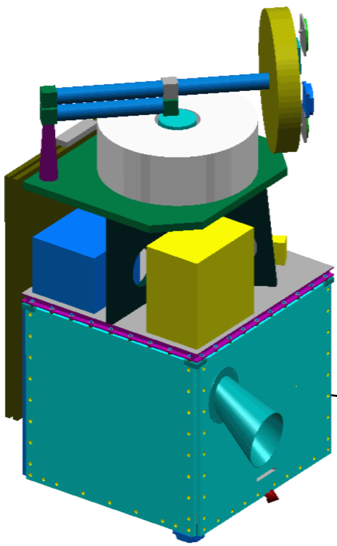

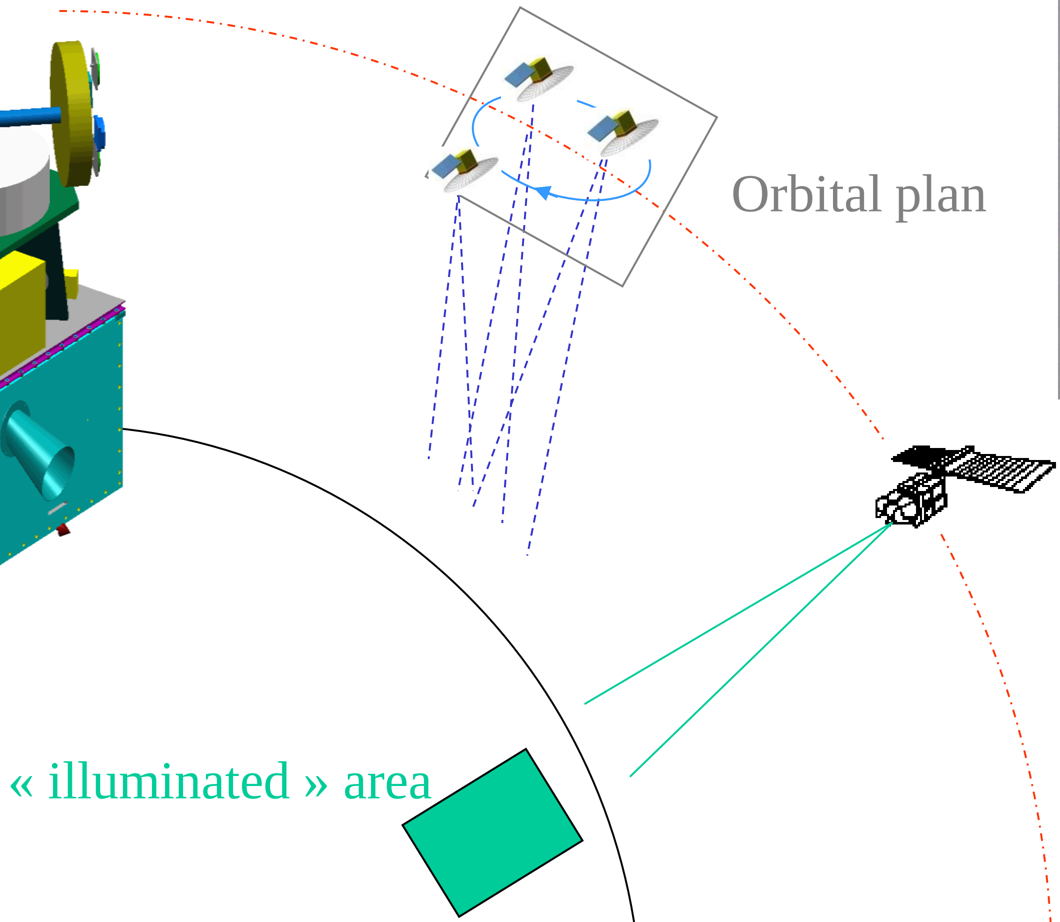

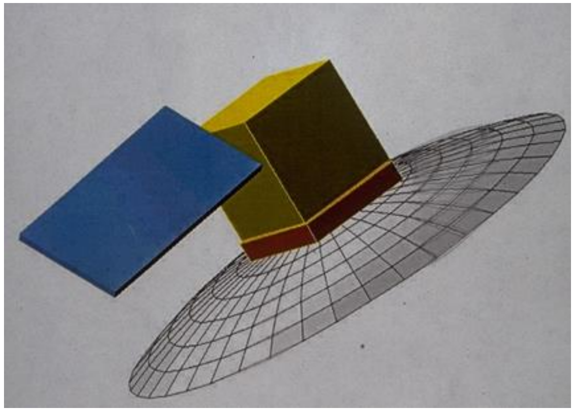

Dedicated systems are interesting only if they achieve significant improvement and low cost

70 cm vertical resolution
on 15 m cells in single pass

Large crosstrack baseline for DEM
Small crosstrack baseline for surface change
Along track baseline for motion detection

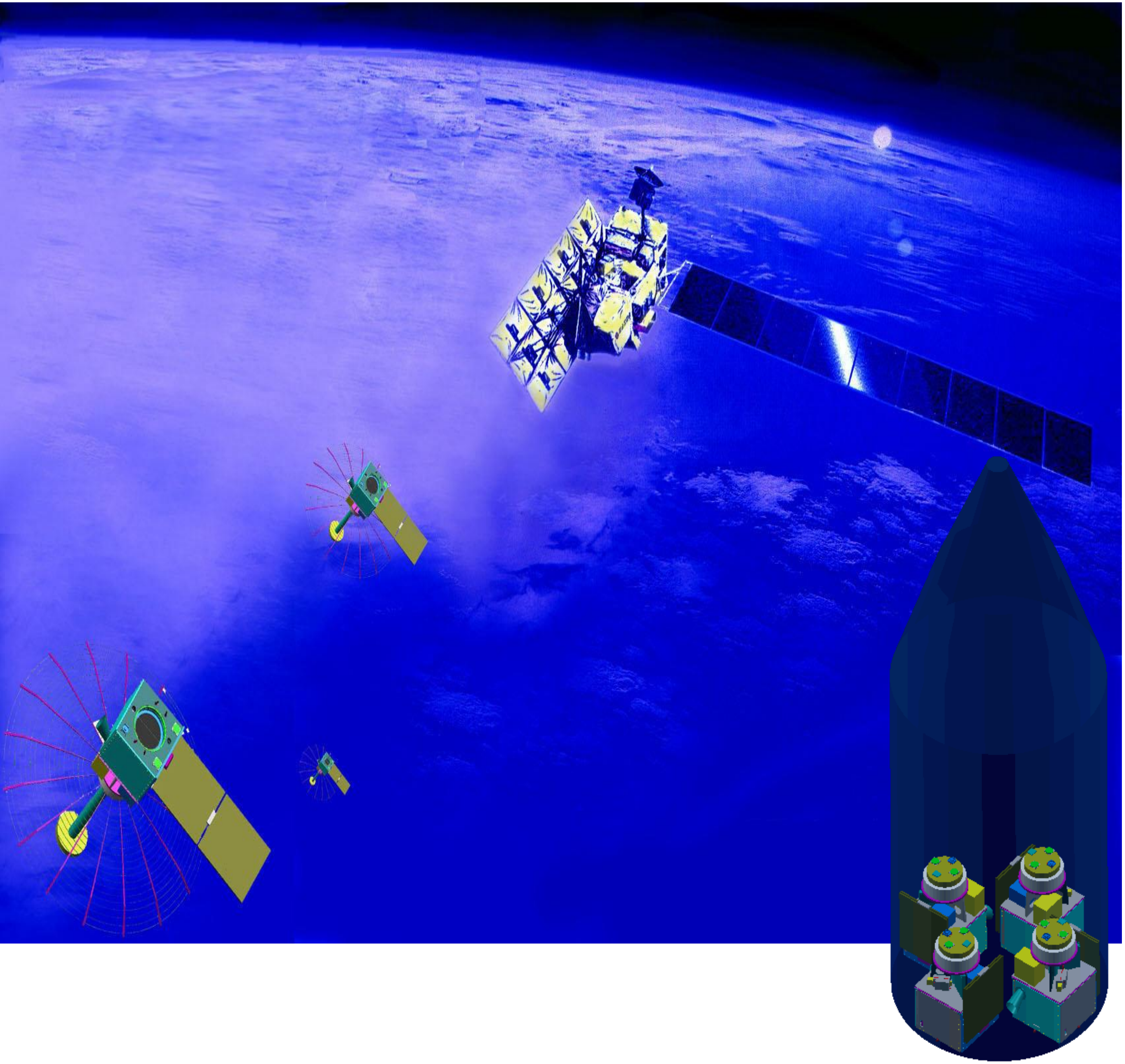

An artist 's Rendering of Cartwheel

But the scales are wrong !

The receivers fly a few km apart !

The companion is more than 100 km away !